



8-2013

# The N-terminus of the *Saccharomyces cerevisiae* G protein-coupled receptor Ste2p: formation of dimer interfaces and negative regulation

Mohammad Seraj Uddin  
muddin@utk.edu

---

## Recommended Citation

Uddin, Mohammad Seraj, "The N-terminus of the *Saccharomyces cerevisiae* G protein-coupled receptor Ste2p: formation of dimer interfaces and negative regulation." PhD diss., University of Tennessee, 2013.  
[https://trace.tennessee.edu/utk\\_graddiss/2490](https://trace.tennessee.edu/utk_graddiss/2490)

This Dissertation is brought to you for free and open access by the Graduate School at Trace: Tennessee Research and Creative Exchange. It has been accepted for inclusion in Doctoral Dissertations by an authorized administrator of Trace: Tennessee Research and Creative Exchange. For more information, please contact [trace@utk.edu](mailto:trace@utk.edu).

To the Graduate Council:

I am submitting herewith a dissertation written by Mohammad Seraj Uddin entitled "The N-terminus of the *Saccharomyces cerevisiae* G protein-coupled receptor Ste2p: formation of dimer interfaces and negative regulation." I have examined the final electronic copy of this dissertation for form and content and recommend that it be accepted in partial fulfillment of the requirements for the degree of Doctor of Philosophy, with a major in Microbiology.

Jeffrey M Becker, Major Professor

We have read this dissertation and recommend its acceptance:

Tim E. Sparer, Todd B. Reynolds, Cynthia B. Peterson

Accepted for the Council:

Dixie L. Thompson

Vice Provost and Dean of the Graduate School

(Original signatures are on file with official student records.)

---

The N-terminus of the *Saccharomyces cerevisiae*  
G protein-coupled receptor Ste2p: formation of  
dimer interfaces and negative regulation

A Dissertation Presented for the  
Doctor of Philosophy  
Degree  
The University of Tennessee, Knoxville

Mohammad Seraj Uddin

August 2013

**Copyright©2013 by Mohammad Seraj Uddin**  
**All rights reserved**

## **Dedication**

*This dissertation is dedicated to my parents, Rashid Ahmed and Laila Begum, for their endless love and support. I would also dedicate this work to all family members, my wife Fahmida Chowdhury, my son Zarif and my parents-in-law for their encouragement and love.*

## Acknowledgments

I would like to thank many people who, without their help, this dissertation would not be possible. My first and deepest appreciation goes to my mentor Dr. Jeffrey M. Becker. It was really a great pleasure to work for such an enthusiastic scientist whose knowledge, guidance, support and directions will be with me for the rest of my career. I could not have done it without him. I am thankful that he was so patient and supportive during the time I was struggling with my projects. His critical suggestions and guidance helped me overcome lots of stumbling blocks that I would not even try without him. It is a great pleasure and honor to work for such a great scientist.

I also would like to give my very appreciation to my committee members Dr. Timothy E. Sparer, Dr. Todd B. Reynolds, and Dr. Cynthia Peterson for their suggestions, critical reviews and guidance during my studies. Their extraordinary patience and encouragement motivated me. I would like to thank Dr. Fred Naider for his support and valuable ideas on critical decisions throughout these studies. I also want to thank all the Dr. Naider laboratory members for the peptide syntheses that made this study possible.

I really appreciate all the lab members in Dr. Becker's laboratory: Special thanks to Dr. Melinda Hauser, Dr. Byung-Kwon Lee, and Dr. Tom Masi for their guidance and help during my study. I also want to thank Sarah Kauffman, George Umanah, Liyin Huang, Elena Ganusova, Steve Minkin, Heejung Kim, Giljun Park, Kyung Sik, Amanda Deyo, Madelyn Crawford, Jordan Kim, Brandon Sidney, Julie Maccarone, John Lockart, who made Becker lab such an enjoyable and fun place to work at.

Finally I am greatly indebted to my family in Bangladesh, Fahmida Chowdhury and my little son Zarif for all the love and support they gave me during all these years. And a big thank you to everyone who has been a friend and colleague throughout this process. I could not have it without you all.

## Abstract

G protein-coupled receptors (GPCRs), the largest family of membrane proteins on the cell surface, play essential roles in signal transduction in all eukaryotic organisms. These proteins are responsible for sensing and detecting a wide range of extracellular stimuli and translating them to intracellular responses. This signaling requires a tight control for receptor activation without which abnormal signal leads to diseases. In fact, malfunctions of these receptors are associated with numerous pathological conditions and currently an estimated 40-50% of therapeutic drugs are designed to target these receptors suggesting that further increases in understanding of GPCRs and the signaling pathways they initiate will lead to new and more specific drug targets. We have used *Saccharomyces cerevisiae* GPCR Ste2p as a model system to understand structure-function relationships of these receptors. In this study, the role of the extracellular N-terminus has been examined using various biophysical methods with the anticipation to uncover its role in receptor function. It was found that some residues in the extracellular N-terminus were not accessible to a sulfhydryl reagent and that the alternating pattern of accessibility is consistent with the structure of a beta strand. This beta strand was found to be involved in dimer formation. Moreover, a conserved tyrosine residue in the middle of the beta strand was found to interact with two residues in the extracellular loop 1. It was also found that the N-terminus is involved in negative regulation and important for cell surface expression.

# Table of Contents

<b>Chapter 1: General introduction.....</b>	<b>1</b>
<b>G protein-coupled receptors: an overview .....</b>	<b>2</b>
<b>Classification of GPCRs .....</b>	<b>4</b>
<b>GPCR crystal structures .....</b>	<b>9</b>
<b>Fungal GPCRs.....</b>	<b>12</b>
<b><i>S. cerevisiae</i> GPCRs .....</b>	<b>15</b>
<b>The use of Ste2p as a model GPCR .....</b>	<b>20</b>
<b>References.....</b>	<b>27</b>
<b>Chapter 2 : Identification of residues involved in homodimer formation located within a <math>\beta</math>-strand region of the N-terminus of a yeast G protein-coupled receptor.....</b>	<b>48</b>
<b>Abstract.....</b>	<b>50</b>
<b>Introduction.....</b>	<b>51</b>
<b>Methods.....</b>	<b>53</b>
<b>Results .....</b>	<b>58</b>
<b>Discussion .....</b>	<b>74</b>
<b>Conclusion .....</b>	<b>78</b>
<b>Acknowledgements .....</b>	<b>79</b>
<b>References.....</b>	<b>80</b>

<b>Chapter 3: The N-terminus of <i>Saccharomyces cerevisiae</i> G protein-coupled receptor Ste2p is involved in negative regulation .....</b>	<b>89</b>
<b>Abstract.....</b>	<b>90</b>
<b>Introduction.....</b>	<b>91</b>
<b>Methods.....</b>	<b>94</b>
<b>Results .....</b>	<b>100</b>
<b>Discussion .....</b>	<b>124</b>
<b>Acknowledgments .....</b>	<b>129</b>
<b>References.....</b>	<b>130</b>
<b>Chapter 4: Formation of ste2p dimers by a conserved tyrosine residue in the N-terminus that has multiple contacts with the extracellular loop 1.....</b>	<b>138</b>
<b>Abstract.....</b>	<b>139</b>
<b>Introduction.....</b>	<b>140</b>
<b>Materials and methods .....</b>	<b>143</b>
<b>Results .....</b>	<b>148</b>
<b>Discussion .....</b>	<b>165</b>
<b>References.....</b>	<b>171</b>
<b>Chapter 5: Conclusions, summary and future studies .....</b>	<b>183</b>
<b>Summary.....</b>	<b>184</b>
<b>Future studies .....</b>	<b>186</b>
<b>References.....</b>	<b>189</b>
<b>Vita.....</b>	<b>192</b>

## List of Tables

<b>Table 1.1. Sequence-based groupings within the G-protein-coupled receptors.....</b>	<b>6</b>
<b>Table 1.2. GPCR structures solved in the 2000-2013 period .....</b>	<b>11</b>
<b>Table 1.3. Six classes of GPCRs in fungi.....</b>	<b>14</b>
<b>Table 1.4. Proposed roles of GPCR dimerisation/oligomerisation.....</b>	<b>24</b>
<b>Table 2.1. Relative expression levels of Ste2p.....</b>	<b>60</b>
<b>Table 2.2. Biological activities of Cys-less and single Cys mutants of Ste2p .....</b>	<b>64</b>
<b>Table 2.3. Relative MTSEA-biotin labeling of Cys-scanned mutants of Ste2p.....</b>	<b>68</b>
<b>Table 3.1. Total expression, surface expression and binding affinity of Ste2p N-terminal deletion mutants .....</b>	<b>104</b>
<b>Table 3.2. Signaling activities of Ste2p mutants.....</b>	<b>117</b>
<b>Table 4.1. Biological activities of Cys mutant receptors.....</b>	<b>153</b>
<b>Table 4.2. Dimer to monomer ratio of Cys mutants in non-reducing and reducing conditions .....</b>	<b>159</b>

## List of Figures

Figure 1.1. Cartoon of a GPCR showing the seven transmembrane domains.....	3
Figure 1.2. Pheromone mediated mating in <i>Saccharomyces cerevisiae</i> .....	17
Figure 1.3. Schematic diagram of the mating MAPK signaling cascade in <i>S. cerevisiae</i> . ....	19
Figure 2.1. Total expression levels of Ste2p mutants.....	62
Figure 2.2. MTSEA labeling of the N-terminal residues of Ste2p.....	67
Figure 2.3. Dimer formation by the Ste2p N-terminal Cysteine mutants.....	72
Figure 3.1. Diagram of Ste2p. ....	101
Figure 3.2. Schematic representation of the Ste2p mutants analyzed in this study.....	102
Figure 3.3. Ste2p total expression levels.....	103
Figure 3.4. Deglycosylation of N-terminal deletion mutants of Ste2p.....	107
Figure 3.5. Saturation binding of [ <sup>3</sup> H]α factor to various N-terminally deleted Ste2p.. ....	109
Figure 3.6. Growth arrest (halo) assays of wild type and deletion mutant receptors. Cells containing wild type Ste2p or cells with N-terminally truncated Ste2p were plated onto medium.....	111
Figure 3.7. Pheromone-induced <i>FUS1-LacZ</i> induction.....	113
Figure 3.8. Quantitative mating assay of the Ste2p mutants .....	115
Figure 3.9. Normalized <i>FUS1-LacZ</i> activity of each receptor construct as compared the wild type. ....	119
Figure 3.10. Ste2p expression level at the cell surface determined by flow Cytometry. ....	121
Figure 3.11. Signaling activities of the wild type receptor expressed at different levels... ..	123
Figure 4.1. Sequence alignments of pheromone α-factor receptors from different fungi..	149

<b>Figure 4.2. Diagram of Ste2p used in this study.....</b>	<b>150</b>
<b>Figure 4.3. Comparison of the expression levels and signaling activities of the WT and ICL1-Xa<sub>2</sub> receptor used in this study.....</b>	<b>151</b>
<b>Figure 4.4. (A) Ste2p expression levels of various Cys mutants. (B) Effect of reducing agent (β-mercaptoethanol) on dimerization. (C) Effect of ligand binding on dimerization.....</b>	<b>155</b>
<b>Figure 4.5. Effect of ligand binding on dimerization.....</b>	<b>161</b>
<b>Figure 4.6. Diagram showing the schematic of determination of intramolecular interaction using protease Factor Xa digestions followed by immunoblot detection using antibody against the C-terminal FLAG epitope tag. ....</b>	<b>163</b>
<b>Figure 4.7. Disulfide cross-linking and Factor Xa digestion.....</b>	<b>164</b>
<b>Figure 4.8. Ste2p dimer mediated by Y26 and its interaction with ECL1.....</b>	<b>168</b>

**Chapter 1**  
**General introduction**

## **G protein-coupled receptors: an overview**

Signal transduction is an essential biological process that is required to maintain cellular homeostasis and coordinated cellular activity in all organisms. The membrane proteins at the cell surface play crucial roles in these fundamental processes of communicating between the external and internal environment of the cell. The largest and most diverse membrane protein family on the cell surface is the G protein-coupled receptors (GPCRs) that are involved in nearly all important physiological processes in eukaryotic organisms (1). These proteins function by sensing an astonishing variety of extracellular signals, including photons, protons, ions, odorants, amino acids, nucleotides, steroids, fatty acids, proteins and peptides (2).

The GPCR family of proteins comprises approximately 4% of the encoded human genes corresponding to over 800 members (1,3-5). Modifications in the signaling of these receptors are pertinent for many pathological conditions including cardiovascular and pulmonary diseases, pain perception, obesity, cancer, and neurological disorders (1,6,7). In fact, GPCRs are considered one of the most successful therapeutic targets with more than 25% of all modern prescription drugs targeting these receptors (8-12). However, only a very small fraction of the known GPCRs are therapeutic targets. Many GPCRs remain 'orphan', which have not been assigned either ligands and/or functions. Even for many receptors whose ligands are known, there is a need for identifying alternate agonist and antagonist ligands. Regarding these facts, it is suggested that GPCRs will continue to be important drug targets of the future (1,13-15). Thus, the studies of GPCRs will contribute significantly to the understanding and treatment of a variety of diseases.

GPCRs share a common structural organization with an extracellular N-terminus, seven transmembrane domains connected by extracellular and intracellular loops, and a cytoplasmic C-

terminus (16-18). Despite the astounding diversity of their ligands, biological function and lack of strong sequence similarity, all GPCRs share common mechanisms of signal transduction. i.e., they couple the binding of ligands to the activation of specific heterotrimeric guanine nucleotide-binding proteins (G proteins) and/or non-G protein mediated signaling, leading to the modulation of downstream effector proteins and gene expression (19-22).

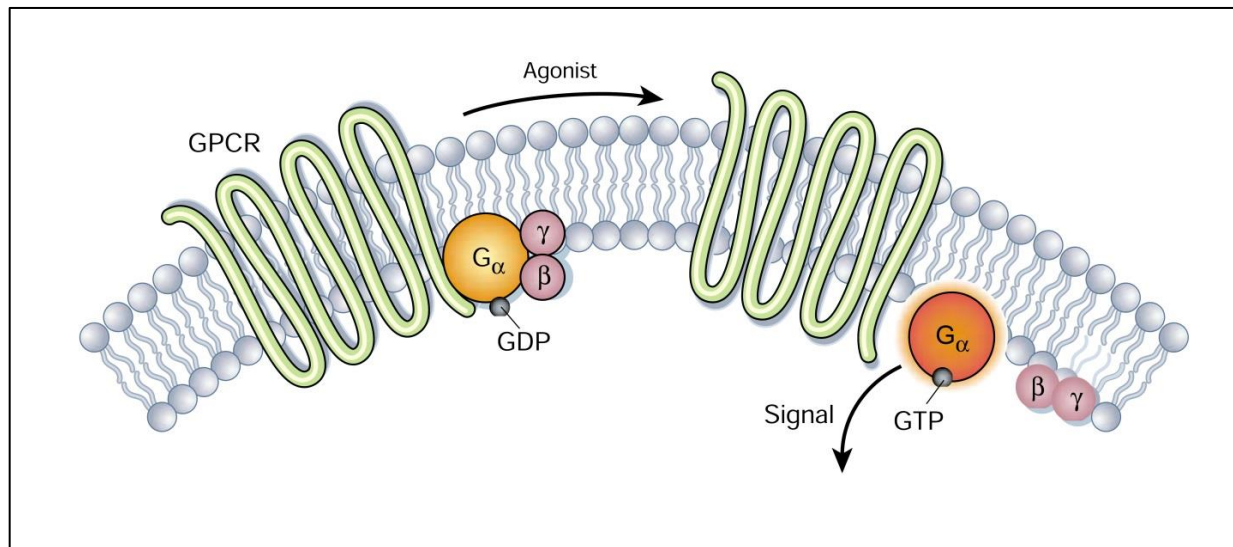


**Figure 1.1. Cartoon of a GPCR showing the seven transmembrane domains connected by alternating extracellular and intracellular loops. Agonist-binding activates the receptor triggering the exchange of GDP by GTP at the  $G\alpha$  subunit of the heterotrimeric G protein. This results in dissociation of the  $G\beta\gamma$  from the  $G\alpha$ . Both GTP-bound  $G\alpha$  and the released  $G\beta\gamma$  can mediate the stimulation or inhibition of intracellular effector proteins. (Taken from (23))**

Upon ligand binding, the receptor induces a conformational change in the intracellular heterotrimeric G proteins that act as molecular switch leading to intracellular responses. The G proteins are composed of three subunits ( $\alpha$ ,  $\beta\gamma$  dimer). For many GPCRs, activation leads to exchange of GDP by GTP on the  $G\alpha$ -subunit triggering the dissociation of the  $\alpha$ -subunit from the receptor and the  $\beta\gamma$  dimer (24). Both the GTP bound  $\alpha$ -subunit and the released  $\beta\gamma$ -dimer can

mediate the stimulation or inhibition of effector proteins such as enzymes and ion channels [e.g., adenylate cyclase, guanylyl cyclase, phospholipase C, mitogen-activated protein kinases (MAPKs), Ca<sup>2+</sup>, and K<sup>+</sup> channels]. Thus, stimulation of GPCRs with specific agonists results in changes in the concentration of second-messenger molecules (24). However, this general mechanism of signal transduction by GPCRs may be different in yeast.

## **Classification of GPCRs**

GPCRs have been organized into groups or classes based on different criteria including how their ligand binds, as well as physiological and structural features of the receptors. The most commonly used systems classify the GPCRs into 6 clans A, B, C, D, E, and F to include all GPCRs in animals and fungi based on sequence similarity in their transmembrane domains (25,26). Each clan is again divided into families based on common biochemical properties (**Table 1.1**). Human GPCRs have been recently classified into five families using a GRAFS (Glutamate, Rhodopsin, Adhesion, Frizzled/taste2, Secretin) system that is based on phylogenetic relationship in the transmembrane regions: rhodopsin (clan A), secretin (clan B), glutamate (clan C), adhesion, and frizzled/taste2 receptor families (4). Additionally, some GPCRs in humans could not be classified into any of the families, as sequences were very divergent. However, the other receptors clearly form five families as determined by the extensive phylogenetic analyses. Members of four of the five families all have long N termini. The exception is the members of the rhodopsin family; most members of the rhodopsin family have short N-termini, however there are instances of members with long N-terminal domains.

The rhodopsin family (class A) has the largest number of receptors. Currently, there are more than 700 receptors in this family as recognized by the IUPHAR database (International Union of basic and clinical PHARmacology, <http://www.iuphar-db.org/>) (27). The members of

the rhodopsin family share several characteristics. Most members of the rhodopsin family contain the NSxxNPxxY motif in transmembrane domain VII (TMVII), and the D(E)-R-Y(F) or “DRY” motif or at the border between transmembrane domain III (TMIII) and intracellular loop 2 (IL2). The ligands for most of the rhodopsin receptors bind within a cavity between the TM regions (28).

The receptors of the secretin family (class B – 55 receptors as recognized by the IUPHAR database (27)) bind large peptide ligands that share high sequence similarity and most often act in a paracrine manner. The N-termini of these receptors are long (~60 and 80 amino acids), and contain conserved Cys-Cys bridges that are important for ligand binding. This family consists of peptide and neuropeptide hormone receptors, such the secretin, calcitonin (CALC), vasoactive intestinal peptide (VIP), glucagon (GCG), parathyroid hormone (PTH), and pituitary adenylyl cyclase-activating protein (PACAP) receptors.

**Table 1.1. Sequence-based groupings within the G-protein-coupled receptors**

<b>Clan A: rhodopsin-like receptors</b>	
Family I	Olfactory receptors, adenosine receptors, melanocortin receptors, and others
Family II	Biogenic amine receptors
Family III	Vertebrate opsins and neuropeptide receptors
Family IV	Invertebrate opsins
Family V	Chemokine, chemotactic, somatostatin, opioids, and others
Family VI	Melatonin receptors and others
<b>Clan B: calcitonin and related receptors</b>	
Family I	Calcitonin, calcitonin-like, and CRF receptors
Family II	PTH/PTHrP receptors
Family III	Glucagon, secretin receptors and others
Family IV	Latrotoxin receptors and others
<b>Clan C: metabotropic glutamate and related receptors</b>	
Family I	Metabotropic glutamate receptors
Family II	Calcium receptors
Family III	GABA-B receptors
Family IV	Putative pheromone receptors
<b>Clan D: STE2 pheromone receptors</b>	
<b>Clan E: STE3 pheromone receptors</b>	
<b>Clan F: cAMP receptors and archaebacterial opsins</b>	

Table adapted from Flower (29)

The glutamate receptor family (class C) consists of eight metabotropic glutamate receptors (GRM), two gamma-aminobutyric acid (GABA) receptors (GABA<sub>B1</sub> GABA<sub>B2</sub>; functional GABA receptors contain both GABA<sub>B1</sub> and GABA<sub>B2</sub> subunits), a single calcium-sensing receptor (CASR), three receptors that are believed to be taste receptors (TAS1) and seven orphan receptors (27). All receptors of this family contain long N-terminus. In particular, the metabotropic glutamate receptors contain a very long N terminus (~280 to 580 amino acids) that forms two distinct lobes separated by a cavity in which glutamate binds, forming the so-called “Venus fly trap” where the glutamate causes the lobes to close around the ligand. The CASR also has a long, cysteine-rich N terminus, which is important for mediating calcium signaling, although it is not known if it is involved in Ca<sup>2+</sup> binding. The GABA receptors have a long N-terminus that contains the ligand-binding site but lacks the cysteine-rich domain found in the other receptors of this family. The TAS1 receptors are expressed in the tongue and believed to mediate taste signals. These receptors also have a long N terminus with a series of conserved Cys residues.

The members of the adhesion family of GPCRs contain N-termini of variable length (~200 to ~2800 amino acids) and are often rich in glycosylation sites and proline residues. The long N-termini of these GPCRs contain motifs that are likely to participate in cell adhesion (30,31).

The frizzled/taste2 receptor family includes two groups: the frizzled and the TAS2 receptors. There are several consensus motifs (IFL in TMII, SFLL in TMV, and SxKTL in TMVII) in the members of this family which are not found in the other four families. The TAS2 receptors are expressed in the tongue and palate epithelium, and are believed to function as bitter taste receptors (4). These receptors have a very short N terminus that is unlikely to contain a

ligand-binding domain. Members of the frizzled family of receptors have a long N-terminus (~200-amino acid) with conserved cysteines that are believed to be involved in ligand binding. The receptors of this family are responsible for controlling cell fate, proliferation, and polarity during metazoan development (4,32,33). Like other eukaryotic organisms, fungi also possess GPCRs that are responsible for sensing extracellular signals. Fungal GPCRs are described later in a separate section.

## GPCR Crystal Structures

Structural information for GPCRs is vital to understand how these signaling molecules carry out their function. This information is also essential for drug design and development. Although structures of a number of GPCRs have been obtained, information about the structure-function relationships of GPCRs is still in its infancy. (34-36). The methods available for use to gain structural information of proteins include X-ray crystallography, electron microscopy or diffraction, NMR spectroscopy and molecular modeling. All of these methods require high concentrations of purified protein. Additionally, crystallization and NMR require proteins in media that provide a good environment for study. In order to maintain their native structures, membrane proteins are required to be maintained in a lipid-like environment making the structural studies by crystallization and NMR more challenging. In fact, crystallization of GPCRs was one of the most challenging subjects in structural biology due to the poor natural abundance and high intrinsic flexibility of these membrane proteins. Bovine rhodopsin was the first GPCR to be crystallized about a decade ago by Palczewski *et al* (37). However, it took several years to solve the crystal structure of a second GPCR (beta 2 adrenergic receptor) in 2007 (38,39). Since then there has been almost an exponential growth in the number of solved structures due to the application of several innovative protein engineering techniques and crystallography methods. Currently there are 75 crystal structures of 18 GPCRs that have been solved (see Table 1.2 adapted from Maeda 2013) (40). These structures provide insights into the structural and functional diversity of these receptors and will be helpful to discover the molecular signatures of the GPCRs. These structures will also aid in understanding the molecular changes that occur during receptor activation. The structural data combined with data from the biophysical,

biochemical and computational studies will allow us to understand the structure-function relationships of GPCRs.

Due to the tremendous diversity of GPCRs and their involvement in so many pathways in the cell, there remains a huge potential for the development of drugs to ameliorate many diseases including neurological disorders, inflammatory diseases, cancer and metabolic imbalances. Therefore, structures of more GPCRs and understanding the molecular mechanism of receptor activation is important for fundamental biology as well as for improving human health by facilitating structure-based *in-silico* drug discovery and the development of drugs with improved specificity and pharmacodynamics.

**Table 1.2. GPCR structures solved in the 2000-2013 period**

<b>GPCR</b>	<b>Species</b>	<b>Year</b>	<b>PDB code</b>	<b>Reference</b>
Rhodopsin	Bovine	2000	1F88	(37)
$\beta$ 1 Adrenergic	Turkey	2008	2VT4	(41)
$\beta$ 2 Adrenergic	Human	2007	2R4R	(38)
D3 dopamine	Human	2010	3PBL	(42)
H1 histamine	Human	2011	3RZE	(43)
M2 muscarinic acetylcholine	Human	2012	3UON	(44)
M3 muscarinic acetylcholine	Rat	2012	4DAJ	(45)
A2A_Adenosine	Human	2008	3EML	(46)
Chemokine CXCR4	Human	2010	3ODU	(47)
Chemokine CXCR1	Human	2012	2LNL	(48)
$\mu$ -Opioid	Mouse	2012	4DKL	(49)
$\kappa$ -Opioid	Human	2012	4DJH	(50).
$\delta$ -Opioid	Mouse	2012	4EJ4	(51)
N/OFQ opioid	Human	2012	4EA3	(52)

**Table 1.2 continued**

<b>GPCR</b>	<b>Species</b>	<b>Year</b>	<b>PDB code</b>	<b>Reference</b>
Neurotensin receptor	Rat	2012	4GRV	(53)
PAR1	Human	2012	3VW7	(54)
Sphingosine 1-phosphate	Human	2012	3V2W	(55)
Smoothened	Human	2013	4JKV	(56)
Serotonin 5-HT <sub>1B</sub>	Human	2013	4IAR	(57)

Table adapted from Maeda (40).

### **Fungal GPCRs**

Like many other eukaryotic organisms, fungi also possess GPCRs that respond to extracellular signals to ensure proper cellular response. Although many GPCRs have been identified in different fungi, only a few were included in the GPCR classification system (A-F system, Table 1.1) described in the previous section (29). As a result, the fungal GPCRs have been categorized separately into six classes based on sequence homology and ligand sensing (**Table 1.3**). These are Ste2p-like pheromone receptors, Ste3p-like pheromone receptors,

carbon/amino acid receptor, putative nutrient receptor, cAMP receptor-like, and microbial opsin (22).

Although a number of GPCRs have been identified in fungi based on conserved sequences and structures, only a few are well studied. Specifically the *Saccharomyces cerevisiae* mating pheromone receptors Ste2p and Ste3p have been studied more extensively than the other GPCRs due to the availability of whole genome sequence and the ability to manipulate easily. In fact, the studies on *S. cerevisiae* GPCR system have considerably advanced our understanding the mating system at molecular level.

**Table 1.3. Six classes of GPCRs in fungi**

Species	Ste2-like pheromone receptor	Ste3-like pheromone receptor	Carbon/ amino acid receptor	Putative nutrient receptor	cAMP receptor-like	Microbial Opsin
<i>Saccharomyces cerevisiae</i>	Ste2	Ste3	Gpr1	SCRG_01312 SCRG_02823 SCRG_00179	–	–
<i>Schizosaccharomyces pombe</i>	Mam2	Map3	Git3	Stm1	–	–
<i>Candida albicans</i>	Ste2	Ste3	Gpr1	CAWG_02899 CAWG_06059 CAWG_02686	–	–
<i>Aspergillus nidulans</i>	GprA	GprB	GprC GprD GprE	GprF GprG AN5720	GprH GprI AN8262	AN3361
<i>Aspergillus fumigatus</i>	Afu3g14330	Afu5g07880	Afu7g04800	Afu5g04100 Afu1g06840 Afu1g11900	Afu3g01750 Afu5g04140 Afu3g00780	Afu7g01430
<i>Neurospora crassa</i>	Pre-2	Pre-1	Gpr-4	Gpr-5 Gpr-6	Gpr-1 Gpr-2 Gpr-3	Nop-1 ORP-1
<i>Magnaporthe grisea</i>	MGG_04711	MGG_06452	MGG_08803	MGG_04698 MGG_02855	MGG_06738	MGG_09015
<i>Cryptococcus neoformans</i>	–	Ste3a/Ste3a Cpr2	Gpr4	Gpr2 Gpr3	Gpr4 Gpr5	CNAG_03572 (Ops1)
<i>Ustilago maydis</i>	–	Pra1 Pra2	–	UM06006 UM01546	UM03423	UM02629 UM04125
<i>Coprinopsis cinerea</i>	–	Rcb1 Rcb2 Rcb3 CC1G_02129	–	CC1G_07132 CC1G_04180	CC1G_02288 CC1G_02310	–

Table adapted from Xue et. al. (22)

## ***S. cerevisiae* GPCRs**

GPCR studies using mammalian systems can be extremely complex due to cross-talk between different types of receptors and the assortment of G proteins present that can regulate multiple pathways. In contrast, the unicellular, genetically tractable eukaryotic organism *S. cerevisiae* provides a simple biological system with only a few GPCRs and G proteins (58,59). *S. cerevisiae* has only three GPCRs: Ste2p, Ste3p and Gpr1p. Ste2p and Ste3p are mating pheromone receptors and Gpr1p is a carbohydrate sensor. Although the pheromone and the carbohydrate sensing receptors share some downstream components, no cross-talk occurs between these two receptor systems as they couple to two different G proteins. The mitogen-activated protein kinase (MAPK) pathway activated by the GPCRs of this organism exhibits high homology to that of the mammalian system (60). In spite of little sequence similarity to the endogenous yeast GPCRs, several mammalian GPCRs were successfully expressed in yeast and were capable of activating the MAPK pathway (59,61,62). Yeast GPCRs have also been shown to exhibit signaling when expressed in mammalian cells (63).

*S. cerevisiae* exists as a haploid or diploid cell (64). The haploid cells exist as one of two mating types, *MATa* and *MAT $\alpha$* , which are distinguished by the expression of a set of genes involved in mating that are not expressed by the diploids. *MATa* cells express the GPCR Ste2p and the pheromone **a**-factor, a hydrophobic, farnesylated, carboxymethylated, dodecapeptide with the sequence YIIKGVFWDPAC(Farnesyl)-OCH<sub>3</sub>. *MAT $\alpha$*  cells express the GPCR Ste3p and the pheromone  $\alpha$ -factor, a tridecapeptide with the sequence WHWLQLKPGQPMY. The pheromones **a**- and  $\alpha$ -factor, bind to Ste3p and Ste2p, respectively, initiating the mating and eventual fusion of the two haploid cells resulting in a diploid cell (Figure 1.2). Pheromone binding causes a conformational change in the receptor that triggers the activation of the intracellular heterotrimeric G proteins consisting of Gpa1p ( $G_{\alpha}$ ), Ste4p ( $G_{\beta}$ ) and Ste18p ( $G_{\gamma}$ ) leading to the G1 cell cycle arrest, polarized growth, dissolution of the cell wall and membranes followed by cellular fusion (65). Receptor activation triggers the exchange of GDP with GTP at Gpa1p ( $G_{\alpha}$ ) subunit releasing the Ste4p/Ste18p ( $G_{\beta\gamma}$ ) dimer which in turn transmits the signal required for mating. The Gpa1p ( $G_{\alpha}$ ) may also promote signaling via the RNA binding protein

Scp160, although the mechanism is unknown (66).

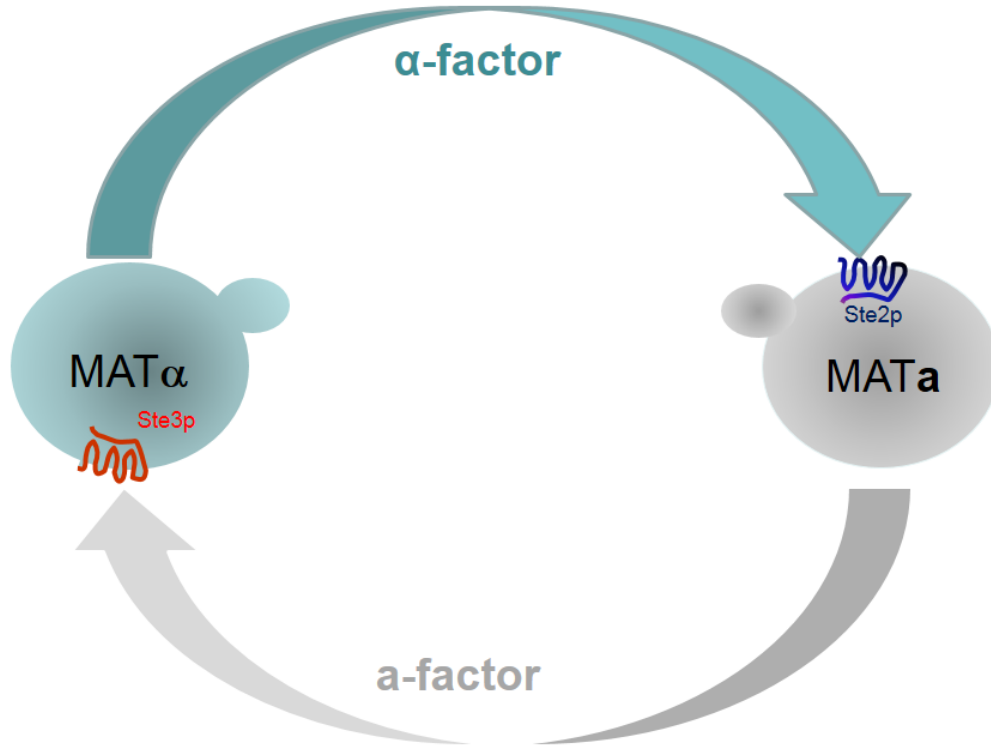


**Figure 1.2. Pheromone mediated mating in *Saccharomyces cerevisiae*. Schematic representation of the pheromone/receptor mediated communication between *MATa* and *MATa* haploid cells prior to mating. The  $\alpha$ -factor pheromone expressed by the *MATa* cells binds with Ste2p expressed on the cell surface of *MATa* cells. The a-factor pheromone expressed by the *MATa* cells binds with Ste3p expressed on the cell surface of *MATa* cells. Pheromone binding activates the receptors resulting in initiation of signaling involving the MAP kinase cascades, and activation of mating specific genes ultimately resulting in the fusion of the two haploid cells.**

The Ste4p/Ste18p complex transmits the signal to a mitogen-activated protein (MAP) kinase cascade through at least three effector proteins: (i) Ste20, a p21-activated protein kinase, (ii) Ste5, a scaffold protein that coordinates the MAPK pathway, and (iii) Far1, a protein involved in cell cycle control (65,67-69). Ste20 phosphorylates and activates Ste11 (MAPKKK), the first kinase in the MAPK pathway, which in turn drives a series of phosphorylation reactions involving Ste7 (MAPKK) and Fus3 (MAPK) (70,71). Phosphorylated Fus3 activates Ste12, the transcription factor required for the expression of mating genes. Fus3 also phosphorylates and inactivates Dig1 and Dig2, two negative regulators of the transcription factor Ste12 (65,72). The scaffold protein Ste5p serves to facilitate interactions among Ste11, Ste7 and Fus3 and delivers these proteins to the plasma membrane via its associated G protein  $\beta$  subunit (73-75). In addition, Ste5 has been shown to also limit cross-talk between alternative MAPK signaling pathways. Ste5 increases the affinity of Ste7 for Fus3 over Kss1 during response to pheromone. Ste7 preferentially targets the Kss1 kinase during filamentous growth (e.g., upon nitrogen starvation) (76). Fus3 phosphorylates and activates Far1 (72), which inhibits Cdc28-G1 cyclin complex thereby promoting cell cycle arrest (77). The transcriptional transactivator Ste12p binds to the pheromone response element (PRE) at the promoter region of target genes such as *FUS1*, *FUS2*, *FIG1*, *FIG2*, and *AGA1* that are induced for cell fusion (78). The two haploid cells of the opposite mating types form shmoo, (79) followed by degradation of the cell wall, plasma membrane and finally fusion of their nuclei to become one a/ $\alpha$  diploid zygote (80).

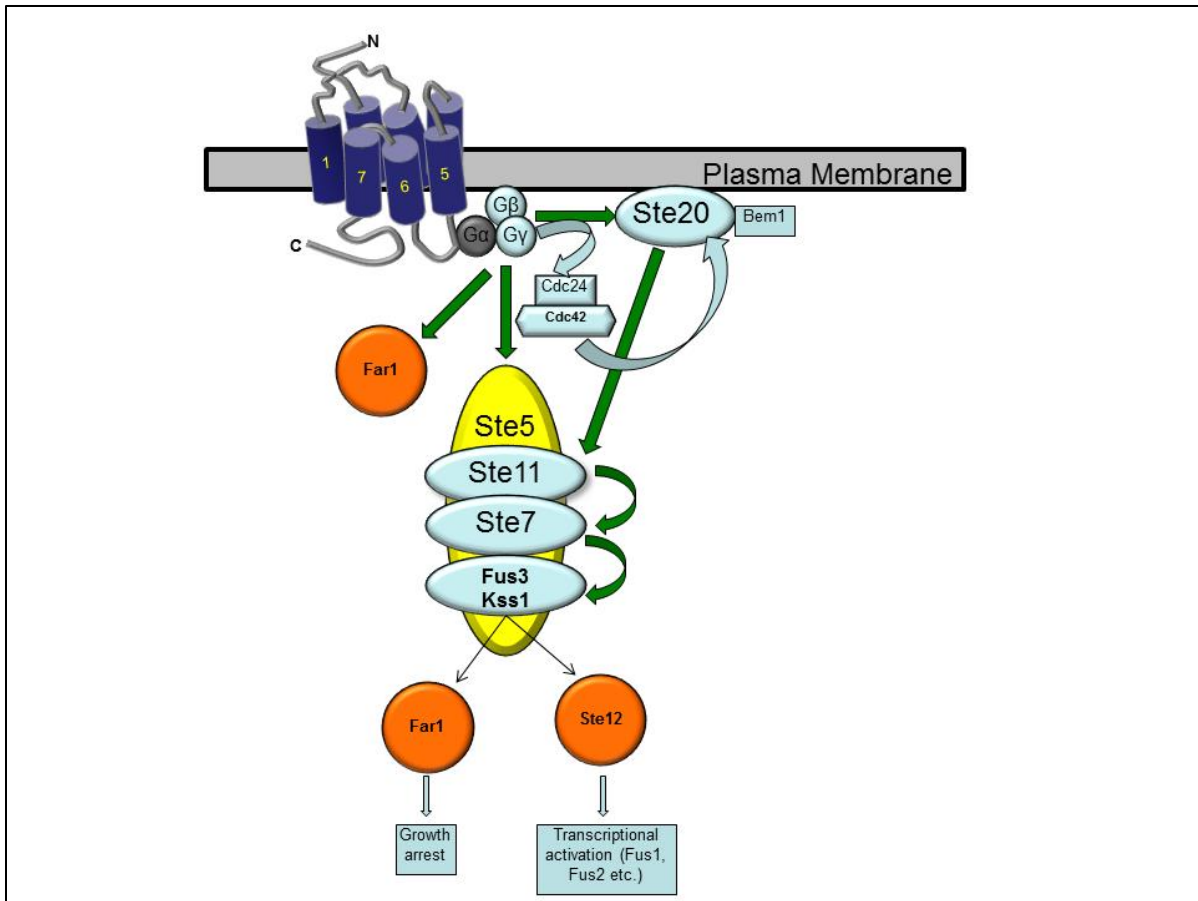


**Figure 1.3. Schematic diagram of the mating MAPK signaling cascade in *S. cerevisiae*.**

Activation of the pheromone receptor after binding with pheromone ( $\alpha$ -factor) leads to the exchange of GDP with GTP in the G protein  $\alpha$  subunit (Gpa1). This results in dissociation of G $\alpha$  from the G protein  $\beta\gamma$  subunits (Ste4 and Ste18). Free  $\beta\gamma$  activates a downstream signaling cascade through the guanine nucleotide exchange factor Cdc24, the protein kinase Ste20, and the kinase scaffold protein Ste5. The MAP kinase Fus3 phosphorylates and activates the transcription factor Ste12, resulting in new gene transcription

Like many other eukaryotic GPCRs, the mating pathway in yeast is highly regulated by several mechanisms. The extracellular protease Bar1p produced by the *MATa* cell cleaves  $\alpha$ -factor (81) allowing the cells to recover from  $\alpha$ -factor induced growth arrest. Sst2p, a member of the regulator of G-protein signaling (RGS) protein family, interferes with GTP-bound Gpa1p and down-regulates mating signal (82). Yeast casein kinases, Yck1p and Yck2p, are involved in budding morphogenesis and internalization of pheromone receptors (83). Yck-mediated phosphorylation of the mating receptors is required for vesicle trafficking at the cell membrane (84). Eventually phosphorylation at the C-terminus of the receptor leads to ubiquitination, internalization and degradation (85).

Taking advantage of the simplicity of the yeast system and the power of yeast genetics along with the low cost of yeast cell culture, the yeast GPCR system have enabled many researchers worldwide to use it as a model for structure-function analysis of GPCRs. Moreover, yeast GPCRs in a haploid cell can be replaced with a mammalian GPCR and the mating pathway can be activated. Heterologous expression of mammalian GPCRs in a yeast host has enabled researchers to develop cell-based functional assays in a eukaryotic system free from cross-talk with other GPCRs and can be used for ligand identification and pharmacological characterization (59,61,63).

### **The use of Ste2p as a model GPCR**

Ste2p, the  $\alpha$ -factor pheromone receptor of *S. cerevisiae*, shares common architectural organization of GPCRs with the signature seven transmembrane domains. Although there is no significant sequence homology across the members of the GPCR superfamily, their mechanism of signal transduction is thought to be similar. In fact, comparative analysis of two widely divergent GPCRs, Ste2p (a Class D GPCR) and rhodopsin (a Class A GPCR) exhibited several

similarities (20). For example, ligand binding occurs within the core of the 7TM helices (86-88); the third intracellular loop plays key roles in G protein activation (89-91); and the C-terminus is the target for desensitization by phosphorylation and ligand-mediated down-regulation by receptor endocytosis (92,93). In addition, conserved residues important for receptor function are located in TM1 and TM3 of both receptors. Strongly polar amino acids in Ste2p that mediate helix interactions are also located in similar positions in rhodopsin. Mutation of these residues leads to phenotypic changes such as loss of function or constitutive activity. In both receptors, small and weakly polar amino acids located in identical positions (TM domains) facilitate tight helix packing. Location of conserved amino acids and sites of constitutively active mutations are located in TM3, TM6 and TM7. Proline is essential at similar positions in TM6 and TM7. Thus these structure-function similarities provide strong support that the underlying mechanism of signal transduction in these receptors is similar.

Although there has been an explosion of X-ray crystal structures of GPCRs since 2007, X-ray crystallography of Ste2p is still not possible due to difficulties in obtaining sufficient amount of pure protein. As a result, structure-function information of Ste2p has been mainly obtained by mutational analysis. Substituted Cysteine Accessibility method (SCAM), modeling, and biophysical analysis have been used in several studies to obtain structural information for Ste2p. A recent study using SCAM proposed that the N-terminus has a  $\beta$ -strand between residues 20-30 and that this  $\beta$ -strand participates in homodimer formation (94). Another study using SCAM by Hauser et al. proposed that residues 106-114 in the EL1 form a  $3_{10}$  helix (95). More details describing the N-terminus and its role in dimerization of Ste2p will be discussed in chapter 2 of this dissertation. Modeling and biophysical studies by Akal-Strader et. al. predicted that the C-terminus of the EL1 comprising residues 126-135 contain two short  $\beta$ -strands (96).

The solvent accessibility of the several residues were also reported to change in a ligand-dependent manner. Hauser et. al. proposed that part of the EL1 is buried in a solvent-inaccessible environment and that this part interacts with the extracellular part of the transmembrane domains 5 and 6. Choi and Konopka (97) used SCAM to determine the TM boundaries. They proposed that TM domains of Ste2p vary in length and that some TM domains are tilted relative to the plane of the membrane in a manner similar to that described in the crystal structure of rhodopsin.

Ste2p is activated upon binding to the  $\alpha$ -factor pheromone (WHWLQLKPGQPMY), a 13-residue peptide. Analysis of  $\alpha$ -factor using alanine scanning mutagenesis studies indicated that residues near the N-terminus (Trp<sup>1</sup>-Leu<sup>4</sup>) of this peptide are involved in receptor activation and signal transduction, while residues near the C-terminus (Gln<sup>10</sup>-Tyr<sup>13</sup>) are associated with ligand binding (58,98). The central region consisting of residues Lys<sup>7</sup>-Gln<sup>10</sup> assumes a  $\beta$ -turn structure that has been shown to be critical for proper orientation of the signaling and the binding domains of the peptide (99-101). It was also demonstrated that deletion of the last two residues (Met<sup>12</sup>Tyr<sup>13</sup>) from the peptide results in a peptide that does not show any significant binding and does not block the binding of the full-length 13-residue peptide, but instead enhances the activity of the intact peptide. It was demonstrated that this 11-residue peptide (WHWLQLKPGQP) enhances the signaling activity of Ste2p when it is added to the wild type thereby acting as a synergist (102). It was also shown that deletion of the N-terminus results in a peptide that lowers the signaling activity of the full-length pheromone thereby acting as an antagonist (103). Thus studies with  $\alpha$ -factor suggested that three regions of the peptide play three different roles, each being dedicated to a certain function.

Cross-linking studies using unnatural amino acid p-benzoylphenylalanine (Bpa) at various positions of  $\alpha$ -factor indicated that residues Trp1, Trp3, Gln5 and Tyr13 residues of  $\alpha$ -factor interact

with residues at the extracellular ends of TM5-TM7 and portions of EL2 and EL3 close to these TMs (104). Several studies indicated that Tyr13 of  $\alpha$ -factor may interact directly with a region of Ste2p (Phe55-Arg58) at the extracellular end of TM1 (86,104,105). In studies using alanine scanning mutagenesis, Lee et al. showed that Tyr266 in the extracellular end of TM6 may be part of the ligand-binding pocket. Tyr266 recognizes the N-terminal portion of  $\alpha$ -factor, and upon ligand binding is involved in the transformation of Ste2p into an activated state (106). Later, Tyr266 was shown to interact with Asn205 (107,108). The 10<sup>th</sup> residue (Gln<sup>10</sup>) of  $\alpha$ -factor was shown to be adjacent to Ser47 and Thr48 of Ste2p (109). Studies by Bajaj et. al. using a fluorescent alpha-factor analogue fluorescent  $\alpha$ -factor analogue [ $K^7$ (NBD),Nle<sup>12</sup>] $\alpha$ -factor in conjunction with flow cytometry and fluorescence microscopy suggested that the  $\alpha$ -factor binds to the receptor in a two-step process: an initial interaction in which the ligand is placed in a hydrophobic environment followed by a conversion to a state in which the ligand moves to a more polar environment (110). Based on these studies a model of ligand binding to the receptor was suggested by our lab (58). According to this model, the  $\alpha$ -factor bends around the Gly<sup>9</sup>-Gln<sup>10</sup>-Pro<sup>11</sup> residues and carboxyl terminal residues Gln<sup>10</sup>-Pro<sup>11</sup>-Met<sup>12</sup>-Tyr<sup>13</sup> side chains of  $\alpha$ -factor interact with TM1 of the receptor while the N-terminal residues Trp<sup>1</sup> and Trp<sup>3</sup> side chains interact with a pocket formed by TM6-ECL3-TM7. (58).

Interactions among proteins play essential roles in the organization and function of cellular signaling. GPCRs have been considered to exist and function as monomers for many years. However, an increasing number of studies demonstrated that GPCRs are able to form dimers or higher order oligomers. Several studies reported that dimerization and /or oligomerization are often essential for modulation of receptor function (**Table 1.4**) (10,111-117).

**Table 1.4. Proposed roles of GPCR dimerisation/oligomerisation**

<b>Role of dimerisation/ oligomerisation</b>	<b>Receptor(s)</b>	<b>References</b>
Protein folding	$\beta_2$ -adrenoceptor	(118)
	CXCR1	(119)
	$\alpha_2$ -adrenoceptors	(120)
	TSH receptor	(121)
	Frizzled 4	(122)
	Calcium sensing receptor	(123)
	Melacortin-1 receptor	(124)
	CXCR1–CXCR2 hetero-dimer	(119)
Efficient signal transduction	Rhodopsin	(125,126)
	BLT1 leukotriene B4 receptor	(127)
G-protein selectivity (hetero-dimers)	MOP and DOP receptors	(128,129)
	D1 and D2 dopamine receptors	(130,131)
Signal alteration/modulation (hetero-dimers)	Orexin-1 receptor and cannabinoid CB1	(132)
	Melatonin MT1 and GPR50	(133)
	MrgD and MrgE	(134)
	DOP receptor and SNSR-4	(135)
	Somatostatin sst2a and sst3	(136)

**Table 1.4 continued**

<b>Role of dimerisation/ oligomerisation</b>	<b>Receptor(s)</b>	<b>References</b>
Control of physiological function (heterodimers)	DOP and KOP receptors	(137)
	Angiotensin AT <sub>1</sub> and Bradykinin B2	(138,139)
	Angiotensin AT <sub>1</sub> and Mas	(140,141)
	EP1 prostanoid receptor and $\beta$ 2-adrenoceptor	(142)
	Various adenosine and dopamine receptors	(143-146)
	Adenosine A <sub>1</sub> and A <sub>2A</sub>	(147)
	Dopamine D2 and cannabinoid CB1?	(148)

Table adapted from Milligan 2007 (111).

Ste2p has also been identified in oligomers in intact cells and membranes, although the functional significance of this oligomerization/dimerization is not clear. Gehret et. al. (149) used bioluminescence resonance energy transfer (BRET) to demonstrate that co-expressed Ste2p tagged with *Renilla* luciferase or a modified green fluorescent proteins co-oligomerize. Their study indicated that individual receptors that form oligomers do not act independently. In an analysis of Ste2p mutants using fluorescence resonance energy transfer (FRET) Overton and Blumer (150) demonstrated that the N-terminus, TM1 and TM2 mediate oligomerization of

Ste2p. Another study used disulfide cross-linking to demonstrate that TM1 and TM4 are dimer interfaces of Ste2p (151). These two transmembrane domains have also been reported to be dimer contacts in rhodopsin, a class A GPCR, providing evidence that structure and function are highly conserved across GPCRs (151). A study by Kim et. al. demonstrated that TM1 and TM7 of Ste2p also participate in dimerization. They demonstrated that the dimers formed by TM7 changes upon receptor activation (152). More recently, Umanah et al. demonstrated that IL3 of Ste2p also participates in the dimerization (153). Uddin et al. (94) demonstrated that the N-terminus of Ste2p also participates in Ste2p dimerization. Thus, several domains of Ste2p have been found to be associated with oligomerization/dimerization, although the precise, functional significance of this observation still unclear. In chapters 2, 3 and 4 of this dissertation, dimerization of Ste2p is discussed in more detail.

This dissertation describes the role of extracellular N-terminus of Ste2p and its interaction with extracellular loop 1. In Chapter 2, substituted Cysteine Accessibility Method (SCAM) was used to determine the solvent accessibility of the N-terminus. This chapter also discusses the possible structure of the N-terminus and its role in receptor dimerization. Chapter 3 describes the role of the N-terminus in receptor function. The interaction between the N-terminus and the extracellular loop 1 is discussed in Chapter 4. Finally, Chapter 5 is an overall evaluation of these studies and future directions. This experimental results presented in this dissertation will provide a better understanding of the structure of the N-terminus of Ste2p and how this structure plays a role in regulation of receptor function. Ultimately these studies will be aid in the understanding of structure-function relationships which regulate receptor signaling.

## References

1. O'Hayre, M., Vazquez-Prado, J., Kufareva, I., Stawiski, E. W., Handel, T. M., Seshagiri, S., and Gutkind, J. S. (2013) The emerging mutational landscape of G proteins and G-protein-coupled receptors in cancer. *Nature reviews. Cancer* **13**, 412-424
2. Maller, J. L. (2003) Signal transduction. Fishing at the cell surface. *Science* **300**, 594-595
3. Ding, X., Zhao, X., and Watts, A. (2013) G-protein-coupled receptor structure, ligand binding and activation as studied by solid-state NMR spectroscopy. *The Biochemical journal* **450**, 443-457
4. Fredriksson, R., Lagerstrom, M. C., Lundin, L. G., and Schioth, H. B. (2003) The G-protein-coupled receptors in the human genome form five main families. Phylogenetic analysis, paralogon groups, and fingerprints. *Molecular pharmacology* **63**, 1256-1272
5. Gloriam, D. E., Fredriksson, R., and Schioth, H. B. (2007) The G protein-coupled receptor subset of the rat genome. *BMC genomics* **8**, 338
6. Salon, J. A., Lodowski, D. T., and Palczewski, K. (2011) The significance of G protein-coupled receptor crystallography for drug discovery. *Pharmacological reviews* **63**, 901-937
7. Kobilka, B. K. (2011) Structural insights into adrenergic receptor function and pharmacology. *Trends in pharmacological sciences* **32**, 213-218
8. Klabunde, T., and Hessler, G. (2002) Drug design strategies for targeting G-protein-coupled receptors. *Chembiochem : a European journal of chemical biology* **3**, 928-944
9. Jacoby, E., Bouhelal, R., Gerspacher, M., and Seuwen, K. (2006) The 7 TM G-protein-coupled receptor target family. *ChemMedChem* **1**, 761-782

10. George, S. R., O'Dowd, B. F., and Lee, S. P. (2002) G-protein-coupled receptor oligomerization and its potential for drug discovery. *Nature reviews. Drug discovery* **1**, 808-820
11. Rask-Andersen, M., Almen, M. S., and Schioth, H. B. (2011) Trends in the exploitation of novel drug targets. *Nature reviews. Drug discovery* **10**, 579-590
12. Ma, P., and Zimmel, R. (2002) Value of novelty? *Nature reviews. Drug discovery* **1**, 571-572
13. Venter, J. C., Adams, M. D., Myers, et. al. (2001) The sequence of the human genome. *Science* **291**, 1304-1351
14. Wise, A., Gearing, K., and Rees, S. (2002) Target validation of G-protein coupled receptors. *Drug discovery today* **7**, 235-246
15. Hopkins, A. L., and Groom, C. R. (2002) The druggable genome. *Nature reviews. Drug discovery* **1**, 727-730
16. Kristiansen, K. (2004) Molecular mechanisms of ligand binding, signaling, and regulation within the superfamily of G-protein-coupled receptors: molecular modeling and mutagenesis approaches to receptor structure and function. *Pharmacology & therapeutics* **103**, 21-80
17. Gether, U. (2000) Uncovering molecular mechanisms involved in activation of G protein-coupled receptors. *Endocrine reviews* **21**, 90-113
18. Venkatakrisnan, A. J., Deupi, X., Lebon, G., Tate, C. G., Schertler, G. F., and Babu, M. M. (2013) Molecular signatures of G-protein-coupled receptors. *Nature* **494**, 185-194
19. Umanah, G. K., Huang, L., Ding, F. X., Arshava, B., Farley, A. R., Link, A. J., Naider, F., and Becker, J. M. (2010) Identification of residue-to-residue contact between a

- peptide ligand and its G protein-coupled receptor using periodate-mediated dihydroxyphenylalanine cross-linking and mass spectrometry. *The Journal of biological chemistry* **285**, 39425-39436
20. Eilers, M., Hornak, V., Smith, S. O., and Konopka, J. B. (2005) Comparison of class A and D G protein-coupled receptors: common features in structure and activation. *Biochemistry* **44**, 8959-8975
  21. Oldham, W. M., and Hamm, H. E. (2008) Heterotrimeric G protein activation by G-protein-coupled receptors. *Nature reviews. Molecular cell biology* **9**, 60-71
  22. Xue, C., Hsueh, Y. P., and Heitman, J. (2008) Magnificent seven: roles of G protein-coupled receptors in extracellular sensing in fungi. *FEMS microbiology reviews* **32**, 1010-1032
  23. Li, J., Ning, Y., Hedley, W., Saunders, B., Chen, Y., Tindill, N., Hannay, T., and Subramaniam, S. (2002) The Molecule Pages database. *Nature* **420**, 716-717
  24. Pierce, K. L., Premont, R. T., and Lefkowitz, R. J. (2002) Seven-transmembrane receptors. *Nature reviews. Molecular cell biology* **3**, 639-650
  25. Attwood, T. K., and Findlay, J. B. (1994) Fingerprinting G-protein-coupled receptors. *Protein engineering* **7**, 195-203
  26. Kolakowski, L. F., Jr. (1994) GCRDb: a G-protein-coupled receptor database. *Receptors & channels* **2**, 1-7
  27. Sharman, J. L., Benson, H. E., Pawson, A. J., Lukito, V., Mpamhanga, C. P., Bombail, V., Davenport, A. P., Peters, J. A., Spedding, M., Harmar, A. J., and Nc, I. (2013) IUPHAR-DB: updated database content and new features. *Nucleic acids research* **41**, D1083-1088

28. Baldwin, J. M. (1994) Structure and function of receptors coupled to G proteins. *Current opinion in cell biology* **6**, 180-190
29. Flower, D. R. (1999) Modelling G-protein-coupled receptors for drug design. *Biochimica et biophysica acta* **1422**, 207-234
30. McKnight, A. J., and Gordon, S. (1998) The EGF-TM7 family: unusual structures at the leukocyte surface. *Journal of leukocyte biology* **63**, 271-280
31. Stacey, M., Lin, H. H., Gordon, S., and McKnight, A. J. (2000) LNB-TM7, a group of seven-transmembrane proteins related to family-B G-protein-coupled receptors. *Trends in biochemical sciences* **25**, 284-289
32. Barnes, M. R., Duckworth, D. M., and Beeley, L. J. (1998) Frizzled proteins constitute a novel family of G protein-coupled receptors, most closely related to the secretin family. *Trends in pharmacological sciences* **19**, 399-400
33. Slusarski, D. C., Corces, V. G., and Moon, R. T. (1997) Interaction of Wnt and a Frizzled homologue triggers G-protein-linked phosphatidylinositol signalling. *Nature* **390**, 410-413
34. Rosenbaum, D. M., Rasmussen, S. G., and Kobilka, B. K. (2009) The structure and function of G-protein-coupled receptors. *Nature* **459**, 356-363
35. Lundstrom, K. (2009) An overview on GPCRs and drug discovery: structure-based drug design and structural biology on GPCRs. *Methods in molecular biology* **552**, 51-66
36. Ratnala, V. R., and Kobilka, B. (2009) Understanding the ligand-receptor-G protein ternary complex for GPCR drug discovery. *Methods in molecular biology* **552**, 67-77
37. Palczewski, K., Kumasaka, T., Hori, T., Behnke, C. A., Motoshima, H., Fox, B. A., Le Trong, I., Teller, D. C., Okada, T., Stenkamp, R. E., Yamamoto, M., and Miyano, M.

- (2000) Crystal structure of rhodopsin: A G protein-coupled receptor. *Science* **289**, 739-745
38. Rasmussen, S. G., Choi, H. J., Rosenbaum, D. M., Kobilka, T. S., Thian, F. S., Edwards, P. C., Burghammer, M., Ratnala, V. R., Sanishvili, R., Fischetti, R. F., Schertler, G. F., Weis, W. I., and Kobilka, B. K. (2007) Crystal structure of the human beta2 adrenergic G-protein-coupled receptor. *Nature* **450**, 383-387
39. Cherezov, V., Rosenbaum, D. M., Hanson, M. A., Rasmussen, S. G., Thian, F. S., Kobilka, T. S., Choi, H. J., Kuhn, P., Weis, W. I., Kobilka, B. K., and Stevens, R. C. (2007) High-resolution crystal structure of an engineered human beta2-adrenergic G protein-coupled receptor. *Science* **318**, 1258-1265
40. Maeda, S., and Schertler, G. F. (2013) Production of GPCR and GPCR complexes for structure determination. *Current opinion in structural biology*
41. Warne, T., Serrano-Vega, M. J., Baker, J. G., Moukhametzianov, R., Edwards, P. C., Henderson, R., Leslie, A. G., Tate, C. G., and Schertler, G. F. (2008) Structure of a beta1-adrenergic G-protein-coupled receptor. *Nature* **454**, 486-491
42. Chien, E. Y., Liu, W., Zhao, Q., Katritch, V., Han, G. W., Hanson, M. A., Shi, L., Newman, A. H., Javitch, J. A., Cherezov, V., and Stevens, R. C. (2010) Structure of the human dopamine D3 receptor in complex with a D2/D3 selective antagonist. *Science* **330**, 1091-1095
43. Shimamura, T., Shiroishi, M., Weyand, S., Tsujimoto, H., Winter, G., Katritch, V., Abagyan, R., Cherezov, V., Liu, W., Han, G. W., Kobayashi, T., Stevens, R. C., and Iwata, S. (2011) Structure of the human histamine H1 receptor complex with doxepin. *Nature* **475**, 65-70

44. Haga, K., Kruse, A. C., Asada, H., Yurugi-Kobayashi, T., Shiroishi, M., Zhang, C., Weis, W. I., Okada, T., Kobilka, B. K., Haga, T., and Kobayashi, T. (2012) Structure of the human M2 muscarinic acetylcholine receptor bound to an antagonist. *Nature* **482**, 547-551
45. Kruse, A. C., Hu, J., Pan, A. C., Arlow, D. H., Rosenbaum, D. M., Rosemond, E., Green, H. F., Liu, T., Chae, P. S., Dror, R. O., Shaw, D. E., Weis, W. I., Wess, J., and Kobilka, B. K. (2012) Structure and dynamics of the M3 muscarinic acetylcholine receptor. *Nature* **482**, 552-556
46. Jaakola, V. P., Griffith, M. T., Hanson, M. A., Cherezov, V., Chien, E. Y., Lane, J. R., Ijzerman, A. P., and Stevens, R. C. (2008) The 2.6 angstrom crystal structure of a human A2A adenosine receptor bound to an antagonist. *Science* **322**, 1211-1217
47. Wu, B., Chien, E. Y., Mol, C. D., Fenalti, G., Liu, W., Katritch, V., Abagyan, R., Brooun, A., Wells, P., Bi, F. C., Hamel, D. J., Kuhn, P., Handel, T. M., Cherezov, V., and Stevens, R. C. (2010) Structures of the CXCR4 chemokine GPCR with small-molecule and cyclic peptide antagonists. *Science* **330**, 1066-1071
48. Park, S. H., Das, B. B., Casagrande, F., Tian, Y., Nothnagel, H. J., Chu, M., Kiefer, H., Maier, K., De Angelis, A. A., Marassi, F. M., and Opella, S. J. (2012) Structure of the chemokine receptor CXCR1 in phospholipid bilayers. *Nature* **491**, 779-783
49. Manglik, A., Kruse, A. C., Kobilka, T. S., Thian, F. S., Mathiesen, J. M., Sunahara, R. K., Pardo, L., Weis, W. I., Kobilka, B. K., and Granier, S. (2012) Crystal structure of the micro-opioid receptor bound to a morphinan antagonist. *Nature* **485**, 321-326
50. Wu, H., Wacker, D., Mileni, M., Katritch, V., Han, G. W., Vardy, E., Liu, W., Thompson, A. A., Huang, X. P., Carroll, F. I., Mascarella, S. W., Westkaemper, R. B.,

- Mosier, P. D., Roth, B. L., Cherezov, V., and Stevens, R. C. (2012) Structure of the human kappa-opioid receptor in complex with JDTic. *Nature* **485**, 327-332
51. Granier, S., Manglik, A., Kruse, A. C., Kobilka, T. S., Thian, F. S., Weis, W. I., and Kobilka, B. K. (2012) Structure of the delta-opioid receptor bound to naltrindole. *Nature* **485**, 400-404
52. Thompson, A. A., Liu, W., Chun, E., Katritch, V., Wu, H., Vardy, E., Huang, X. P., Trapella, C., Guerrini, R., Calo, G., Roth, B. L., Cherezov, V., and Stevens, R. C. (2012) Structure of the nociceptin/orphanin FQ receptor in complex with a peptide mimetic. *Nature* **485**, 395-399
53. White, J. F., Noinaj, N., Shibata, Y., Love, J., Kloss, B., Xu, F., Gvozdenovic-Jeremic, J., Shah, P., Shiloach, J., Tate, C. G., and Grisshammer, R. (2012) Structure of the agonist-bound neurotensin receptor. *Nature* **490**, 508-513
54. Zhang, C., Srinivasan, Y., Arlow, D. H., Fung, J. J., Palmer, D., Zheng, Y., Green, H. F., Pandey, A., Dror, R. O., Shaw, D. E., Weis, W. I., Coughlin, S. R., and Kobilka, B. K. (2012) High-resolution crystal structure of human protease-activated receptor 1. *Nature* **492**, 387-392
55. Hanson, M. A., Roth, C. B., Jo, E., Griffith, M. T., Scott, F. L., Reinhart, G., Desale, H., Clemons, B., Cahalan, S. M., Schuerer, S. C., Sanna, M. G., Han, G. W., Kuhn, P., Rosen, H., and Stevens, R. C. (2012) Crystal structure of a lipid G protein-coupled receptor. *Science* **335**, 851-855
56. Wang, C., Wu, H., Katritch, V., Han, G. W., Huang, X. P., Liu, W., Siu, F. Y., Roth, B. L., Cherezov, V., and Stevens, R. C. (2013) Structure of the human smoothed receptor bound to an antitumour agent. *Nature* **497**, 338-343

57. Wang, C., Jiang, Y., Ma, J., Wu, H., Wacker, D., Katritch, V., Han, G. W., Liu, W., Huang, X. P., Vardy, E., McCorvy, J. D., Gao, X., Zhou, X. E., Melcher, K., Zhang, C., Bai, F., Yang, H., Yang, L., Jiang, H., Roth, B. L., Cherezov, V., Stevens, R. C., and Xu, H. E. (2013) Structural basis for molecular recognition at serotonin receptors. *Science* **340**, 610-614
58. Naider, F., and Becker, J. M. (2004) The alpha-factor mating pheromone of *Saccharomyces cerevisiae*: a model for studying the interaction of peptide hormones and G protein-coupled receptors. *Peptides* **25**, 1441-1463
59. Minic, J., Sautel, M., Salesse, R., and Pajot-Augy, E. (2005) Yeast system as a screening tool for pharmacological assessment of g protein coupled receptors. *Current medicinal chemistry* **12**, 961-969
60. Thalhauser, C. J., and Komarova, N. L. (2010) Signal response sensitivity in the yeast mitogen-activated protein kinase cascade. *PloS one* **5**, e11568
61. Dowell, S. J., and Brown, A. J. (2009) Yeast assays for G protein-coupled receptors. *Methods in molecular biology* **552**, 213-229
62. King, K., Dohlman, H. G., Thorner, J., Caron, M. G., and Lefkowitz, R. J. (1990) Control of yeast mating signal transduction by a mammalian beta 2-adrenergic receptor and Gs alpha subunit. *Science* **250**, 121-123
63. Yin, D., Gavi, S., Shumay, E., Duell, K., Konopka, J. B., Malbon, C. C., and Wang, H. Y. (2005) Successful expression of a functional yeast G-protein-coupled receptor (Ste2) in mammalian cells. *Biochemical and biophysical research communications* **329**, 281-287

64. Sprague, G. F., Jr., Jensen, R., and Herskowitz, I. (1983) Control of yeast cell type by the mating type locus: positive regulation of the alpha-specific STE3 gene by the MAT alpha 1 product. *Cell* **32**, 409-415
65. Bardwell, L. (2005) A walk-through of the yeast mating pheromone response pathway. *Peptides* **26**, 339-350
66. Guo, M., Aston, C., Burchett, S. A., Dyke, C., Fields, S., Rajarao, S. J., Uetz, P., Wang, Y., Young, K., and Dohlman, H. G. (2003) The yeast G protein alpha subunit Gpa1 transmits a signal through an RNA binding effector protein Scp160. *Molecular cell* **12**, 517-524
67. Chen, R. E., and Thorner, J. (2007) Function and regulation in MAPK signaling pathways: lessons learned from the yeast *Saccharomyces cerevisiae*. *Biochimica et biophysica acta* **1773**, 1311-1340
68. Jones, S. K., Jr., and Bennett, R. J. (2011) Fungal mating pheromones: choreographing the dating game. *Fungal genetics and biology : FG & B* **48**, 668-676
69. Hoffman, C. S. (2005) Except in every detail: comparing and contrasting G-protein signaling in *Saccharomyces cerevisiae* and *Schizosaccharomyces pombe*. *Eukaryotic cell* **4**, 495-503
70. Zhou, Z., Gartner, A., Cade, R., Ammerer, G., and Errede, B. (1993) Pheromone-induced signal transduction in *Saccharomyces cerevisiae* requires the sequential function of three protein kinases. *Molecular and cellular biology* **13**, 2069-2080
71. Choi, K. Y., Satterberg, B., Lyons, D. M., and Elion, E. A. (1994) Ste5 tethers multiple protein kinases in the MAP kinase cascade required for mating in *S. cerevisiae*. *Cell* **78**, 499-512

72. Elion, E. A., Satterberg, B., and Kranz, J. E. (1993) FUS3 phosphorylates multiple components of the mating signal transduction cascade: evidence for STE12 and FAR1. *Molecular biology of the cell* **4**, 495-510
73. Printen, J. A., and Sprague, G. F., Jr. (1994) Protein-protein interactions in the yeast pheromone response pathway: Ste5p interacts with all members of the MAP kinase cascade. *Genetics* **138**, 609-619
74. Flotho, A., Simpson, D. M., Qi, M., and Elion, E. A. (2004) Localized feedback phosphorylation of Ste5p scaffold by associated MAPK cascade. *The Journal of biological chemistry* **279**, 47391-47401
75. Whiteway, M. S., Wu, C., Leeuw, T., Clark, K., Fourest-Lieuvin, A., Thomas, D. Y., and Leberer, E. (1995) Association of the yeast pheromone response G protein beta gamma subunits with the MAP kinase scaffold Ste5p. *Science* **269**, 1572-1575
76. Good, M., Tang, G., Singleton, J., Remenyi, A., and Lim, W. A. (2009) The Ste5 scaffold directs mating signaling by catalytically unlocking the Fus3 MAP kinase for activation. *Cell* **136**, 1085-1097
77. Olson, K. A., Nelson, C., Tai, G., Hung, W., Yong, C., Astell, C., and Sadowski, I. (2000) Two regulators of Ste12p inhibit pheromone-responsive transcription by separate mechanisms. *Molecular and cellular biology* **20**, 4199-4209
78. Bardwell, L. (2004) A walk-through of the yeast mating pheromone response pathway. *Peptides* **25**, 1465-1476
79. Melloy, P., Shen, S., White, E., McIntosh, J. R., and Rose, M. D. (2007) Nuclear fusion during yeast mating occurs by a three-step pathway. *The Journal of cell biology* **179**, 659-670

80. Philips, J., and Herskowitz, I. (1997) Osmotic balance regulates cell fusion during mating in *Saccharomyces cerevisiae*. *The Journal of cell biology* **138**, 961-974
81. MacKay, V. L., Welch, S. K., Insley, M. Y., Manney, T. R., Holly, J., Saari, G. C., and Parker, M. L. (1988) The *Saccharomyces cerevisiae* BAR1 gene encodes an exported protein with homology to pepsin. *Proceedings of the National Academy of Sciences of the United States of America* **85**, 55-59
82. Dohlman, H. G., Song, J., Ma, D., Courchesne, W. E., and Thorner, J. (1996) Sst2, a negative regulator of pheromone signaling in the yeast *Saccharomyces cerevisiae*: expression, localization, and genetic interaction and physical association with Gpa1 (the G-protein alpha subunit). *Molecular and cellular biology* **16**, 5194-5209
83. Babu, P., Bryan, J. D., Panek, H. R., Jordan, S. L., Forbrich, B. M., Kelley, S. C., Colvin, R. T., and Robinson, L. C. (2002) Plasma membrane localization of the Yck2p yeast casein kinase 1 isoform requires the C-terminal extension and secretory pathway function. *Journal of cell science* **115**, 4957-4968
84. Panek, H. R., Stepp, J. D., Engle, H. M., Marks, K. M., Tan, P. K., Lemmon, S. K., and Robinson, L. C. (1997) Suppressors of YCK-encoded yeast casein kinase 1 deficiency define the four subunits of a novel clathrin AP-like complex. *The EMBO journal* **16**, 4194-4204
85. Dohlman, H. G., and Thorner, J. W. (2001) Regulation of G protein-initiated signal transduction in yeast: paradigms and principles. *Annual review of biochemistry* **70**, 703-754
86. Henry, L. K., Khare, S., Son, C., Babu, V. V., Naider, F., and Becker, J. M. (2002) Identification of a contact region between the tridecapeptide alpha-factor mating

- pheromone of *Saccharomyces cerevisiae* and its G protein-coupled receptor by photoaffinity labeling. *Biochemistry* **41**, 6128-6139
87. Lin, J. C., Duell, K., and Konopka, J. B. (2004) A microdomain formed by the extracellular ends of the transmembrane domains promotes activation of the G protein-coupled alpha-factor receptor. *Molecular and cellular biology* **24**, 2041-2051
88. Chen, S., Lin, F., Xu, M., Riek, R. P., Novotny, J., and Graham, R. M. (2002) Mutation of a single TMVI residue, Phe(282), in the beta(2)-adrenergic receptor results in structurally distinct activated receptor conformations. *Biochemistry* **41**, 6045-6053
89. O'Dowd, B. F., Hnatowich, M., Regan, J. W., Leader, W. M., Caron, M. G., and Lefkowitz, R. J. (1988) Site-directed mutagenesis of the cytoplasmic domains of the human beta 2-adrenergic receptor. Localization of regions involved in G protein-receptor coupling. *The Journal of biological chemistry* **263**, 15985-15992
90. Schandel, K. A., and Jenness, D. D. (1994) Direct evidence for ligand-induced internalization of the yeast alpha-factor pheromone receptor. *Molecular and cellular biology* **14**, 7245-7255
91. Stefan, C. J., and Blumer, K. J. (1994) The third cytoplasmic loop of a yeast G-protein-coupled receptor controls pathway activation, ligand discrimination, and receptor internalization. *Molecular and cellular biology* **14**, 3339-3349
92. Chen, Q., and Konopka, J. B. (1996) Regulation of the G-protein-coupled alpha-factor pheromone receptor by phosphorylation. *Molecular and cellular biology* **16**, 247-257
93. Hicke, L., and Riezman, H. (1996) Ubiquitination of a yeast plasma membrane receptor signals its ligand-stimulated endocytosis. *Cell* **84**, 277-287

94. Uddin, M. S., Kim, H., Deyo, A., Naider, F., and Becker, J. M. (2012) Identification of residues involved in homodimer formation located within a beta-strand region of the N-terminus of a Yeast G protein-coupled receptor. *Journal of receptor and signal transduction research* **32**, 65-75
95. Hauser, M., Kauffman, S., Lee, B. K., Naider, F., and Becker, J. M. (2007) The first extracellular loop of the *Saccharomyces cerevisiae* G protein-coupled receptor Ste2p undergoes a conformational change upon ligand binding. *The Journal of biological chemistry* **282**, 10387-10397
96. Akal-Strader, A., Khare, S., Xu, D., Naider, F., and Becker, J. M. (2002) Residues in the first extracellular loop of a G protein-coupled receptor play a role in signal transduction. *The Journal of biological chemistry* **277**, 30581-30590
97. Choi, Y., and Konopka, J. B. (2006) Accessibility of cysteine residues substituted into the cytoplasmic regions of the alpha-factor receptor identifies the intracellular residues that are available for G protein interaction. *Biochemistry* **45**, 15310-15317
98. Abel, M. G., Zhang, Y. L., Lu, H. F., Naider, F., and Becker, J. M. (1998) Structure-function analysis of the *Saccharomyces cerevisiae* tridecapeptide pheromone using alanine-scanned analogs. *The journal of peptide research : official journal of the American Peptide Society* **52**, 95-106
99. Xue, C. B., Eriotou-Bargiota, E., Miller, D., Becker, J. M., and Naider, F. (1989) A covalently constrained congener of the *Saccharomyces cerevisiae* tridecapeptide mating pheromone is an agonist. *The Journal of biological chemistry* **264**, 19161-19168

100. Antohi, O., Marepalli, H. R., Yang, W., Becker, J. M., and Naider, F. (1998) Conformational analysis of cyclic analogues of the *Saccharomyces cerevisiae* alpha-factor pheromone. *Biopolymers* **45**, 21-34
101. Zhang, Y. L., Marepalli, H. R., Lu, H. F., Becker, J. M., and Naider, F. (1998) Synthesis, biological activity, and conformational analysis of peptidomimetic analogues of the *Saccharomyces cerevisiae* alpha-factor tridecapeptide. *Biochemistry* **37**, 12465-12476
102. Eriotou-Bargiota, E., Xue, C. B., Naider, F., and Becker, J. M. (1992) Antagonistic and synergistic peptide analogues of the tridecapeptide mating pheromone of *Saccharomyces cerevisiae*. *Biochemistry* **31**, 551-557
103. Liu, S., Henry, L. K., Lee, B. K., Wang, S. H., Arshava, B., Becker, J. M., and Naider, F. (2000) Position 13 analogs of the tridecapeptide mating pheromone from *Saccharomyces cerevisiae*: design of an iodinated ligand for receptor binding. *The journal of peptide research : official journal of the American Peptide Society* **56**, 24-34
104. Son, C. D., Sargsyan, H., Naider, F., and Becker, J. M. (2004) Identification of ligand binding regions of the *Saccharomyces cerevisiae* alpha-factor pheromone receptor by photoaffinity cross-linking. *Biochemistry* **43**, 13193-13203
105. Son, C. D., Sargsyan, H., Hurst, G. B., Naider, F., and Becker, J. M. (2005) Analysis of ligand-receptor cross-linked fragments by mass spectrometry. *The journal of peptide research : official journal of the American Peptide Society* **65**, 418-426
106. Lee, B. K., Lee, Y. H., Hauser, M., Son, C. D., Khare, S., Naider, F., and Becker, J. M. (2002) Tyr266 in the sixth transmembrane domain of the yeast alpha-factor receptor plays key roles in receptor activation and ligand specificity. *Biochemistry* **41**, 13681-13689

107. Lee, Y. H., Naider, F., and Becker, J. M. (2006) Interacting residues in an activated state of a G protein-coupled receptor. *The Journal of biological chemistry* **281**, 2263-2272
108. Naider, F., Becker, J. M., Lee, Y. H., and Horovitz, A. (2007) Double-mutant cycle scanning of the interaction of a peptide ligand and its G protein-coupled receptor. *Biochemistry* **46**, 3476-3481
109. Lee, B. K., Khare, S., Naider, F., and Becker, J. M. (2001) Identification of residues of the *Saccharomyces cerevisiae* G protein-coupled receptor contributing to alpha-factor pheromone binding. *The Journal of biological chemistry* **276**, 37950-37961
110. Bajaj, A., Celic, A., Ding, F. X., Naider, F., Becker, J. M., and Dumont, M. E. (2004) A fluorescent alpha-factor analogue exhibits multiple steps on binding to its G protein coupled receptor in yeast. *Biochemistry* **43**, 13564-13578
111. Milligan, G. (2007) G protein-coupled receptor dimerisation: molecular basis and relevance to function. *Biochimica et biophysica acta* **1768**, 825-835
112. Bouvier, M. (2001) Oligomerization of G-protein-coupled transmitter receptors. *Nature reviews. Neuroscience* **2**, 274-286
113. Devi, L. A. (2001) Heterodimerization of G-protein-coupled receptors: pharmacology, signaling and trafficking. *Trends in pharmacological sciences* **22**, 532-537
114. Milligan, G. (2004) G protein-coupled receptor dimerization: function and ligand pharmacology. *Molecular pharmacology* **66**, 1-7
115. Milligan, G. (2008) A day in the life of a G protein-coupled receptor: the contribution to function of G protein-coupled receptor dimerization. *British journal of pharmacology* **153 Suppl 1**, S216-229

116. Maurice, P., Kamal, M., and Jockers, R. (2011) Asymmetry of GPCR oligomers supports their functional relevance. *Trends in pharmacological sciences* **32**, 514-520
117. Ferre, S., Ciruela, F., Woods, A. S., Lluís, C., and Franco, R. (2007) Functional relevance of neurotransmitter receptor heteromers in the central nervous system. *Trends in neurosciences* **30**, 440-446
118. Salahpour, A., Angers, S., Mercier, J. F., Lagace, M., Marullo, S., and Bouvier, M. (2004) Homodimerization of the beta2-adrenergic receptor as a prerequisite for cell surface targeting. *The Journal of biological chemistry* **279**, 33390-33397
119. Wilson, S., Wilkinson, G., and Milligan, G. (2005) The CXCR1 and CXCR2 receptors form constitutive homo- and heterodimers selectively and with equal apparent affinities. *The Journal of biological chemistry* **280**, 28663-28674
120. Zhou, F., Filipeanu, C. M., Duvernay, M. T., and Wu, G. (2006) Cell-surface targeting of alpha2-adrenergic receptors -- inhibition by a transport deficient mutant through dimerization. *Cellular signalling* **18**, 318-327
121. Calebiro, D., de Filippis, T., Lucchi, S., Covino, C., Panigone, S., Beck-Peccoz, P., Dunlap, D., and Persani, L. (2005) Intracellular entrapment of wild-type TSH receptor by oligomerization with mutants linked to dominant TSH resistance. *Human molecular genetics* **14**, 2991-3002
122. Kaykas, A., Yang-Snyder, J., Heroux, M., Shah, K. V., Bouvier, M., and Moon, R. T. (2004) Mutant Frizzled 4 associated with vitreoretinopathy traps wild-type Frizzled in the endoplasmic reticulum by oligomerization. *Nature cell biology* **6**, 52-58
123. Pidasheva, S., Grant, M., Canaff, L., Ercan, O., Kumar, U., and Hendy, G. N. (2006) Calcium-sensing receptor dimerizes in the endoplasmic reticulum: biochemical and

- biophysical characterization of CASR mutants retained intracellularly. *Human molecular genetics* **15**, 2200-2209
124. Sanchez-Laorden, B. L., Sanchez-Mas, J., Martinez-Alonso, E., Martinez-Menarguez, J. A., Garcia-Borron, J. C., and Jimenez-Cervantes, C. (2006) Dimerization of the human melanocortin 1 receptor: functional consequences and dominant-negative effects. *The Journal of investigative dermatology* **126**, 172-181
125. Fotiadis, D., Jastrzebska, B., Philippsen, A., Muller, D. J., Palczewski, K., and Engel, A. (2006) Structure of the rhodopsin dimer: a working model for G-protein-coupled receptors. *Current opinion in structural biology* **16**, 252-259
126. Fotiadis, D., Liang, Y., Filipek, S., Saperstein, D. A., Engel, A., and Palczewski, K. (2004) The G protein-coupled receptor rhodopsin in the native membrane. *FEBS letters* **564**, 281-288
127. Baneres, J. L., and Parello, J. (2003) Structure-based analysis of GPCR function: evidence for a novel pentameric assembly between the dimeric leukotriene B4 receptor BLT1 and the G-protein. *Journal of molecular biology* **329**, 815-829
128. George, S. R., Fan, T., Xie, Z., Tse, R., Tam, V., Varghese, G., and O'Dowd, B. F. (2000) Oligomerization of mu- and delta-opioid receptors. Generation of novel functional properties. *The Journal of biological chemistry* **275**, 26128-26135
129. Fan, T., Varghese, G., Nguyen, T., Tse, R., O'Dowd, B. F., and George, S. R. (2005) A role for the distal carboxyl tails in generating the novel pharmacology and G protein activation profile of mu and delta opioid receptor hetero-oligomers. *The Journal of biological chemistry* **280**, 38478-38488

130. So, C. H., Varghese, G., Curley, K. J., Kong, M. M., Alijaniam, M., Ji, X., Nguyen, T., O'Dowd B, F., and George, S. R. (2005) D1 and D2 dopamine receptors form heterooligomers and cointernalize after selective activation of either receptor. *Molecular pharmacology* **68**, 568-578
131. Lee, S. P., So, C. H., Rashid, A. J., Varghese, G., Cheng, R., Lanca, A. J., O'Dowd, B. F., and George, S. R. (2004) Dopamine D1 and D2 receptor Co-activation generates a novel phospholipase C-mediated calcium signal. *The Journal of biological chemistry* **279**, 35671-35678
132. Hilairret, S., Bouaboula, M., Carriere, D., Le Fur, G., and Casellas, P. (2003) Hypersensitization of the Orexin 1 receptor by the CB1 receptor: evidence for cross-talk blocked by the specific CB1 antagonist, SR141716. *The Journal of biological chemistry* **278**, 23731-23737
133. Levoye, A., Dam, J., Ayoub, M. A., Guillaume, J. L., Couturier, C., Delagrang, P., and Jockers, R. (2006) The orphan GPR50 receptor specifically inhibits MT1 melatonin receptor function through heterodimerization. *The EMBO journal* **25**, 3012-3023
134. Milasta, S., Pediani, J., Appelbe, S., Trim, S., Wyatt, M., Cox, P., Fidock, M., and Milligan, G. (2006) Interactions between the Mas-related receptors MrgD and MrgE alter signalling and trafficking of MrgD. *Molecular pharmacology* **69**, 479-491
135. Breit, A., Gagnidze, K., Devi, L. A., Lagace, M., and Bouvier, M. (2006) Simultaneous activation of the delta opioid receptor (deltaOR)/sensory neuron-specific receptor-4 (SNSR-4) hetero-oligomer by the mixed bivalent agonist bovine adrenal medulla peptide 22 activates SNSR-4 but inhibits deltaOR signaling. *Molecular pharmacology* **70**, 686-696

136. Pfeiffer, M., Koch, T., Schroder, H., Klutzny, M., Kirscht, S., Kreienkamp, H. J., Holtt, V., and Schulz, S. (2001) Homo- and heterodimerization of somatostatin receptor subtypes. Inactivation of sst(3) receptor function by heterodimerization with sst(2A). *The Journal of biological chemistry* **276**, 14027-14036
137. Waldhoer, M., Fong, J., Jones, R. M., Lunzer, M. M., Sharma, S. K., Kostenis, E., Portoghese, P. S., and Whistler, J. L. (2005) A heterodimer-selective agonist shows in vivo relevance of G protein-coupled receptor dimers. *Proceedings of the National Academy of Sciences of the United States of America* **102**, 9050-9055
138. AbdAlla, S., Abdel-Baset, A., Lothar, H., el Massiery, A., and Quitterer, U. (2005) Mesangial AT1/B2 receptor heterodimers contribute to angiotensin II hyperresponsiveness in experimental hypertension. *Journal of molecular neuroscience : MN* **26**, 185-192
139. AbdAlla, S., Lothar, H., el Massiery, A., and Quitterer, U. (2001) Increased AT(1) receptor heterodimers in preeclampsia mediate enhanced angiotensin II responsiveness. *Nature medicine* **7**, 1003-1009
140. Kostenis, E., Milligan, G., Christopoulos, A., Sanchez-Ferrer, C. F., Heringer-Walther, S., Sexton, P. M., Gembardt, F., Kellett, E., Martini, L., Vanderheyden, P., Schultheiss, H. P., and Walther, T. (2005) G-protein-coupled receptor Mas is a physiological antagonist of the angiotensin II type 1 receptor. *Circulation* **111**, 1806-1813
141. Canals, M., Jenkins, L., Kellett, E., and Milligan, G. (2006) Up-regulation of the angiotensin II type 1 receptor by the MAS proto-oncogene is due to constitutive activation of Gq/G11 by MAS. *The Journal of biological chemistry* **281**, 16757-16767

142. McGraw, D. W., Mihlbachler, K. A., Schwarb, M. R., Rahman, F. F., Small, K. M., Almoosa, K. F., and Liggett, S. B. (2006) Airway smooth muscle prostaglandin-EP1 receptors directly modulate beta2-adrenergic receptors within a unique heterodimeric complex. *The Journal of clinical investigation* **116**, 1400-1409
143. Fuxe, K., Ferre, S., Canals, M., Torvinen, M., Terasmaa, A., Marcellino, D., Goldberg, S. R., Staines, W., Jacobsen, K. X., Lluis, C., Woods, A. S., Agnati, L. F., and Franco, R. (2005) Adenosine A2A and dopamine D2 heteromeric receptor complexes and their function. *Journal of molecular neuroscience : MN* **26**, 209-220
144. Gines, S., Hillion, J., Torvinen, M., Le Crom, S., Casado, V., Canela, E. I., Rondin, S., Lew, J. Y., Watson, S., Zoli, M., Agnati, L. F., Verniera, P., Lluis, C., Ferre, S., Fuxe, K., and Franco, R. (2000) Dopamine D1 and adenosine A1 receptors form functionally interacting heteromeric complexes. *Proceedings of the National Academy of Sciences of the United States of America* **97**, 8606-8611
145. Torvinen, M., Marcellino, D., Canals, M., Agnati, L. F., Lluis, C., Franco, R., and Fuxe, K. (2005) Adenosine A2A receptor and dopamine D3 receptor interactions: evidence of functional A2A/D3 heteromeric complexes. *Molecular pharmacology* **67**, 400-407
146. Tsai, S. J. (2005) Adenosine A2a receptor/dopamine D2 receptor hetero-oligomerization: a hypothesis that may explain behavioral sensitization to psychostimulants and schizophrenia. *Medical hypotheses* **64**, 197-200
147. Ciruela, F., Casado, V., Rodrigues, R. J., Lujan, R., Burgueno, J., Canals, M., Borycz, J., Rebola, N., Goldberg, S. R., Mallol, J., Cortes, A., Canela, E. I., Lopez-Gimenez, J. F., Milligan, G., Lluis, C., Cunha, R. A., Ferre, S., and Franco, R. (2006) Presynaptic control of striatal glutamatergic neurotransmission by adenosine A1-A2A receptor heteromers.

*The Journal of neuroscience : the official journal of the Society for Neuroscience* **26**, 2080-2087

148. Rios, C., Gomes, I., and Devi, L. A. (2006) mu opioid and CB1 cannabinoid receptor interactions: reciprocal inhibition of receptor signaling and neuritogenesis. *British journal of pharmacology* **148**, 387-395
149. Gehret, A. U., Bajaj, A., Naider, F., and Dumont, M. E. (2006) Oligomerization of the yeast alpha-factor receptor: implications for dominant negative effects of mutant receptors. *The Journal of biological chemistry* **281**, 20698-20714
150. Overton, M. C., and Blumer, K. J. (2002) The extracellular N-terminal domain and transmembrane domains 1 and 2 mediate oligomerization of a yeast G protein-coupled receptor. *The Journal of biological chemistry* **277**, 41463-41472
151. Wang, H. X., and Konopka, J. B. (2009) Identification of amino acids at two dimer interface regions of the alpha-factor receptor (Ste2). *Biochemistry* **48**, 7132-7139
152. Kim, H., Lee, B. K., Naider, F., and Becker, J. M. (2009) Identification of specific transmembrane residues and ligand-induced interface changes involved in homo-dimer formation of a yeast G protein-coupled receptor. *Biochemistry* **48**, 10976-10987
153. Umanah, G. K., Huang, L. Y., Maccarone, J. M., Naider, F., and Becker, J. M. (2011) Changes in conformation at the cytoplasmic ends of the fifth and sixth transmembrane helices of a yeast G protein-coupled receptor in response to ligand binding. *Biochemistry* **50**, 6841-6854

## **Chapter 2**

**Identification of residues involved in homodimer formation located within a  $\beta$ -strand region of the N-terminus of a Yeast G protein-coupled receptor.**

This section is a version of an article that first appeared in the *Journal of Receptors and Signal Transduction* under the same title by M. Seraj Uddin, Heejung Kim, Amanda Deyo, Fred Naider, and Jeffrey M. Becker.

M. Seraj Uddin, Heejung Kim, Amanda Deyo, Fred Naider, and Jeffrey M. Becker Identification of residues involved in homodimer formation located within a  $\beta$ -strand region of the N-terminus of a Yeast G protein-coupled receptor. *J Recept Signal Transduct Res.* 2012 Apr;32(2):65-75. doi: 10.3109/10799893.2011.647352.

My contribution to this paper was to make Ste2p mutants, determination of signaling activities and accessibility of the residues, and much of the literature review and writing.

## Abstract

G protein-coupled receptors (GPCRs) are members of a superfamily of cell surface signaling proteins that play critical roles in many physiological functions; malfunction of these proteins is associated with multiple diseases. Understanding the structure-function relationships of these proteins is important, therefore, for GPCR-based drug discovery. The yeast *Saccharomyces cerevisiae* tridecapeptide pheromone  $\alpha$ -factor receptor Ste2p has been studied as a model to explore the structure-function relationships of this important class of cell surface receptors. Although transmembrane domains of GPCRs have been examined extensively, the extracellular N-terminus and loop regions have received less attention. We have used the substituted cysteine accessibility method (SCAM) to probe the solvent accessibility of single cysteine residues engineered to replace residues Gly20 through Gly33 of the N-terminus of Ste2p. Unexpectedly, our analyses revealed that the residues Ser22, Ile24, Tyr26, and Ser28 in the N-terminus were solvent inaccessible, whereas all other residues of the targeted region were solvent accessible. The periodicity of accessibility from residues Ser22 to Ser28 is indicative of an underlying structure consistent with a  $\beta$ -strand that was predicted computationally in this region. Moreover, a number of these Cys-substituted Ste2p receptors (G20C, S22C, I24C, Y26C, S28C and Y30C) were found to form increased dimers compared to the Cys-less Ste2p. Based on these data, we propose that part of the N-terminus of Ste2p is structured and that this structure forms a dimer interface for Ste2p molecules. Dimerization mediated by the N-terminus was affected by ligand binding indicating an unanticipated conformational change in the N-terminus upon receptor activation.

## **Introduction**

G protein-coupled receptors (GPCRs) belong to a superfamily of cell surface signaling proteins that play pivotal roles in many physiological processes including responses to hormones and neurotransmitters as well as being responsible for vision, olfaction and taste (1). Malfunction of GPCRs is associated with multiple diseases including Alzheimer's, Parkinson's, diabetes, color blindness, asthma, depression, hypertension, stress, cardiovascular, and immune disorders. Because these receptors are involved in a wide range of cellular functions, modulation of GPCR function is an important therapeutic goal with about 40-50% of drugs used in clinical medicine designed to affect GPCRs (2-4). Nonetheless, only a fraction of the GPCR superfamily is targeted by current drugs (5).

To date detailed atomic-level structural information for seven GPCRs has been obtained (6-12). These crystal structures have played a crucial role in understanding the structure-function relationships of these receptors. However, further structural information for additional GPCRs is vital for a more comprehensive understanding of receptor function and ultimately for drug development (1, 2, 13). In addition, most of the studies have revealed structural information focused on the transmembrane domains, although a large portion of all GPCRs is composed of intracellular and extracellular loops as well as N- and C- termini. These regions have received less consideration with respect to structural analysis because many of the crystals analyzed contained a large unnatural replacement within the third intracellular loop and the extracellular regions were not always visualized. It is generally believed that the loop regions and N- and C-termini are flexible and all the residues in the extracellular domains are solvent accessible. However, accessibility analysis of extracellular loop 1 of Ste2p indicated that all extracellular residues are not accessible; and the accessibility of some residues changes upon receptor activation (14). Therefore, we decided that a rational first approach to studying the structure and

function of the N-terminus was to probe systematically its solvent accessibility by the substituted cysteine accessibility method (SCAM) so that we might uncover structural elements of the N-terminus and their functional roles. Solvent accessibility determines whether particular Cys residues are in a hydrophilic or hydrophobic environment. Residues that face the low dielectric of the membrane or are located in tightly packed regions are inaccessible to a highly soluble, hydrophilic SCAM reagent. Conversely, Cys residues that react well with the reagent are predominantly exposed to a hydrophilic milieu outside the membrane or are not packed closely in a solvent excluding environment.

We carried out Cys scanning mutagenesis of residues G20 to G33 of Ste2p and probed the solvent accessibility of the Cys residue in these mutant receptors using SCAM (15, 16). Our analysis revealed a periodicity of accessible residues in the N-terminus which supported the computational prediction of a  $\beta$ -strand in this portion of Ste2p. In addition, we observed that certain Cys residues in the N-terminus promoted dimer formation suggesting the involvement of a 14-amino acid region of the N-terminus in Ste2p dimerization.

## Methods

**Media, Reagents, Strains, and Plasmids:** *S. cerevisiae* strain LM102 [*MATa ste2 FUS1-lacZ::URA3 bar1 ura3 leu2 his4 trp1 met1*] (17) was used for growth arrest, *FUS1-lacZ* gene induction and saturation binding assays, and the protease-deficient strain BJS21 [*MATa, prc1-407 prb1-1122 pep4-3 leu2 trp1 ura3-52 ste2::Kan<sup>R</sup>*] (18) was used for protein isolation, SCAM and immunoblot analyses to decrease receptor degradation during analyses (19). The plasmid pBEC2 containing C-terminal FLAG<sup>TM</sup> and His-tagged *STE2* (14) was transformed by the method of Geitz (20). Transformants were selected by growth on yeast media (21) lacking tryptophan (designated as MLT) to maintain selection for the plasmid. The cells were cultured in MLT and grown to mid log phase at 30°C with shaking (200 rpm) for all assays.

**Growth Arrest Assays:** *S. cerevisiae* LM102 cells expressing Cys-less Ste2p and single Cys mutants were grown at 30°C overnight in MLT, harvested, washed three times with water, and resuspended at a final concentration of  $5 \times 10^6$  cells/mL (22). Cells (1 mL) were combined with 3.5 mL of agar noble (1.1%) and poured as a top agar lawn onto a MLT medium agar plate. Filter disks (BD, Franklin Lakes, NJ) impregnated with  $\alpha$ -factor (2, 1, 0.5, 0.25 and 0.125  $\mu$ g/disk) were placed on the top agar. The plates were incubated at 30°C for 24h and then observed for clear halos around the disks. The experiment was repeated at least three times, and reported values represent the mean of these tests.

***FUS1-lacZ* Gene Induction Assay:** LM102 cells expressing Cys-less Ste2p and single Cys mutants were grown at 30 °C in selective media, harvested, washed three times with fresh media and resuspended at a final concentration of  $5 \times 10^7$  cells/mL. Cells (500  $\mu$ l) were combined with

$\alpha$ -factor pheromone (final concentration of 1  $\mu$ M) and incubated at 30°C for 90 min. The cells were transferred to a 96-well flat bottom plate (Corning Incorporated, Corning, NY) in triplicate, permeabilized with 0.5% Triton X-100 in 25 mM PIPES buffer (pH 7.2) and then  $\beta$ -galactosidase assays were carried out using fluorescein di- $\beta$ -galactopyranoside (Molecular Probes, Inc., Eugene, OR) as a substrate as described previously (18, 23). The reaction mixtures were incubated at 37°C for 60 min and 1.0 M Na<sub>2</sub>CO<sub>3</sub> was added to stop the reaction. The fluorescence of the samples (excitation of 485 nm and emission of 530 nm) was determined using a 96-well plate reader Synergy2 (BioTek Instruments, Inc., Winooski, VT). The data were analyzed using Prism software (GraphPad Prism version 5.03 for Windows, GraphPad Software, San Diego CA). The experiments were repeated at least three times and reported values represent the mean of these tests.

**Binding Assays:** Tritiated [<sup>3</sup>H]  $\alpha$ -factor (9.33 Ci/mmol) prepared as previously described (24) was used in saturation binding assays on whole cells. LM102 cells expressing Cys-less or single Cys mutant of Ste2p were harvested, washed 3 times with YM1 (25), and adjusted to a final concentration of  $3 \times 10^7$  cells/mL. Cells (600  $\mu$ L) were combined with 150  $\mu$ L of ice-cold 5X binding medium (YM1 plus protease inhibitors [YM1i] (25) supplemented with [<sup>3</sup>H] $\alpha$ -factor and incubated at room temperature for 30 min. The final concentration of [<sup>3</sup>H] $\alpha$ -factor ranged from  $0.5 \times 10^{-10}$  to  $1 \times 10^{-6}$  M. Upon completion of the incubation interval, 200  $\mu$ L aliquots of the cell-pheromone mixture were collected in triplicate and washed over glass fiber filter mats using the Standard Cell Harvester (Skatron Instruments, Sterling, VA). Retained radioactivity on the filter was counted by liquid scintillation spectroscopy. LM102 cells lacking Ste2p were used as a nonspecific binding control for the assays. Binding assays were repeated a minimum of three times, and similar results were observed for each replicate. Specific binding for each mutant

receptor was calculated by subtracting the nonspecific values from those obtained for total binding. Specific binding data were analyzed by nonlinear regression analysis for single-site binding using Prism software (GraphPad Software, San Diego, CA) to determine the  $K_d$  and  $B_{max}$  values for each mutant receptor.

**Immunoblots:** BJS21 cells expressing Cys-less or single Cys mutants grown in MLT were used to prepare total cell membranes isolated as previously described (25). Protein concentration was determined by BioRad protein assay (BioRad, Hercules, CA)(14), and membranes were solubilized in sodium dodecyl sulfate (SDS) sample buffer (10% glycerol, 5% 2-mercaptoethanol, 1% SDS, 0.03% bromophenol blue, 62.5 mM Tris, pH 6.8). For studies of disulfide cross-linking, membranes were solubilized in SDS sample buffer without 2-mercaptoethanol. Proteins were fractioned by SDS-PAGE (10% acrylamide) along with pre-stained Precision Plus protein standards (BioRad) and transferred to an Immobilon<sup>TM</sup>P membrane (Millipore Corp., Bedford, MA). The blot was probed with anti-FLAG<sup>TM</sup> M2 antibody (Sigma/Aldrich Chemical, St. Louis, MO), and bands were visualized with the West Pico chemiluminescent detection system (Pierce). The total intensity of all Ste2p bands in each lane was determined using a ChemiDoc XRS photodocumentation system with Quantity One one-dimensional analysis software (version 4.6.9, BioRad, Hercules, CA). Multiple repeats of immunoblot experiments yielded similar results. Constitutively-expressed membrane protein Pma1p was used as a loading control as described previously (26) using Pma1p antibody (Thermo Scientific, Rockford, IL).

### ***Whole-cell MTSEA Labeling, Membrane Preparation, and Immunoblots:***

MTSEA-biotin (2-((biotinoyl)amino)ethyl methanethiosulfonate) (Biotium, Hayward, CA) labeling was performed as described previously (14). To eliminate reaction with native Cys in Ste2p, all the mutants were constructed in a Cys-less receptor background. This Cys-less receptor contained a FLAG<sup>TM</sup> epitope tag and a 6XHis tag at the C-terminus of the receptor. Experiments were completed at least three times as described below. BJS21 cells expressing single Cys mutations in Ste2p or Cys-less receptor were grown in MLT at 30°C overnight. Cells were harvested at mid-log phase ( $A_{600} \sim 1.5$ ), washed, and resuspended in phosphate-buffered saline (PBS; 10 mM Na<sub>2</sub>HPO<sub>4</sub>, 1.5 mM KH<sub>2</sub>PO<sub>4</sub>, 3.0 mM KCl, 150 mM NaCl, pH 7.4) at 20-fold concentration. One ml of this cell suspension was warmed to room temperature and then supplemented with MTSEA-biotin (20 mM in dimethyl sulfoxide) to a final concentration of 0.1 mM. The reaction was stopped after 2 min by the addition of ice-cold citrate buffer to a final concentration of 50 mM (0.25M Citric Acid/KH<sub>2</sub>PO<sub>4</sub>, pH 4.0) and was incubated on ice for an additional 5 min. The low pH has previously been shown to prevent disulfide exchange reactions that might complicate the analysis (27). All subsequent steps were performed at 4°C unless otherwise indicated. MTSEA-biotin-treated cells were pelleted, resuspended in PBS, and lysed by vortexing with glass beads. Following a low speed spin (700 X g, 5 min) to remove cell wall debris, unbroken cells, and glass beads, the resulting supernatant was centrifuged at high speed (15,000 X g, 30 min) to pellet membranes. The pellet was resuspended in PBS, and protein concentration was determined using the BioRad (BioRad, Hercules, CA) protein assay. Membranes were solubilized in RIPA buffer (0.1% SDS, 1% Triton X-100, 0.5% deoxycholic acid, 1 mM EDTA in 1X PBS, pH 7.4) for 1 h at room temperature with end-over-end mixing. The solubilized, biotinylated proteins

were collected on UltraLink Immobilized Streptavidin Plus beads (Thermo Scientific, Rockford, IL) by incubation overnight at 4°C with end-over-end mixing. The beads were washed four times with ice-cold RIPA buffer, once with 2% SDS in PBS (room temperature), followed by a final wash with ice-cold RIPA buffer. During the washes the beads were resuspended and then allowed to settle by gravity for 20 min prior to removal of the supernatant. Bound proteins were extracted from the beads using SDS sample buffer (10% glycerol, 5% 2-mercaptoethanol, 1% SDS, 0.03% bromophenol blue, 62.5 mM Tris, pH 6.8, 55°C, 5 min) and used for immunoblot analysis. Solubilized proteins were resolved by SDS-PAGE and immunoblotted using anti-FLAG™ M2 antibody as described under “immunoblots” in Methods. To verify Ste2p expression levels, an aliquot of total membrane proteins was solubilized in SDS sample buffer, fractionated by SDS-PAGE (5-10 µg/lane), and immuno-blotted in parallel with the biotinylated proteins extracted from the beads.

***Disulfide Cross-Linking with Cu-Phenanthroline:*** One hundred µg of membrane protein preparation was treated with a fresh preparation (pH 7.4) of Cu(II)-1,10-phenanthroline (Cu-P; final concentration, 2.5 µM CuSO<sub>4</sub> and 7.5 µM phenanthroline). The reaction was carried out at room temperature for 20 min, terminated with 50 mM EDTA, and kept on ice for 20 min followed by adding SDS sample buffer without 2-mercaptoethanol. In experiments designed to prevent disulfide bond formation, the membranes were treated with 5 mM NEM (N-ethylmaleimide) for 20 min prior to incubation with Cu-P reagent. Alpha-factor or antagonist (desW<sup>1</sup>,desH<sup>2</sup>-α-factor) (10 µM final concentration) were added to the membrane preparation and incubation was allowed to proceed for 30 min prior to Cu-P treatment in experiments performed to examine the influence of ligand on dimerization.

## Results

### *Expression and Biological Activities of Single Cys and Cys-less Receptors*

We targeted residues G20 to G33 in the N-terminus of Ste2p, which comprised the predicted  $\beta$ -strand (T23 to Y30) (28, 29) and an additional three residues on both the N- and C-termini of the strand, for determining the solvent accessibility. To eliminate any non-specific reactivity with MTSEA-biotin in SCAM experiments (reported below), we used the Cys-less receptor that had been used previously for SCAM studies in our lab and those of others. In this receptor, the two native cysteine residues at C59 and C252 were replaced with serine resulting in a fully active receptor (30). Individual residues in the region of interest were replaced one at a time with cysteine to generate a total of 14 Cys mutants of Ste2p. Before embarking on SCAM, expression level and biological activities of each mutant receptor were measured.

For determination of total receptor expression levels, membranes from yeast cells harboring a plasmid with each single Cys mutant receptor tagged with a FLAG- epitope were prepared, run on SDS-PAGE under reducing conditions, and immunoblotted using the FLAG™ antibody. Two additional single-Cys mutants (T199C and Y266C) were also studied as they served as controls in SCAM experiments reported below. Multiple repeats of immunoblot experiments yielded similar results and the standard deviation for each expression is indicated for each receptor (**Table 2.1**). Representative blots are shown in figure 2.1. Relative total expression level of the mutant receptors (monomers and dimers were both included in the calculated total expression; dimer formation is examined in greater detail below) was compared to the Cys-less receptor and normalized to the constitutively-expressed membrane protein Pma1p which was used as a loading control (**Table 2.1**). Expression levels of different mutants varied from ~4 fold lower (S22C) to ~1.6 fold higher (G31C) than the Cys-less Ste2p. Because SCAM experiments were

carried out in whole cells using a membrane impermeable reagent, surface expression of the receptors will directly affect the relative solvent accessibility of the mutants as reported below. Therefore, surface expression of the mutants was measured by saturation binding assays using tritiated [ $^3\text{H}$ ] $\alpha$ -factor in whole cells. Since the relative Bmax value from saturation binding experiments represents the relative surface expression of a receptor, the Bmax values of the mutants were compared to that of the Cys-less receptors. As shown in Table 2.1, mutant surface expressions varied from ~5 fold lower (Y26C) to ~1.8 fold higher (T23C) as compared to the Cys-less Ste2p. When experimental error was taken into account 9 of the 14 Cys mutants showed a good correlation between the relative total expression and surface expression. Most significantly, correlation was quite good for the poorly expressed (G20C, S22C and Y26C) mutants. Three of the mutants (Q21C, T27C and N32C) showed a low surface expression compared to total expression and two (T23C and Y30C) showed a higher relative surface expression compared to total expression.

**Table 2.1. Relative expression levels of Ste2p**

Receptor	Relative Total Expression Level <sup>a</sup>			Relative Surface Expression Level <sup>b</sup>		
		±			±	
Cys-less	1.00	±	0.06	1.00	±	0.01
T199C	0.81	±	0.10	1.25	±	0.36
Y266C	0.72	±	0.13	1.14	±	0.15
G20C	0.49	±	0.06	0.43	±	0.13
Q21C	1.06	±	0.02	0.69	±	0.05
S22C	0.25	±	0.06	0.20	±	0.07
T23C	1.13	±	0.17	1.85	±	0.05
I24C	0.64	±	0.20	0.75	±	0.37
N25C	1.09	±	0.33	0.87	±	0.36
Y26C	0.26	±	0.07	0.19	±	0.04
T27C	1.35	±	0.21	0.78	±	0.05
S28C	0.63	±	0.09	0.57	±	0.21
I29C	1.33	±	0.08	1.57	±	0.24
Y30C	0.95	±	0.14	1.51	±	0.04
G31C	1.56	±	0.27	1.26	±	0.07
N32C	1.30	±	0.13	0.76	±	0.08
G33C	1.06	±	0.05	0.84	±	0.05

<sup>a</sup>Relative expression level of the Cys mutants of Ste2p. Ste2p band intensity was quantitated by Quantity One software (BioRad) and normalized to the Pma1p band intensity (amount of light emitted from the chemiluminescent signal as read by Quantity One) (for protein loading on the gel) and the Cys-less receptor. Expression level of each receptor on the same PAGE immunoblot was calculated as

$$\left\{ \frac{\textit{Ste2p Cys-mutant band intensity}}{\textit{Pma1p band intensity of the mutant}} \right\} \times \left\{ \frac{\textit{Pma1p band intensity of Cys-less}}{\textit{Ste2p Cys-less band intensity}} \right\}$$

<sup>b</sup>Relative surface expression Cys mutants of Ste2p. Surface expression was determined by saturation binding assay using tritiated [<sup>3</sup>H]  $\alpha$ -factor with whole cells. The surface expression of receptors was determined from the Bmax values obtained from saturation binding assays using tritiated [<sup>3</sup>H]  $\alpha$ -factor with whole cells and the relative surface expression was expressed as

$$\frac{\text{Bmax value of the mutant}}{\text{Bmax value of the Cys-less receptor}}$$

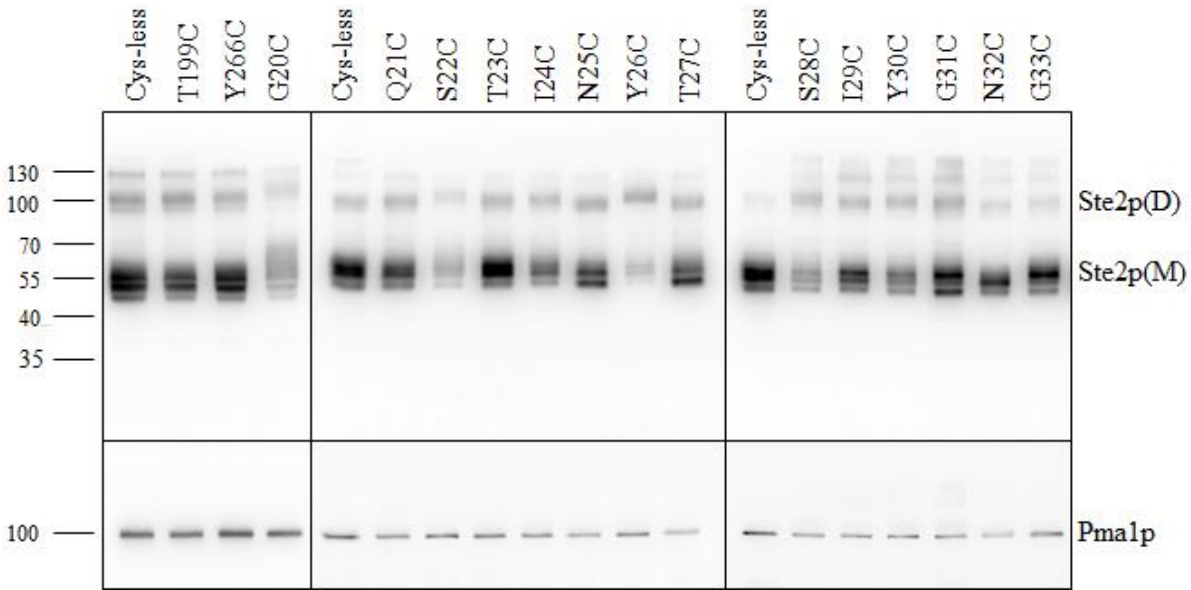


**Figure 2.1. Ste2p expression levels.** Total membranes prepared from cells expressing single Cys mutants of Ste2p (G20C to G33C, T199C, and Y266C) and the Cys-less receptor were run on separate gels shown in the three panels. Five  $\mu\text{g}$  of total membrane preparations from each mutant was immunoblotted using antibody against the C-terminal FLAG<sup>TM</sup> epitope tag. Molecular mass markers (kDa) are indicated on the left-hand side. M and D indicate the monomeric and dimeric forms of Ste2p, respectively. The same blot was stripped and then re-probed with anti-Pma1p antibody as a loading control.

The biological activities of each mutant were measured by growth arrest, reporter gene activity, and binding assays and were normalized to those of the Cys-less receptor (**Table 2.2**). Pheromone-induced growth arrest activity of all the mutants was similar to that of the Cys-less receptor (between 85% and 103% of Cys-less receptor). One receptor, Y26C, was reported in a previous study to fail to trigger growth arrest (29). We believe the discrepancy between our study and that of Shi *et al.* (29) is due to differences in the strain background used. Signaling activity

as measured by the pheromone-induced *FUS1-lacZ* reporter gene activation assay was between 57% (Y30C) and 127% (I24C) of the Cys-less receptor. Although expression of two receptors [S22C (25%) and Y26C (26%)] was lower than 50%, these mutants exhibited effective growth arrest and  $\beta$ -galactosidase activities suggesting that even the low expression of Ste2p was sufficient to elicit a strong biological response to pheromone. Previous studies also indicated that low levels of Ste2p were sufficient to manifest full biological responses (31-34). Finally, the alpha-factor binding affinity of each mutant was measured by saturation binding assays using whole cells. The binding affinity varied from ~50% (I29C) lower to ~50% (G33C) higher in comparison to that of the Cys-less receptor (**Table 2.2**). From the results of the above experiments, we conclude that all the single Cys mutants of Ste2p exhibited effective signaling and strong binding, and therefore Cys substitution did not cause any global change in the receptor conformation.

**Table 2.2.** Biological activities of Cys-less and single Cys mutants of Ste2p

<b>Receptor</b>	<b>Growth Arrest Activity (%)<sup>a</sup></b>	<b><math>\beta</math>-galactosidase Activity (%)<sup>b</sup></b>	<b>Relative Kd<sup>c</sup></b>
Cys-less	100 $\pm$ 0.3	100 $\pm$ 2.0	1.00 $\pm$ 0.21
T199C	93 $\pm$ 7.0	96 $\pm$ 5.0	0.99 $\pm$ 0.20
G20C	89 $\pm$ 0.7	71 $\pm$ 2.1	1.15 $\pm$ 0.50
Q21C	97 $\pm$ 3.0	125 $\pm$ 4.4	0.71 $\pm$ 0.06
S22C	87 $\pm$ 8.1	89 $\pm$ 4.4	1.38 $\pm$ 0.79
T23C	97 $\pm$ 3.7	113 $\pm$ 2.7	1.44 $\pm$ 0.05
I24C	101 $\pm$ 3.5	127 $\pm$ 6.2	0.78 $\pm$ 0.39
N25C	89 $\pm$ 3.5	108 $\pm$ 3.8	0.75 $\pm$ 0.49
Y26C	85 $\pm$ 7.5	113 $\pm$ 8.3	1.09 $\pm$ 0.23
T27C	98 $\pm$ 8.0	65 $\pm$ 8.2	1.06 $\pm$ 0.08
S28C	103 $\pm$ 1.3	58 $\pm$ 2.9	0.65 $\pm$ 0.28
I29C	100 $\pm$ 2.3	96 $\pm$ 3.6	1.52 $\pm$ 0.20
Y30C	97 $\pm$ 3.5	57 $\pm$ 4.6	1.13 $\pm$ 0.30

**Table 2.2 Continued**

<b>Receptor</b>	<b>Growth Arrest Activity (%)<sup>a</sup></b>	<b><i>β</i>-galactosidase Activity (%)<sup>b</sup></b>	<b>Relative Kd<sup>c</sup></b>
G31C	101 ± 3.5	71 ± 2.1	1.49 ± 0.21
N32C	99 ± 1.3	117 ± 2.4	0.88 ± 0.15
G33C	100 ± 4.0	61 ± 1.2	0.53 ± 0.13

<sup>a</sup>Relative growth arrest activity (halo size ±standard deviation) was compared to that of the Cys-less receptor at 0.5 µg of α-factor applied to a disk (the halo size of Cys-less was 23mm).

<sup>b</sup>Relative β-galactosidase activity (±standard deviation) was compared with that of Cys-less at 1 µM α-factor.

<sup>c</sup>The Kd values (±standard deviation) are presented relative to those of the Cys-less receptor. The Kd was determined by saturation binding of radioactive α-factor according to the protocol described in experimental procedures. (Kd of Cys-less receptor was 10.8 nM).

### *Accessibility of N-terminal Cys residues*

The substituted cysteine accessibility method (SCAM) has proven to be an important means to determine the accessibility of residues as well as to gain knowledge about the secondary structure of transmembrane proteins. SCAM was performed in order to uncover the solvent accessibility of a portion of the N-terminus previously predicted to have secondary structure. For SCAM we used MTSEA-biotin, a thiol-specific, membrane-impermeable reagent. To ensure that the topology of the receptor was not perturbed by membrane preparation, whole cells were used instead of isolated membranes as in previous SCAM experiments in our laboratory which probed the first extracellular domain of Ste2p (14). The receptors T199C and Y266C were used as accessibility controls as they were shown to be fully accessible (T199C) and inaccessible (Y266C) to MTSEA-Biotin in previous studies (14, 35). Representative examples of immunoblots are shown in Figure 2.2. As shown in all panels, no detectable labeling was observed in the Cys-less and Y266C receptors but strong labeling was observed in T199C as had been reported previously. However, substantial variation in the labeling of the mutants was observed. Since cell surface expression of each mutant was different, the labeling of each mutant was normalized to its cell surface expression to determine accessibility. This was done to ensure that the solvent accessibility was not affected by the differential surface expression. Finally, accessibility of each mutant was normalized to that of T199C, which was assigned as the positive control for accessibility (100% labeling by MTSEA-biotin) (Table 2.3).

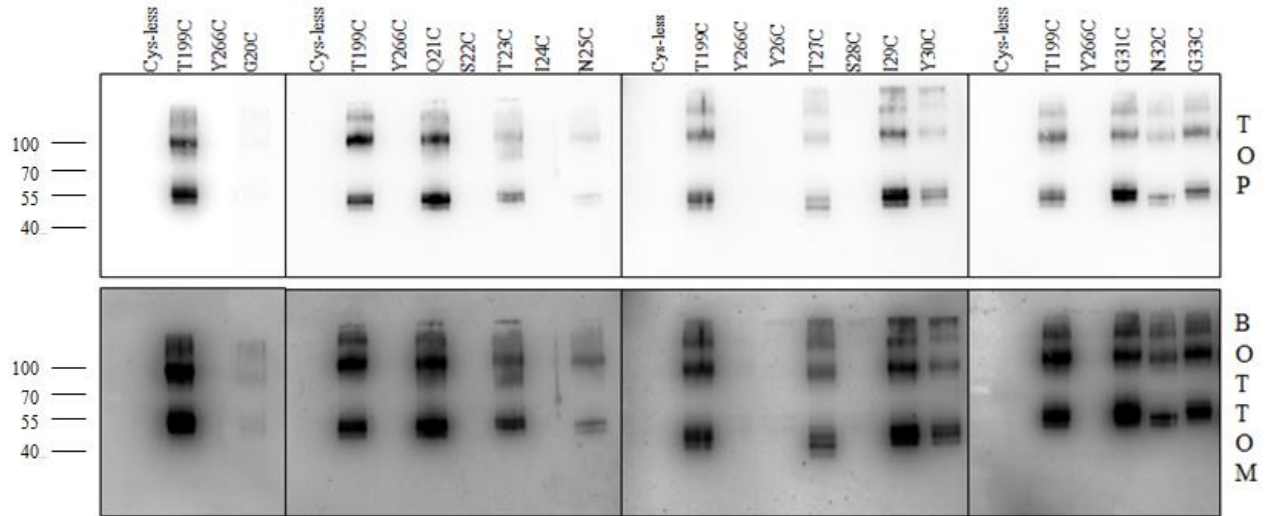


**Figure 2.2. MTSEA labeling of the N-terminal residues of Ste2p. Ste2p Cys mutants at positions G20-G33 were labeled with MTSEA as described under Methods. T199C was used as a positive control, and Y266C and Cys-less receptors were used as negative controls. Molecular mass markers (kDa) are indicated on the left-hand side of the Fig. The bottom panel shows overexposed immunoblots of the top panels.**

**Table 2.3. Relative MTSEA-biotin labeling of Cys-scanned mutants of Ste2p**

<b>Receptor</b>	<b>Labeling<sup>a</sup></b>
T199C	1.00 ± 0.15
Y266C	0
Cys-less	0
G20C	0.09 ± 0.06
Q21C	2.19 ± 0.05
S22C	0
T23C	0.32 ± 0.02
I24C	0
N25C	0.19 ± 0.04
Y26C	0
T27C	1.08 ± 0.02
S28C	0
I29C	2.00 ± 0.20
Y30C	0.71 ± 0.02
G31C	1.30 ± 0.03
N32C	0.61 ± 0.04
G33C	1.19 ± 0.06

<sup>a</sup>MTSEA-biotin labeling was adjusted to the surface expression of each mutant and normalized to the labeling of T199C as calculated as  $\{(Band\ intensity\ of\ mutant/B_{max}\ of\ mutant) \times B_{max}\ of\ T199C / Band\ intensity\ of\ T199C\}$ .

Examination of normalized accessibilities revealed that the residues in the target region are not equally solvent accessible despite the fact that the N-terminus of Ste2p is extracellular; residues in this region are expected to be equally solvent accessible. We found that four residues (S22C, I24C, Y26C and S28C) were not detectably labeled (even when the gels were overexposed, Figure 2.2 bottom). G20C, T23C and N25C were poorly labeled (<40%) and all of the other residues in this targeted region (Q21C, T27C, I29C, Y30, G31, N32, and G33) were labeled to 60% or more of the positive control. The amount of accessibility varied from ~5-fold less (N25C) to ~2-fold higher (Q21C and I29C) as compared to T199C (Table 2.3). Many mutants exhibited a lack of correlation between the surface expression and the solvent accessibility. For example, residues I24C and N32C have similar surface expression (75% and 76%, respectively) as compared to the Cys-less, receptor (Table 2.1) but their accessibility is entirely different, i.e., N32C is highly accessible but I24C is completely inaccessible.

The periodicity of accessibility from S22 to S28 in the N-terminus with residues S22, I24, Y26, and S28 showing no apparent accessibility and residues Q21, T23, N25, T27, and I29 demonstrating accessibility would be consistent with that region of the N-terminus forming a  $\beta$ -strand structure as predicted in previous studies (28, 29) with one face of the  $\beta$ -strand being shielded from solvent. One explanation for the solvent inaccessibility would be involvement of that portion of the N-terminus in a dimer interface. Previous studies have shown that deletion of the first 45 residues of the N-terminus decreased dimerization of Ste2p (36). Thus we explored the involvement of these  $\beta$ -strand residues in Ste2p dimerization.

### ***Involvement of specific N-terminal residues in dimer formation***

Cells expressing each of the different Cys mutants were grown and membranes were prepared. The samples were analyzed by SDS-PAGE in non-reducing conditions and probed with anti-FLAG™ antibody. A small dimer band at ~110 kD was observed with the Cys-less Ste2p and all of the Ste2p Cys mutants under non-reducing (Figure 2.3A) and reducing conditions (Figure 2.1). This “SDS-resistant” band has been observed consistently in studies of Ste2p (29, 33, 37, 38). Under the non-reducing conditions (Figure 2.3A) there was an increase in the dimer/monomer for many of the mutants. For example in Fig. 1 under reducing conditions I24C is mostly in the monomeric form whereas in non-reducing conditions (Figure 2.3A) it is mostly dimeric. We attribute the increased dimers to disulfide formation between the Cys-substituted residues in the N-terminus as evidenced by the reversal of dimer formation by NEM pretreatment (compare Figure 2.3B & Figure 2.3E) and by the lower dimer/monomer ratio under reducing conditions (Figure 2.1). Under non-reducing conditions and in the absence of a catalyst, whereas the majority species was monomeric in the Cys-less and the Q21C, T23C, N25C, T27C, I29C, G31C, N32C, and G33C receptors, the G20C, S22C, I24C, Y26C, S28C, and Y30C receptors were mostly in the dimer form (Figure 2.3A). In previous studies, we have shown that Cys cross-linking of Ste2p transmembrane domains and intracellular residues was promoted by Cu-P (Cu(II)-1,10-phenanthroline) treatment. Cu-P treatment provides a more oxidative environment and has been used in many experiments to determine Cys-Cys disulfide formation in membrane proteins (39-43). With Cu-P treatment, many of the six Cys mutants (G20C, S22C, I24C, Y26C, S28C, and Y30C) that showed a high dimer formation under non-reducing conditions (Figure 2.3A) exhibited an even higher dimer population (Figure 2.3B). In addition, in the presence of Cu-P three mutants (N25C, T27C, and I29C), which did not form a significant proportion of

dimer under non-reducing conditions, showed increased dimerization (compare Figure 2.3A and Figure 2.3B). Dimer formation in the other mutants (Q21C, T23C, G31C, N32C, and G33C) was not affected to a major extent by Cu-P treatment. To verify that the Cu-P stimulated increase in higher molecular weight band was due to disulfide bond formation, samples were treated with NEM (N-ethylmaleimide) prior to Cu-P addition. NEM alkylates the free –SH group of cysteine irreversibly, so that disulfide bond formation cannot occur after NEM treatment. Representative data for five mutants (N25C to I29C) are shown in Figure 2.3E. NEM pre-treatment was found to block Cu-P stimulated dimerization for mutants N25C, T27C, and I29C (compare Figure 2.3B and Figure 2.3E).

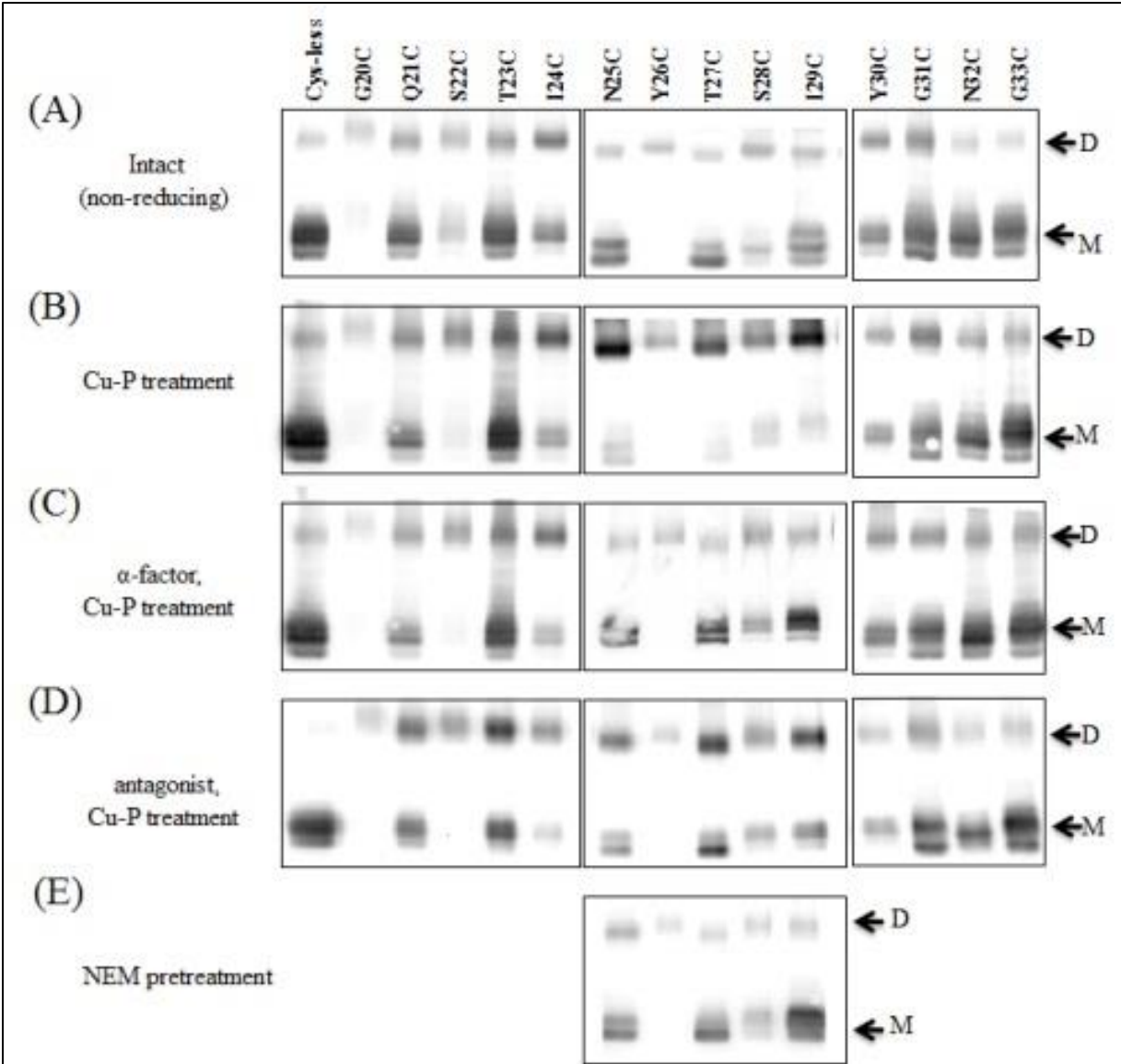


**Figure 2.3. Dimer formation by the Ste2p N-terminal Cysteine mutants. Membrane proteins untreated (A), treated with Cu-P (B), incubated with  $\alpha$ -factor followed by Cu-P (C), incubated with antagonist followed by Cu-P (D) or NEM added prior to Cu-P (E) were separated by SDS-PAGE, then immunoblotted and probed with anti-FLAG™ antibody. The upper band (~110 kDa) represents dimerized receptor (indicated by “D”) and the lower band (~55 kDa) represents monomer (indicated by “M”).**

### ***Effect of ligand binding on dimerization***

It has been observed that ligand binding can induce a change in a GPCR dimer interface (44, 45). To examine the effect of ligand on Cys-mediated dimerization, membranes were incubated with either  $\alpha$ -factor (agonist) or [desW<sup>1</sup>desH<sup>2</sup>] $\alpha$ -factor (an antagonist) prior to Cu-P treatment. Notable reduction was observed in dimer formation for the N25C, T27C, and I29C mutants in the presence of  $\alpha$ -factor (compare Figure 2.3B to Figure 2.3C). In contrast, dimerization of receptors with Cys in the other residues of this region was not greatly affected by agonist binding. In addition, Cu-P stimulated dimerization was not affected significantly by antagonist treatment for the mutants analyzed (compare Figure 2.3B and Figure 2.3D).

## Discussion

Binding of ligand to its cognate GPCR induces conformational changes in the receptor which promote signal transduction across the membrane and activate a G-protein mediated signal transduction cascade (46, 47). Ste2p, the  $\alpha$ -factor pheromone receptor, is a GPCR expressed in the yeast *Saccharomyces cerevisiae* and has been used extensively as a model for peptide-responsive GPCRs (48-50). Although Ste2p does not share sequence similarity with mammalian GPCRs or even with Ste3p, the  $\alpha$ -factor pheromone receptor of yeast, all GPCRs have the same overall membrane architecture and manifest functional similarities such as G-protein coupling. The extracellular N-termini of GPCRs are highly variable differing greatly in length and sequence. Even within subfamilies, the N-termini often show low sequence homology. However, recent studies have indicated that the N-terminal regions of GPCRs play important roles in receptor function. For example, the N-terminus of several GPCRs has been found to be involved in ligand binding (51-53), and receptor dimerization (36, 54), and cell surface targeting (55).

For Ste2p, extensive structure and function studies have been conducted on the intracellular domains and transmembrane domains, while fewer studies have focused on the extracellular N-terminal region. In those studies where this portion of Ste2p was studied, the role of the N-terminus in glycosylation (56), dimerization (36) and mating (28, 29) was examined. The Ste2p N-terminus is 48 amino acids long, and residues N25 and N32 are sites of N-linked glycosylation (56). Nevertheless, removal of these glycosylation sites still resulted in a fully active receptor (56). Deletion of the N-terminal 45 residues yielded a receptor that was deficient in dimer formation (36), and deletion of the first 30 amino acids of the N-terminus of Ste2p resulted in a cell that could not mate and showed weak signaling after pheromone addition (28). In another study, 17 residues in the N-terminus (P15, P19, T23 to I36 and, N46) were

investigated by substituting with Cys and Ala. This study showed that none of the substitutions affected signaling, but mutation of residues P15, I24 and I29 greatly lowered the mating ability of the cells carrying these mutations (29).

In this study we have explored the solvent accessibility and involvement in dimer formation of a portion of the N-terminus of Ste2p to gain insights into the structure and function of this domain of the receptor. SCAM has been used previously to study the lining of pores of channels and transport proteins (57-59) and the binding site of acetylcholine receptors (60). More recently, this method has been applied to study G protein-coupled receptors (14, 15, 27, 61-64). Previous studies had suggested that certain residues in the N-terminus of Ste2p were critical for pheromone induced mating but not for G1 arrest. Marsh and co-workers using *S. cerevisiae/S. kluyveri* chimeras concluded that residues 1-45 were not involved in pheromone binding specificity (65). Our binding studies on the Cys mutants of residues 20-33 of Ste2p would be consistent with this observation. Despite the minor influence of the Cys mutations on receptor signaling and pheromone binding here we report the first experimental evidence that all residues in the N-terminus are not equally accessible and that the part of the N-terminus of Ste2p that putatively contains a  $\beta$ -strand participates in dimerization of Ste2p. Notably, we uncovered a change in the conformation of the N-terminus upon agonist binding as determined by differences in disulfide-mediated dimer formation in the active and inactive stages of Ste2p (Figure 2.3).

Our accessibility analyses showed that there were striking variations in the solvent exposure of residues in the region of the N-terminus between residues S22 and S28. Residues S22C, I24C, Y26C, and S28C were completely inaccessible to a membrane-impermeable, hydrophilic, thiol-specific reagent MTSEA-biotin even though I24C and S28C receptors were expressed at the cell surface as well as, or nearly as well as residues (Q21C, T27C, N32C, and

G33C) whose Cys residues were accessible to MTSEA-biotin (Table 2.1 and Table 2.3).

Residues adjacent to the inaccessible residues readily reacted with the reagent. The differential labeling of residues G20-S33 of the N-terminal residues is surprising since all these extracellular residues were expected to be readily solvent accessible. The alternating pattern of accessibility of consecutive engineered cysteines suggests an underlying structure of this region which is consistent with predicted  $\beta$ -strand spanning from Thr 23 to Tyr 30 (28, 29).

Based on the above SCAM analysis we hypothesized that the putative  $\beta$ -strand in the N-terminus of Ste2p may be involved in dimerization of Ste2p, as the N-terminus of Ste2p had been shown previously to be part of the Ste2p dimer interface (36). Indeed, our results show that the cysteine-substituted residues S22, I24, Y26 and S28, which were not solvent accessible as judged by disulfide crosslinking to a biotinylation reagent, were involved in dimer formation. On the other hand, residues (Q21C, T23C, N25C, T27C, I29C) which would be on the opposite face of the  $\beta$ -strand and thereby accessible to biotinylation were not involved in dimer formation under non-reducing conditions. Dimerization of the S28C mutant was blocked by NEM pre-treatment (Figure 2.3E) corroborating the fact that dimerization was mediated by disulfide crosslinking of two nearby Cys residues. Disulfide bond formation suggests that the  $\alpha$ -carbons of the two Cys residues are located close to each other, within 7Å as the maximum distance, in order to result in a disulfide bond (33, 66-68). Our modeling shows that disulfide formation between residues in the N-terminus the putative  $\beta$ -strand region would require a parallel arrangement of two Ste2p molecules. In contrast to our results, previous studies indicated that residue I24C was accessible in a SCAM experiment (29). The different outcomes between our and the previous investigation may reflect differences in the assay conditions used. In our assay, labeling experiments were performed with MTSEA-biotin using intact cells, whereas Shi and co-workers

used isolated membranes and fluorescein-5-maleimide. We have observed that accessibility was found to differ in experiments performed on isolated membranes versus whole cells in a study of Ste2p EL1 residues (14).

Our results also demonstrate that agonist-induced conformational changes occur in the N-terminus of Ste2p as indicated by  $\alpha$ -factor induced changes in the Cu-P catalyzed oxidation of dimerization for the N25C, T27C, and I29C mutants (compare Figure 2.3B and Figure 2.3CC). However, treatment with antagonist, which binds but does not activate the receptor, did not prevent the Cu-P-mediated increase in dimerization (compare Figure 2.3B, Figure 2.3C and Figure 2.3D). We postulate that the conformation of the N-terminus changes in the active state of the receptor such that the distance between these residues is too great for Cu-P induced disulfide bond formation. In contrast, the residues involved in dimer formation in the non-reducing conditions (22, 24, 26, and 28) still form a dimer interface in the activated state of the receptor. For these interactions between receptor monomers to occur, the parallel  $\beta$ -strands must have enough flexibility to allow formation of disulfide bonds with residues on both faces of the  $\beta$ -strands as observed with Cu-P in the absence of alpha-factor.

## Conclusion

In conclusion SCAM analysis and disulfide crosslinking clearly show that in a short segment of the N-terminus of Ste2p certain residues do not react with a soluble biotinylation reagent and appear to be involved in receptor dimerization. The accessibility pattern, in particular, is consistent with a stretch of  $\beta$ -sheet-like structure involving residues G20-Y30. Based on oxidative disulfide crosslinking studies, the dimer interface of the receptor changes in response to pheromone indicating a change in conformation of the N-terminus of the receptor during receptor activation. These studies provide evidence that the N-terminus of Ste2p possesses a discrete structural domain that appears to participate in the signaling mechanism. Information on the extracellular surface of other GPCRs should be useful in designing agents that can modulate signaling and thereby influence cell physiology. The methods applied to Ste2p should be applicable, therefore, to mammalian G protein-coupled receptors.

## **Acknowledgements**

We thank Li-yin Huang for help in the binding assay.

## References

1. Rosenbaum DM, Rasmussen SG, Kobilka BK. The structure and function of G-protein-coupled receptors. *Nature*. 2009;459(7245):356-63.
2. Lundstrom K. An overview on GPCRs and drug discovery: structure-based drug design and structural biology on GPCRs. *Methods Mol Biol*. 2009;552:51-66.
3. Williams C, Hill SJ. GPCR signaling: understanding the pathway to successful drug discovery. *Methods Mol Biol*. 2009;552:39-50.
4. De Amici M, Dallanoce C, Holzgrabe U, Trankle C, Mohr K. Allosteric ligands for G protein-coupled receptors: a novel strategy with attractive therapeutic opportunities. *Med Res Rev*. 2010;30(3):463-549.
5. Lappano R, Maggiolini M. G protein-coupled receptors: novel targets for drug discovery in cancer. *Nat Rev Drug Discov*. 2011;10(1):47-60.
6. Palczewski K, Kumasaka T, Hori T, Behnke CA, Motoshima H, Fox BA, et al. Crystal structure of rhodopsin: A G protein-coupled receptor. *Science*. 2000;289(5480):739-45.
7. Jaakola VP, Griffith MT, Hanson MA, Cherezov V, Chien EY, Lane JR, et al. The 2.6 angstrom crystal structure of a human A2A adenosine receptor bound to an antagonist. *Science*. 2008;322(5905):1211-7.
8. Wu B, Chien EY, Mol CD, Fenalti G, Liu W, Katritch V, et al. Structures of the CXCR4 chemokine GPCR with small-molecule and cyclic peptide antagonists. *Science*. 2010;330(6007):1066-71.

9. Chien EY, Liu W, Zhao Q, Katritch V, Han GW, Hanson MA, et al. Structure of the human dopamine D3 receptor in complex with a D2/D3 selective antagonist. *Science*. 2010;330(6007):1091-5.
10. Warne T, Moukhametzianov R, Baker JG, Nehme R, Edwards PC, Leslie AG, et al. The structural basis for agonist and partial agonist action on a beta(1)-adrenergic receptor. *Nature*. 2011;469(7329):241-4.
11. Warne T, Serrano-Vega MJ, Baker JG, Moukhametzianov R, Edwards PC, Henderson R, et al. Structure of a beta1-adrenergic G-protein-coupled receptor. *Nature*. 2008;454(7203):486-91.
12. Cherezov V, Rosenbaum DM, Hanson MA, Rasmussen SG, Thian FS, Kobilka TS, et al. High-resolution crystal structure of an engineered human beta2-adrenergic G protein-coupled receptor. *Science*. 2007;318(5854):1258-65.
13. Ratnala VR, Kobilka B. Understanding the ligand-receptor-G protein ternary complex for GPCR drug discovery. *Methods Mol Biol*. 2009;552:67-77.
14. Hauser M, Kauffman S, Lee BK, Naider F, Becker JM. The first extracellular loop of the *Saccharomyces cerevisiae* G protein-coupled receptor Ste2p undergoes a conformational change upon ligand binding. *J Biol Chem*. 2007;282(14):10387-97.
15. Javitch JA, Shi L, Liapakis G. Use of the substituted cysteine accessibility method to study the structure and function of G protein-coupled receptors. *Methods Enzymol*. 2002;343:137-56.
16. Karlin A, Akabas MH. Substituted-cysteine accessibility method. *Methods Enzymol*. 1998;293:123-45.

17. Marsh L. Substitutions in the hydrophobic core of the alpha-factor receptor of *Saccharomyces cerevisiae* permit response to *Saccharomyces kluyveri* alpha-factor and to antagonist. *Mol Cell Biol.* 1992;12(9):3959-66.
18. Umanah GK, Huang L, Ding FX, Arshava B, Farley AR, Link AJ, et al. Identification of residue-to-residue contact between a peptide ligand and its G protein-coupled receptor using periodate-mediated dihydroxyphenylalanine cross-linking and mass spectrometry. *J Biol Chem.* 2010;285(50):39425-36.
19. Son CD, Sargsyan H, Naider F, Becker JM. Identification of ligand binding regions of the *Saccharomyces cerevisiae* alpha-factor pheromone receptor by photoaffinity cross-linking. *Biochemistry.* 2004;43(41):13193-203.
20. Turcatti G, Nemeth K, Edgerton MD, Meseth U, Talabot F, Peitsch M, et al. Probing the structure and function of the tachykinin neurokinin-2 receptor through biosynthetic incorporation of fluorescent amino acids at specific sites. *J Biol Chem.* 1996;271(33):19991-8.
21. Sherman F. Getting started with yeast. *Methods Enzymol.* 1991;194:3-21.
22. Huang LY, Umanah G, Hauser M, Son C, Arshava B, Naider F, et al. Unnatural amino acid replacement in a yeast G protein-coupled receptor in its native environment. *Biochemistry.* 2008;47(20):5638-48.
23. Slauch JM, Mahan MJ, Mekalanos JJ. Measurement of transcriptional activity in pathogenic bacteria recovered directly from infected host tissue. *Biotechniques.* 1994;16(4):641-4.

24. Raths SK, Naider F, Becker JM. Peptide analogues compete with the binding of alpha-factor to its receptor in *Saccharomyces cerevisiae*. *J Biol Chem*. 1988;263(33):17333-41.
25. David NE, Gee M, Andersen B, Naider F, Thorner J, Stevens RC. Expression and purification of the *Saccharomyces cerevisiae* a-factor receptor (Ste2p), a 7-transmembrane-segment G protein-coupled receptor. *Faseb Journal*. 1997;11(9):2805.
26. Pinson B, Chevallier J, Urban-Grimal D. Only one of the charged amino acids located in membrane-spanning regions is important for the function of the *Saccharomyces cerevisiae* uracil permease. *Biochem J*. 1999;339 ( Pt 1):37-42.
27. Choi Y, Konopka JB. Accessibility of cysteine residues substituted into the cytoplasmic regions of the alpha-factor receptor identifies the intracellular residues that are available for G protein interaction. *Biochemistry*. 2006;45(51):15310-7.
28. Shi C, Kaminskyj S, Caldwell S, Loewen MC. A role for a complex between activated G protein-coupled receptors in yeast cellular mating. *Proc Natl Acad Sci U S A*. 2007;104(13):5395-400.
29. Shi C, Kendall SC, Grote E, Kaminskyj S, Loewen MC. N-terminal residues of the yeast pheromone receptor, Ste2p, mediate mating events independently of G1-arrest signaling. *J Cell Biochem*. 2009;107(4):630-8.
30. Akal-Strader A, Khare S, Xu D, Naider F, Becker JM. Residues in the first extracellular loop of a G protein-coupled receptor play a role in signal transduction. *J Biol Chem*. 2002;277(34):30581-90.

31. Martin NP, Celic A, Dumont ME. Mutagenic mapping of helical structures in the transmembrane segments of the yeast alpha-factor receptor. *J Mol Biol.* 2002;317(5):765-88.
32. Shah A, Marsh L. Role of Sst2 in modulating G protein-coupled receptor signaling. *Biochem Biophys Res Commun.* 1996;226(1):242-6.
33. Kim H, Lee BK, Naider F, Becker JM. Identification of specific transmembrane residues and ligand-induced interface changes involved in homo-dimer formation of a yeast G protein-coupled receptor. *Biochemistry.* 2009;48(46):10976-87.
34. Stefan CJ, Overton MC, Blumer KJ. Mechanisms governing the activation and trafficking of yeast G protein-coupled receptors. *Mol Biol Cell.* 1998;9(4):885-99.
35. Lin JC, Duell K, Konopka JB. A microdomain formed by the extracellular ends of the transmembrane domains promotes activation of the G protein-coupled alpha-factor receptor. *Mol Cell Biol.* 2004;24(5):2041-51.
36. Overton MC, Blumer KJ. The extracellular N-terminal domain and transmembrane domains 1 and 2 mediate oligomerization of a yeast G protein-coupled receptor. *J Biol Chem.* 2002;277(44):41463-72.
37. Reneke JE, Blumer KJ, Courchesne WE, Thorner J. *Cell.* 1988;55(null):221.
38. Yesilaltay A, Jenness DD. Homo-oligomeric complexes of the yeast alpha-factor pheromone receptor are functional units of endocytosis. *Mol Biol Cell.* 2000;11(9):2873-84.
39. Li JH, Hamdan FF, Kim SK, Jacobson KA, Zhang X, Han SJ, et al. Ligand-specific changes in M3 muscarinic acetylcholine receptor structure detected by a disulfide scanning strategy. *Biochemistry.* 2008;47(9):2776-88.

40. Li JH, Han SJ, Hamdan FF, Kim SK, Jacobson KA, Bloodworth LM, et al. Distinct structural changes in a G protein-coupled receptor caused by different classes of agonist ligands. *J Biol Chem.* 2007;282(36):26284-93.
41. Ward SD, Hamdan FF, Bloodworth LM, Siddiqui NA, Li JH, Wess J. Use of an in situ disulfide cross-linking strategy to study the dynamic properties of the cytoplasmic end of transmembrane domain VI of the M3 muscarinic acetylcholine receptor. *Biochemistry.* 2006;45(3):676-85.
42. Yu H, Kono M, McKee TD, Oprian DD. A general method for mapping tertiary contacts between amino acid residues in membrane-embedded proteins. *Biochemistry.* 1995;34(46):14963-9.
43. Yu H, Kono M, Oprian DD. State-dependent disulfide cross-linking in rhodopsin. *Biochemistry.* 1999;38(37):12028-32.
44. Guo W, Shi L, Filizola M, Weinstein H, Javitch JA. Crosstalk in G protein-coupled receptors: changes at the transmembrane homodimer interface determine activation. *Proc Natl Acad Sci U S A.* 2005;102(48):17495-500.
45. Mancia F, Assur Z, Herman AG, Siegel R, Hendrickson WA. Ligand sensitivity in dimeric associations of the serotonin 5HT<sub>2c</sub> receptor. *EMBO Rep.* 2008;9(4):363-9.
46. Eilers M, Hornak V, Smith SO, Konopka JB. Comparison of class A and D G protein-coupled receptors: common features in structure and activation. *Biochemistry.* 2005;44(25):8959-75.
47. Karnik SS, Gogonea C, Patil S, Saad Y, Takezako T. Activation of G-protein-coupled receptors: a common molecular mechanism. *Trends Endocrinol Metab.* 2003;14(9):431-7.

48. Naider F, Becker JM. The alpha-factor mating pheromone of *Saccharomyces cerevisiae*: a model for studying the interaction of peptide hormones and G protein-coupled receptors. *Peptides*. 2004;25(9):1441-63..
49. Celic A, Connelly SM, Martin NP, Dumont ME. Intensive mutational analysis of G protein-coupled receptors in yeast. *Methods Mol Biol*. 2004;237:105-20.
50. Dohlman HG, Thorner J, Caron MG, Lefkowitz RJ. Model systems for the study of seven-transmembrane-segment receptors. *Annu Rev Biochem*. 1991;60:653-88.
51. Ho HH, Du D, Gershengorn MC. The N terminus of Kaposi's sarcoma-associated herpesvirus G protein-coupled receptor is necessary for high affinity chemokine binding but not for constitutive activity. *J Biol Chem*. 1999;274(44):31327-32.
52. Hawtin SR, Wesley VJ, Parslow RA, Simms J, Miles A, McEwan K, et al. A single residue (arg46) located within the N-terminus of the V1a vasopressin receptor is critical for binding vasopressin but not peptide or nonpeptide antagonists. *Mol Endocrinol*. 2002;16(3):600-9.
53. Hagemann IS, Narzinski KD, Floyd DH, Baranski TJ. Random mutagenesis of the complement factor 5a (C5a) receptor N terminus provides a structural constraint for C5a docking. *J Biol Chem*. 2006;281(48):36783-92.
54. Gurevich VV, Gurevich EV. How and why do GPCRs dimerize? *Trends Pharmacol Sci*. 2008;29(5):234-40.
55. Dong C, Wu G. Regulation of anterograde transport of alpha2-adrenergic receptors by the N termini at multiple intracellular compartments. *J Biol Chem*. 2006;281(50):38543-54.

56. Montesana PE, Konopka JB. Mutational analysis of the role of N-glycosylation in alpha-factor receptor function. *Biochemistry*. 2001;40(32):9685-94.
57. Akabas MH, Stauffer DA, Xu M, Karlin A. Acetylcholine receptor channel structure probed in cysteine-substitution mutants. *Science*. 1992;258(5080):307-10.
58. Javitch JA. Probing structure of neurotransmitter transporters by substituted-cysteine accessibility method. *Methods Enzymol*. 1998;296:331-46.
59. Mueckler M, Makepeace C. Analysis of transmembrane segment 8 of the GLUT1 glucose transporter by cysteine-scanning mutagenesis and substituted cysteine accessibility. *J Biol Chem*. 2004;279(11):10494-9.
60. Stauffer DA, Karlin A. Electrostatic potential of the acetylcholine binding sites in the nicotinic receptor probed by reactions of binding-site cysteines with charged methanethiosulfonates. *Biochemistry*. 1994;33(22):6840-9.
61. Prevost M, Vertongen P, Raussens V, Roberts DJ, Cnudde J, Perret J, et al. Mutational and cysteine scanning analysis of the glucagon receptor N-terminal domain. *J Biol Chem*. 2010;285(40):30951-8.
62. Lemaire K, Van de Velde S, Van Dijck P, Thevelein JM. Glucose and sucrose act as agonist and mannose as antagonist ligands of the G protein-coupled receptor Gpr1 in the yeast *Saccharomyces cerevisiae*. *Mol Cell*. 2004;16(2):293-9.
63. Chen S, Lin F, Xu M, Graham RM. Phe(303) in TMVI of the alpha(1B)-adrenergic receptor is a key residue coupling TM helical movements to G-protein activation. *Biochemistry*. 2002;41(2):588-96.
64. Xu W, Li J, Chen C, Huang P, Weinstein H, Javitch JA, et al. Comparison of the amino acid residues in the sixth transmembrane domains accessible in the binding-

- site crevices of mu, delta, and kappa opioid receptors. *Biochemistry*. 2001;40(27):8018-29.
65. Sen M, Marsh L. Noncontiguous domains of the alpha-factor receptor of yeasts confer ligand specificity. *J Biol Chem*. 1994;269(2):968-73.
66. Wang HX, Konopka JB. Identification of amino acids at two dimer interface regions of the alpha-factor receptor (Ste2). *Biochemistry*. 2009;48(30):7132-9.
67. Falke JJ, Dernburg AF, Sternberg DA, Zalkin N, Milligan DL, Koshland DE, Jr. Structure of a bacterial sensory receptor. A site-directed sulfhydryl study. *J Biol Chem*. 1988;263(29):14850-8.
68. Srinivasan N, Sowdhamini R, Ramakrishnan C, Balaram P. Conformations of disulfide bridges in proteins. *Int J Pept Protein Res*. 1990;36(2):147-55.

### **Chapter 3**

**The N-terminus of *Saccharomyces cerevisiae* G protein-coupled receptor Ste2p is involved in negative regulation**

## **Abstract**

Yeast pheromone receptor Ste2p is a G protein-coupled receptor that initiates cellular responses to  $\alpha$ -mating pheromone, a 13-residue peptide. We have examined the role of the extracellular N-terminus of this receptor in signal transduction. Sequential deletion of the N-terminal residues affected cell surface expression without affecting ligand-binding affinity suggesting that the N-terminus is required for efficient cell surface targeting. Deletion of portions of the N-terminus was found to affect signaling activity as determined by quantitative FUS1-LacZ gene reporter induction assay. However, when the receptor surface expression levels of deletion mutants were taken into account, the signaling activity was found to increase. This provides evidence that the N-terminus of Ste2p is involved in the negative regulation of receptor signaling.

## Introduction

Signal transduction is a fundamental biological process that is essential to maintain cellular homeostasis and processes in all organisms. The cells' membrane proteins at the cell surface communicate between the extracellular and intracellular environments of the cell and respond accordingly to maintain cellular function. G protein-coupled receptors (GPCRs) represent one of the largest families of plasma membrane receptors in eukaryotes. More than 800 GPCRs are encoded in the human genomes (1,2). These receptors play central roles in human physiology and thus modifications in the signaling of these receptors are pertinent for many diseases or pathological conditions including cardiovascular and pulmonary diseases, pain perception, obesity, cancer, and neurological disorders. (3-5)

GPCRs share a common structural organization with an extracellular N-terminus, seven transmembrane domains connected by extracellular and intracellular loops, and a cytoplasmic C-terminus (6,7). Despite the diversity of their ligands and a lack of strong sequence similarity, the underlying mechanisms of signal transduction are similar as GPCRs couple the binding of ligands to the activation of specific heterotrimeric guanine nucleotide-binding proteins (G proteins) and/or non-G protein mediated signaling, leading to the modulation of downstream effector proteins and gene expression (8-10).

The GPCR superfamily of receptors is divided into several subgroups on the basis of phylogenetic criteria, conserved residues within the transmembrane helices and according to the size and characteristics of the N-terminal domain of its members. Historically, the bulk of attention of GPCR studies have focused on the transmembrane helices. However, a number of studies indicate that the N-terminus also plays an important role in receptor function (6,11,12). A conserved N-terminal cysteine network in class B secretin receptors stabilizes their structure, the

alteration of which impairs ligand interactions (13). Likewise, a diverse variety of N-terminal domain motifs in the N-terminal domain of class B adhesion receptors determine ligand specificity. The conserved N-terminal Venus flytrap domain in Class C glutamate receptors and N-terminal Wnt-binding domains in Frizzled/Smoothed receptors have been reported to regulate ligand binding and receptor activation (6,11,12,14). The N-terminal domain of protease-activated receptors (PARs) and glycoprotein hormone receptors (GpHRs) plays an important role in their activation (15,16). Recently, the N-terminus of GPR56, an adhesion G protein-coupled receptor that plays a key role in cortical development, has been reported to constrain receptor activity (17). Truncation of the N-terminus of several GPCRs including CB1 cannabinoid (18),  $\alpha_{1D}$  adrenergic (19) and GPR37 (20) has been shown to enhance cell surface expression.

Here we investigate the function of the N-terminus of the  $\alpha$ -factor pheromone receptor Ste2p of *Saccharomyces cerevisiae*, which has been studied as a model for peptide-responsive GPCRs (21,22). Although there has been considerable study of the extracellular and intracellular loops as well as the C-terminus and transmembrane domains of Ste2p, less is known about the role of the N-terminal domain in signaling. The N-terminus of Ste2p is ~48 amino acids long, and it harbors two glycosylation sites (N25 and N32) which were eliminated by mutation (N25A and N32A) without affecting receptor function (23). Other studies indicated that the N-terminus contributed to receptor dimerization(24,25), and three residues (Pro 15, Ile24, and Ile29) were found to be essential for mating but not for signaling as measured by growth arrest and reporter gene (*FUS1*) activation assays (26). Truncation of parts of the N-terminus implicated this domain in cellular fusion (mating) during late stages of conjugation of opposite mating types (26). We performed deletion mutagenesis on the N-terminus and analyzed the mutant receptors by protein expression, ligand binding, and signaling assays. The results showed that deletion of the N-

terminus affected the surface expression levels of the receptor and results in enhanced signaling activities of the receptor, suggesting that the N-terminus is involved in negative regulation of signaling.

## Methods

**Media, Reagents, Strains, and Plasmids:** *S. cerevisiae* strain LM102 [*MATa ste2 FUS1-lacZ::URA3 bar1 ura3 leu2 his4 trp1 met1*] (27) was used for growth arrest, *FUS1-lacZ* gene induction, mating and saturation binding assays, and the protease-deficient strain BJS21 [*MATa, prc1-407 prb1-1122 pep4-3 leu2 trp1 ura3-52 ste2::Kan<sup>R</sup>*] (8) was used for protein isolation to decrease receptor degradation during immunoblot analyses (28). *S. cerevisiae* strain DK102 [*MATa, Ste2::HIS3, bar1 ade2, trp1, ura3, his, leu2, lys2*] (29) was used for expression of the receptor under the control of Cu-inducible promoter *CUP1*. The plasmid pBEC2 containing C-terminal FLAG<sup>TM</sup> and His-tagged *STE2* (30) was transformed by the method of Geitz (31). The construction of pCUP1-BEC2 for expression of the C-terminal FLAG<sup>TM</sup>-His-tagged *STE2* under the *CUP1* promoter was done by inserting *CUP1* from plasmid pmCUPNMsGFPX (32) as the promoter of *STE2*. Yeast transformants were selected by growth on yeast minimal medium (33) lacking tryptophan and supplemented with casamino acids (10g/L, Research Products International Corp., Prospect, IL.) designated as MLT to maintain selection for the plasmid. The cells were cultured in MLT and grown to mid log phase at 30°C with shaking (200 rpm) for all assays. *S. cerevisiae* strain TBR1 [*MATα FLO11 ura3 his2 leu2*] (34) was used the opposite mating type (LM102 *MATa*) for mating assays. [ $\text{Lys}^7$  (7-nitrobenz-2-oxa-1,3-diazol-4-yl),Nle<sup>12</sup>] $\alpha$ -factor abbreviated as [K<sup>7</sup>(NBD),Nle<sup>12</sup>] $\alpha$ -factor was synthesized as previously described (35).

**Growth Arrest Assays:** *S. cerevisiae* LM102 cells, expressing Cys-less Ste2p and single Cys mutants, were grown at 30°C overnight in MLT, harvested, washed three times with water, and resuspended at a final concentration of  $5 \times 10^6$  cells/mL (36). Cells (1 mL) were combined with

3.5 mL of agar noble (1.1%) and poured as a top agar lawn onto a MLT medium agar plate. Filter disks (BD, Franklin Lakes, NJ) impregnated with  $\alpha$ -factor (4, 2, 1, 0.5, 0.25  $\mu\text{g}/\text{disk}$ ) were placed on the top agar. The plates were incubated at 30°C for 24h and then observed for clear halos around the disks. The experiment was repeated at least three times, and reported values represent the mean of these tests. For determination of growth arrest at various receptor expression levels, DK102 cells expressing receptors under the control of *CUP1* promoter were grown for 16 hrs at 30C in minimal media. Cells were mixed with various final concentrations of  $\text{CuSO}_4$  and poured onto agar plates with minimal media.

***FUS1-lacZ Gene Induction Assay:*** LM102 cells, expressing Cys-less Ste2p and single Cys mutants, were grown at 30 °C in selective media, harvested, washed three times with fresh media and resuspended at a final concentration of  $5 \times 10^7$  cells/mL. Cells (500  $\mu\text{l}$ ) were combined with  $\alpha$ -factor (final concentration of 1.0  $\mu\text{M}$ ; this concentration is expected to saturate all the receptors on the surface) and incubated at 30°C for 90 min. The cells were transferred to a 96-well flat bottom plate (Corning Incorporated, Corning, NY) in triplicate, permeabilized with 0.5% Triton X-100 in 25 mM PIPES buffer (pH 7.2) and then  $\beta$ -galactosidase assays were carried out using fluorescein di- $\beta$ -galactopyranoside (Molecular Probes, Inc., Eugene, OR) as a substrate as described previously (8,37). The reaction mixtures were incubated at 37°C for 60 min and 1.0 M  $\text{Na}_2\text{CO}_3$  was added to stop the reaction. The fluorescence of the samples (excitation of 485 nm and emission of 530 nm) was determined using a 96-well plate reader Synergy2 (BioTek Instruments, Inc., Winooski, VT). The data were analyzed using Prism software (GraphPad Prism version 5.03 for Windows, GraphPad Software, San Diego CA). The experiments were repeated at least three times and reported values represent the mean of these tests. For *FUS1-*

*LacZ* induction in DK102 cells expressing wild type Ste2p under the control of *CUP1* promoter, cells were grown overnight in minimal media containing adenine, histidine, tryptophan and lysine in the presence of various concentrations of CuSO<sub>4</sub> (0.1-200 μM) before incubation with α-factor.

**Whole cell radioligand binding experiments:** Tritiated [<sup>3</sup>H] α-factor (9.33 Ci/mmol) prepared as previously described previously (38) was used in saturation binding assays on whole cells. Cells (LM102) expressing wild type or mutant Ste2p were harvested, washed 3 times with YM1 (39), and adjusted to a final concentration of  $3 \times 10^7$  cells/mL. Cells (600 μL) were combined with 150 μL of ice-cold 5× binding medium (YM1 plus protease inhibitors [YM1i] (39) supplemented with [<sup>3</sup>H]α-factor and incubated at room temperature for 30 min. The final concentration of [<sup>3</sup>H]α-factor ranged from  $0.5 \times 10^{-10}$  to  $1 \times 10^{-6}$  M. Upon completion of the incubation interval, 200 μL aliquots of the cell-pheromone mixture were collected in triplicate on glass fiber filter mats and washed for 5 seconds with phosphate buffered saline, pH 7.4 using the Standard Cell Harvester (Skatron Instruments, Sterling, VA). Retained radioactivity on the filter was counted by liquid scintillation spectroscopy. Cells lacking Ste2p were used as a nonspecific binding control for the assays. Binding assays were repeated a minimum of three times, and similar results were observed for each replicate. Specific binding for each mutant receptor was calculated by subtracting the nonspecific values (radioactivity obtained from cells lacking receptor) from those obtained for total binding. Specific binding data were analyzed by nonlinear regression analysis for single-site binding using GraphPad Prism 5.04 (GraphPad Software, San Diego, CA) to determine the  $K_d$  and  $B_{max}$  values for each mutant receptor.

**Immunoblots:** BJS21 cells, expressing wild type or the N-terminal deletion mutants of Ste2p grown in MLT, were used to prepare total cell membranes isolated as previously described (39). Protein concentration was determined by the BioRad protein assay (BioRad, Hercules, CA)(30), and membranes were solubilized in sodium dodecyl sulfate (SDS) sample buffer (10% glycerol, 5% 2-mercaptoethanol, 1% SDS, 0.03% bromophenol blue, 62.5 mM Tris, pH 6.8). Proteins were fractionated by SDS-PAGE (10% acrylamide with 5% stacking gel) along with pre-stained Precision Plus protein standards (BioRad) and transferred to an Immobilon<sup>TM</sup>P membrane (Millipore Corp., Bedford, MA). The blot was probed with anti-FLAG<sup>TM</sup> M2 antibody (Sigma/Aldrich Chemical, St. Louis, MO), and bands were visualized with the West Pico chemiluminescent detection system (Pierce). The total intensity of all Ste2p bands in each lane was determined using a ChemiDoc XRS photodocumentation system with Quantity One one-dimensional analysis software (version 4.6.9, BioRad, Hercules, CA). Immunoblot experiments were repeated at least three times and yielded similar results. Constitutively-expressed membrane protein Pma1p was used as a loading control as described previously (40) using Pma1p antibody (Thermo Scientific, Rockford, IL).

**Deglycosylation of Membrane Proteins:** Total membrane proteins prepared as described above were resuspended in sodium phosphate (50 mM, pH 7.5), supplemented with 500 units of glycerol-free PNGase F (New England Biolabs, Inc., Beverly, MA), and incubated at 37 °C for 2 h. A negative control was run in parallel in which no enzyme was added prior to incubation at 37 °C. Upon termination of the incubation interval, the membranes were pelleted by centrifugation (15,000 × g, 10 min), and the resulting pellet was dissolved in SDS sample buffer. The samples were used for FLAG immunoblot analysis as described above.

**Quantitative Mating Assay:** *MATa* cells expressing various Ste2p constructs and *MATα* cells expressing wild type receptor were grown overnight at 30°C, harvested by centrifugation, resuspended in fresh YEPD, and counted using a hemocytometer. *MATa* cells ( $2 \times 10^6$ ) were mixed with *MATα* cells ( $1 \times 10^7$ ) in a final volume of 100 μL, incubated at 30°C for 5 hours, washed three times with water and resuspended in a final volume of 1 ml water. Then 20 μL of the cell suspension was plated on minimal media lacking lysine and tryptophan and containing histidine and leucine and incubated for 2 days at 30°C. Diploid colonies formed on the plates were counted and analyzed by using GraphPad Prism. This experiment was repeated at least three times and the mating efficiency was expressed as a percentage of diploid colonies formed by mating between the wild type *MATa* (LM102) and *MATα* (TBR1) strains.

**Flow Cytometry:** *S. cerevisiae* strain DK102 expressing wild type Ste2p under the control of *CUPI* promoter was grown for 16 hrs at 30C with various concentrations of CuSO<sub>4</sub> and washed three times with 15 mM sodium acetate buffer (pH 4.6) containing sodium azide. Cells were resuspended in the same buffer to a final concentration of  $1.5 \times 10^6$  cells/ml. Cells (500 μl of the suspension) were incubated with 1 μM final concentration of a fluorescent α-factor analogue [K<sup>7</sup>(NBD),Nle<sup>12</sup>]α-factor for 30 minutes at room temperature with end-over-end mixing. The cells were then washed three times with the same buffer containing sodium azide (10 mM) and 200 μl of this cell suspension were added into a well of a 96-well plate and analyzed on a EMD Millipore (MA, USA) flow cytometer (Guava 6HT-2L) using excitation at 488 nm and emission at 525/30 nm (as specified by the Guava instrument). The samples were protected from light during pre-incubations and flow cytometry analysis. The mean fluorescence intensity obtained at various concentrations of CuSO<sub>4</sub> was used to calculate relative cell surface expression. The mean

fluorescence data obtained from the Guava were analyzed by GraphPad Prism using non-linear regression analysis.

## Results

### *The mutant receptors are expressed but differentially glycosylated:*

To gain insight into the role of the N-terminus of the yeast  $\alpha$ -factor receptor Ste2p in receptor function, we set out to identify specific regions in the N-terminus that influence receptor function (See Figure 3.1 for Ste2p snake diagram). For this purpose, we carried out deletion mutagenesis of the region between residues S2 to Y30 generating five mutants [Ste2p $\Delta$ 2-10, Ste2p $\Delta$ 11-20, Ste2p $\Delta$ 21-30, Ste2p $\Delta$ 2-20 and Ste2p $\Delta$ 2-30 (Figure 3.2)] on the backbone of the full-length, Cys-less receptor (Ste2p-C52S and C259S) with a His and FLAG tag extending from the C-terminus of Ste2p that we refer to herein as the wild type (Figure 3.1). Previous studies have established that this “wild-type” receptor was equivalent in expression and activity to the naturally occurring wild-type Ste2p (25,30,41). All mutants as well as the wild type receptor were expressed from a high copy yeast expression vector under the control of the constitutive *GPD* promoter (8,30).

To test the mutant receptor expression, total membranes were prepared from yeast carrying each of the mutant constructs and the wild type control, the membrane proteins were solubilized and run on SDS-PAGE, immunoblotted, and probed with FLAG<sup>TM</sup> antibody (Figure 3.3). As a loading control for immunoblot experiments, the same immunoblots were washed and re-probed with antibody against the constitutively expressed membrane protein Pma1p. The experiment was repeated at least three times with similar results obtained in each experiment. Wild type Ste2p (Lane 2) appeared as a set of three major bands between 50 and 55 kDa, plus small amounts of higher molecular weight dimers (~100 kD) and oligomers, as observed in many previous studies, for example (30,42,43). Based on the primary amino acid sequence of the FLAG- and His-tagged receptor construct used in this study, the predicted molecular mass is

50.8 kDa (30). Glycosylation of the protein has been shown to result in the disparity of molecular weights of the Ste2p monomer (23,30,44,45).

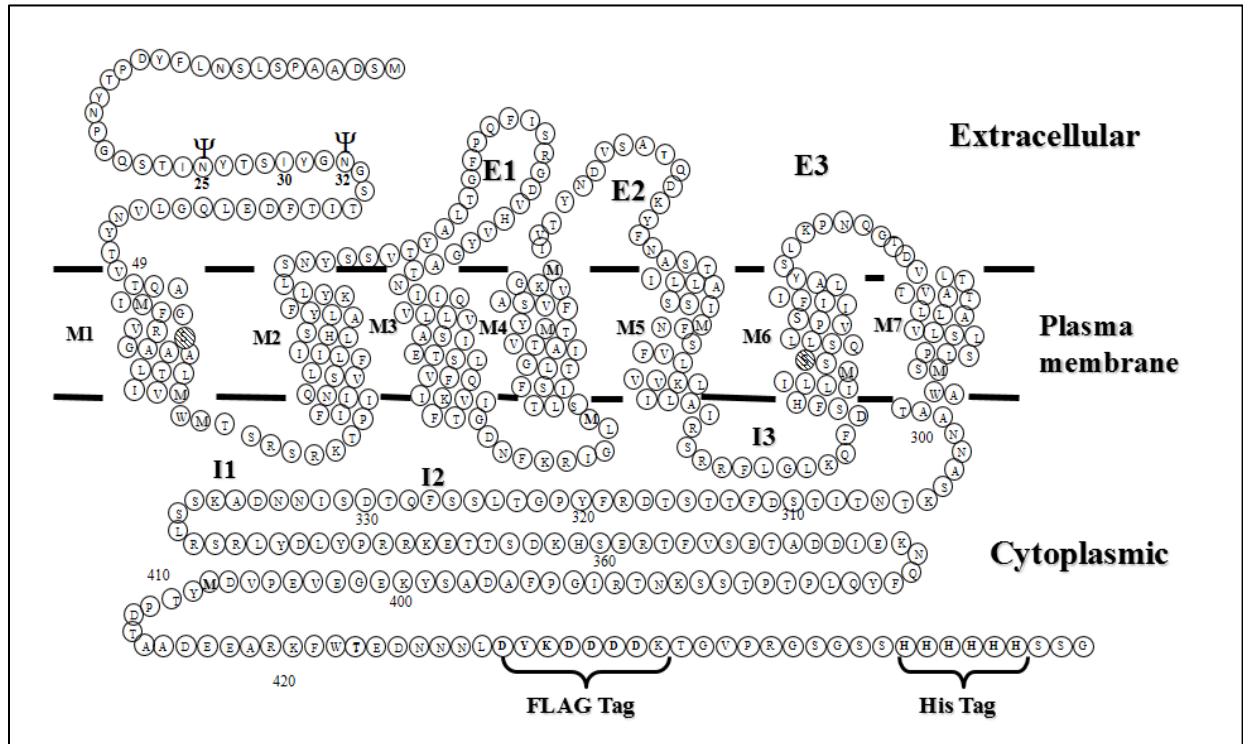


**Figure 3.1. Diagram of Ste2p.** The transmembrane domains are shown between the two parallel lines indicating the leaflets of the lipid bilayer. The intracellular and extracellular boundaries for the transmembrane domains are based on information obtained by SCAM analysis as reported previously (46). The receptor residues are numbered from the N terminus (residue 1) to the C terminus (residue 458) and include the inserted FLAG and His epitope tags (residues 432– 439 and 450 – 455, respectively), and spacer residues between the FLAG and His tags in the C-terminal portion. The two endogenous Cys residues mutated to Ser to generate the Cys-less Ste2p background are indicated by cross-hatching in TM1 and TM6.



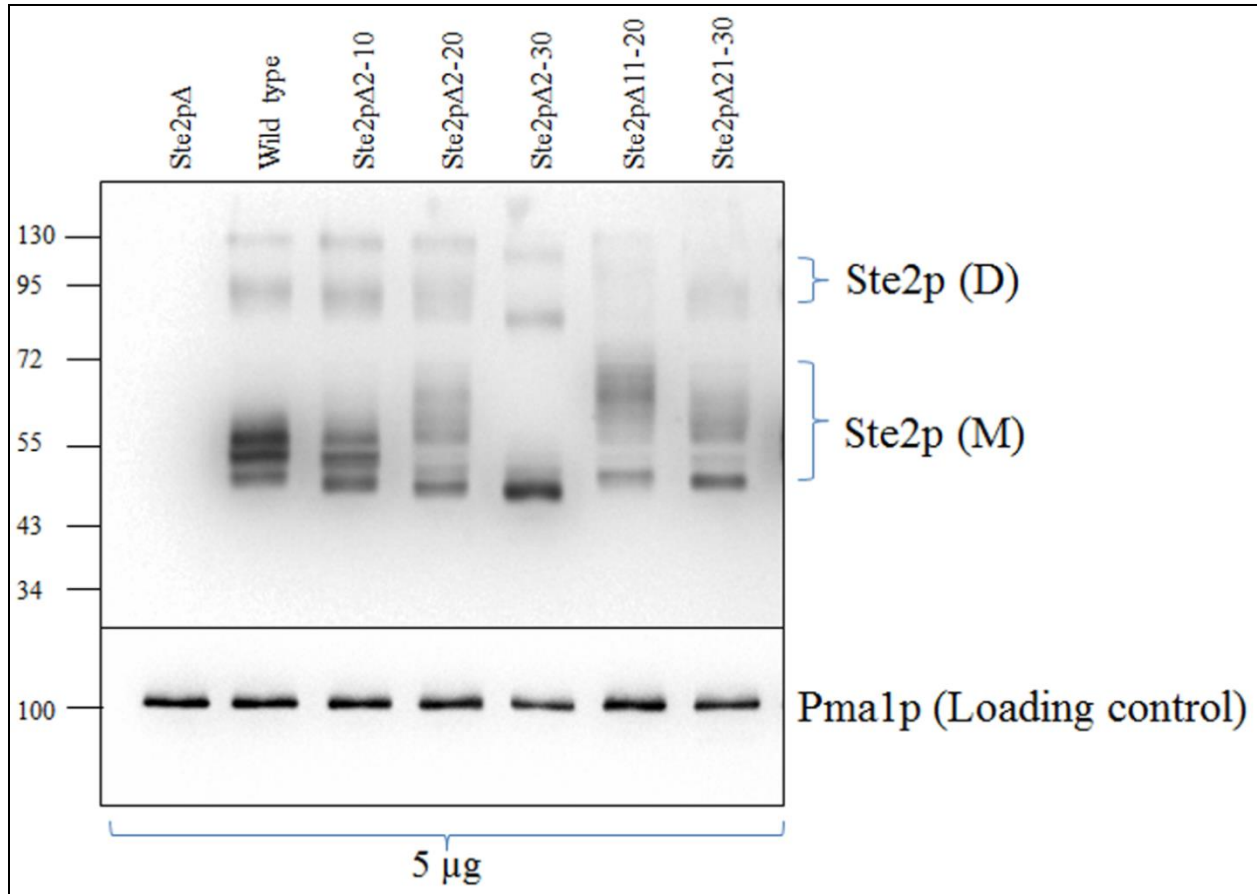


**Figure 3.3. Ste2p total expression levels. Proteins were solubilized from total membranes (5  $\mu$ g) prepared from cells expressing various N-terminal deletion mutants (Ste2p $\Delta$ 2-10, Ste2p $\Delta$ 2-20, Ste2p $\Delta$ 2-30, Ste2p $\Delta$ 11-20, Ste2p $\Delta$ 21-30) and the wild type receptor and run on a SDS-PAGE gel and immunoblotted using antibody against the C-terminal FLAG<sup>TM</sup> epitope tag. M and D indicate the monomeric and dimeric forms of Ste2p, respectively. Molecular mass markers (kDa) are indicated on the left-hand side. The same blot was stripped and then re-probed with anti-Pma1p antibody as a loading control.**

The expression level of each mutant receptor in the total membrane preparation was determined from the FLAG-reactive bands in each lane (monomer, dimer, and higher molecular weight bands), the loading in each lane was normalized to the Pma1p control, and then the expression levels were compared to the wild type receptor, the wild type receptor expression level was considered 100%). The total membrane expression levels were found to range from 54% (Ste2p $\Delta$ 2-30) to 81% (Ste2p $\Delta$ 11-20) of the wild type.

In addition to the reduced levels of expression, the mutants Ste2p $\Delta$ 2-20, Ste2p $\Delta$ 2-30, Ste2p $\Delta$ 11-20, and Ste2p $\Delta$ 21-30 exhibited altered banding patterns as compared with the wild type (Figure 3.3; Figure 3.4 lanes designated by C). We postulated that the different banding patterns were due to differential glycosylation of the mutant receptors as the two glycosylation sites of the receptor (N25 and N32) are located either within or adjacent to the deletion sites. To test this assumption, membranes were prepared from the mutants as well as the wild type cells, treated with PNGase F at 37°C to deglycosylate the receptor, and the banding pattern was examined. The higher molecular weight forms (greater than 130Kda) of Ste2p are attributable to receptor aggregation as a result of the incubation of the sample at 37°C for 2 hours which are conditions necessary for the deglycosylation reaction [Figure 3.4, Lanes (-) and Lanes (+)]. The aggregation of the receptor is likely responsible for the significant reduction in the overall intensity of the Ste2p monomer band after the treatment (Compare lanes C and \_ or + in Figure 3.4). Such temperature-dependent aggregation has been observed previously by our lab (30). The results indicated that the variability in the number of bands was diminished after PNGaseF treatment with most receptors exhibiting a prominent single band and the aforementioned high MW aggregate near the top of the gel (except Ste2p $\Delta$ 2-30 which was not glycosylated) (Figure

3.4). The collapse of the multiple bands at 50-55 kDa into one major band at about 50 kDa after PNGaseF treatment has been reported previously (23,30).

**Table 3.1. Total expression, surface expression and binding affinity of Ste2p N-terminal deletion mutants**

Receptors	Relative total expression levels <sup>a</sup>	Relative $B_{\max}$ <sup>b</sup>	Relative $K_d$ <sup>c</sup>
Wild type	1.00 ± 0.07	1.00 ± 0.08	1.00 ± 0.16
Ste2pΔ2-10	0.79 ± 0.08	0.89 ± 0.07	1.33 ± 0.22
Ste2pΔ2-20	0.62 ± 0.06	0.31 ± 0.02	1.18 ± 0.17
Ste2pΔ11-20	0.81 ± 0.07	0.26 ± 0.03	0.93 ± 0.22
Ste2pΔ21-30	0.56 ± 0.06	0.17 ± 0.03	1.48 ± 0.49
Ste2pΔ2-30	0.54 ± 0.05	0.09 ± 0.01	1.00 ± 0.23

<sup>a</sup>Relative total expression level (±SEM) of the N-terminal deletion mutants of Ste2p. Ste2p band intensity was quantitated by Quantity One software (BioRad) and normalized to the Pma1p band intensity (for protein loading on the gel) and the Cys-less wild type receptor. Expression level of each receptor was calculated as

$$\left\{ \frac{\text{Ste2p mutant band intensity}}{\text{Pma1p band intensity of the mutant}} \right\} \times \left\{ \frac{\text{Pma1p band intensity of Cys-less WT}}{\text{Ste2p Cys-less WT band intensity}} \right\}$$

<sup>b</sup>Relative surface expression (±SEM) of N-terminal deletion mutants of Ste2p. Surface expression was determined by saturation binding assay using tritiated [<sup>3</sup>H] α-factor with whole cells. The relative surface expression was expressed as  $\frac{\text{Bmax value of the mutant}}{\text{Bmax value of the Cys-less WT receptor}}$

<sup>c</sup>The  $K_d$  values (±SEM) are presented relative to those of the Cys-less wild type receptor. The  $K_d$  was determined by saturation binding of radioactive α-factor according to the protocol described in experimental procedures. ( $K_d$  of wild type receptor was 21.93 nM).

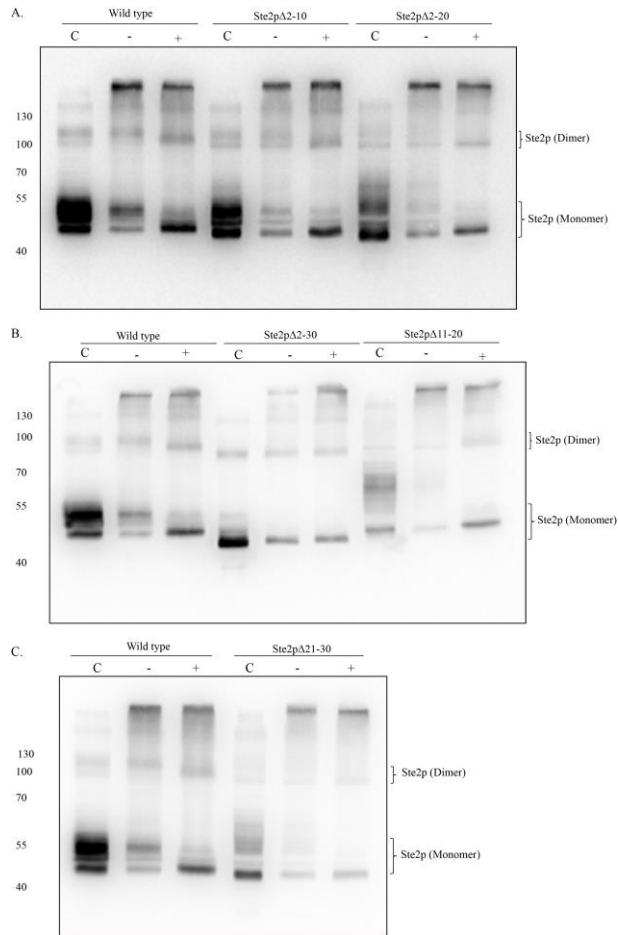


**Figure 3.4. Deglycosylation of N-terminal deletion mutants of Ste2p. Total membrane proteins derived from cells expressing wild-type or deletion mutant receptors indicated were treated (+) with PNGase F as described under “Experimental Procedures” or incubated in parallel in the absence of enzyme (-) to control for degradation or aggregation which might occur as a result of exposure to elevated temperature. The proteins were then analyzed by immunoblot analysis using the anti-FLAG antibody. In control lanes (C) membrane proteins were solubilized directly into denaturing sample buffer immediately prior to SDS-PAGE and subsequent immunoblot analysis. Molecular mass markers (kDa) are indicated on the left-hand side of each panel. The prominent bands visible at ~50 kDa corresponds to the monomeric forms of glycosylated Ste2p, whereas deglycosylated receptor (Ste2p, degly-M) appears as a band of reduced molecular weight.**

***The N-terminus is important for efficient surface expression but not required for ligand-binding:***

The immunoblot analysis measured total receptor expression in the membrane fraction, but it did not provide information regarding receptor expression on the cell surface. Consequently, the surface expression of the mutants was determined by whole cell saturation binding assays using [<sup>3</sup>H]α-factor as described previously (39,41,47). The B<sub>max</sub> values from the saturation binding curves (Figure 3.5) were used to calculate the number of receptors on the cell surface (47). The surface expression level of Ste2pΔ2-10 was approximately 90% of the wild type, but the surface expression levels of the other mutants were significantly lower (p= 0.05) and varied between 9% (Ste2pΔ2-30) and 31% (Ste2pΔ2-20) of the wild type (**Table 3.1**). These results indicate that receptors with N-terminal deletions are well expressed as judged by total expression levels but they exhibited reduced cell surface expression. The involvement of the N-terminus in surface expression is consistent with our previous study (25) and those of others (48,49).

The binding affinities of the receptors as determined by whole cell saturation binding assays (30,39) were not significantly different (p= 0.05) from the wild type receptor (**Table 3.1**). These results indicated that the N-terminus was not directly involved in ligand binding and did not influence the formation of the ligand-binding pocket which is consistent with the observation by Sen and Marsh that the N-terminus of Ste2p was not involved in determining ligand specificity (50).

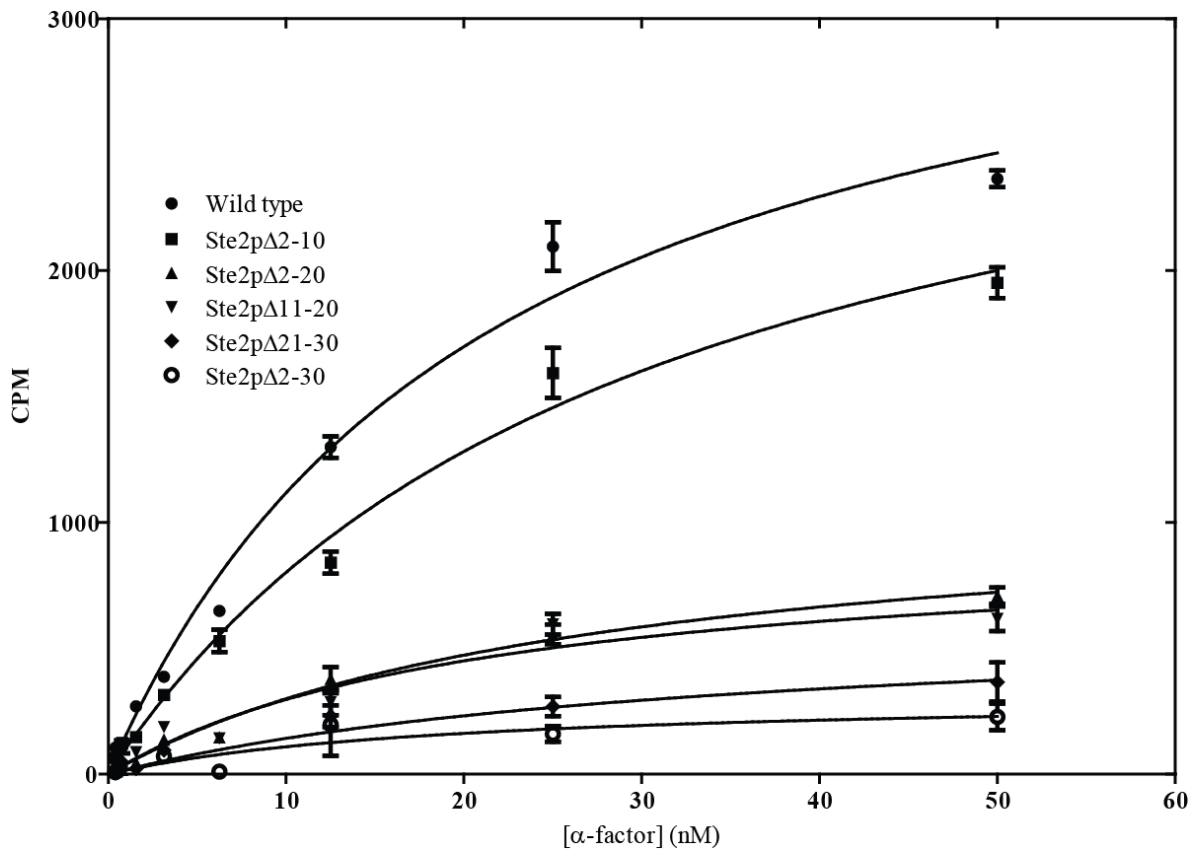


**Figure 3.5. Saturation binding of [ $^3\text{H}$ ] $\alpha$  factor to various N-terminally deleted Ste2p. Whole cell saturation binding assay of [ $^3\text{H}$ ] $\alpha$ -factor to wild type Ste2p and N-terminal deletion mutants were determined. From these saturation curves the binding affinities were determined by nonlinear regression analysis using GraphPad Prism. The data represent specific binding to cells as determined by subtracting the binding to an isogenic strain lacking the receptor from binding to cells containing wild type or mutant Ste2p.**

***Deletion of portions of the N-terminal enhanced pheromone-induced signaling activity:***

To investigate the role of the N-terminus in signaling activities, we examined the mutant receptors by pheromone-induced growth arrest and *FUS1-LacZ* induction assays as well as quantitative mating assays. The growth arrest assay measures the response of cells expressing

Ste2p to arrest growth at the G1 phase based on the size of halos surrounding disks impregnated with various amounts of pheromone applied to lawn of pheromone-responsive cells. This assay measures response over a 24 to 48 h time frame. The *FUS1-LacZ* induction assay measures an early response (1 to 2 h) of the yeast cells to pheromone as detected by induction of  $\beta$ -galactosidase activity through a reporter gene construct consisting of a fusion between *FUS1*, a pheromone-responsive promoter, and the *LacZ* gene (51). Mating assays measure the ability of the cells to conjugate with cells of the opposite mating type producing diploid cells. The number of diploid colonies formed as a result of mating between the two mating types can be compared to that of the wild type indicating mating efficiency. The signaling responses of the mutants in each experiment were normalized to those of the wild type (Figures 3.6, 3.7, 3.8 and **Table 3.2**).

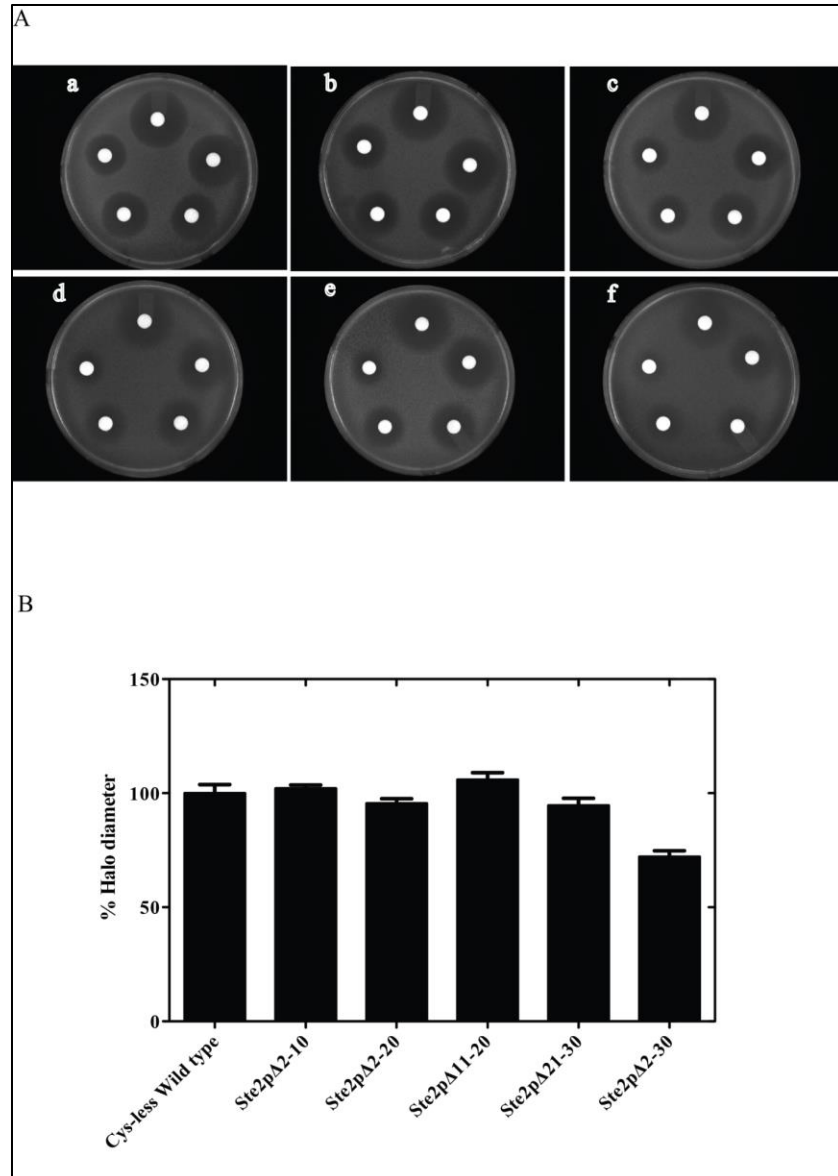


**Figure 3.6. (A) Growth arrest (halo) assays of wild type and deletion mutant receptors. Cells containing wild type Ste2p or cells with N-terminally truncated Ste2p were plated onto medium. Disks containing  $\alpha$ -factor (4.0, 2.0, 1.0, 0.5, and 0.25  $\mu$ g/disk, starting at the 12 O'clock position on each plate and moving clockwise) were placed onto the lawn of cells. The plates were incubated for 48–72 h at 30°C: a) wild type, b) Ste2p $\Delta$ 2-10, c) Ste2p $\Delta$ 11-20 d) Ste2p $\Delta$ 21-30 e) Ste2p $\Delta$ 2-20, f) Ste2p $\Delta$ 2-30. (B) Halo size produced by the wild type and various mutants at 1.0  $\mu$ g  $\alpha$ -factor was compared.**

In growth arrest assays, the halo diameter produced by the same amount of ligand was compared (Figure 3.6B & **Table 3.2**). The results showed that the growth arrest responses of the mutants were nearly the same as those of the wild type, with the exception of Ste2p $\Delta$ 2-30 which had a 25% decrease in halo diameter compared to the wild type at 1.0  $\mu$ g  $\alpha$ -factor (Figure 3.6B). Although the number of receptors on the cell surface of the mutants was different (**Table 3.1**), the growth arrest activity of the mutants was similar with the exception of Ste2p $\Delta$ 2-30. Therefore, the growth arrest response in the N-terminal deletion mutants was not proportional to the level of receptor expressed on the surface.

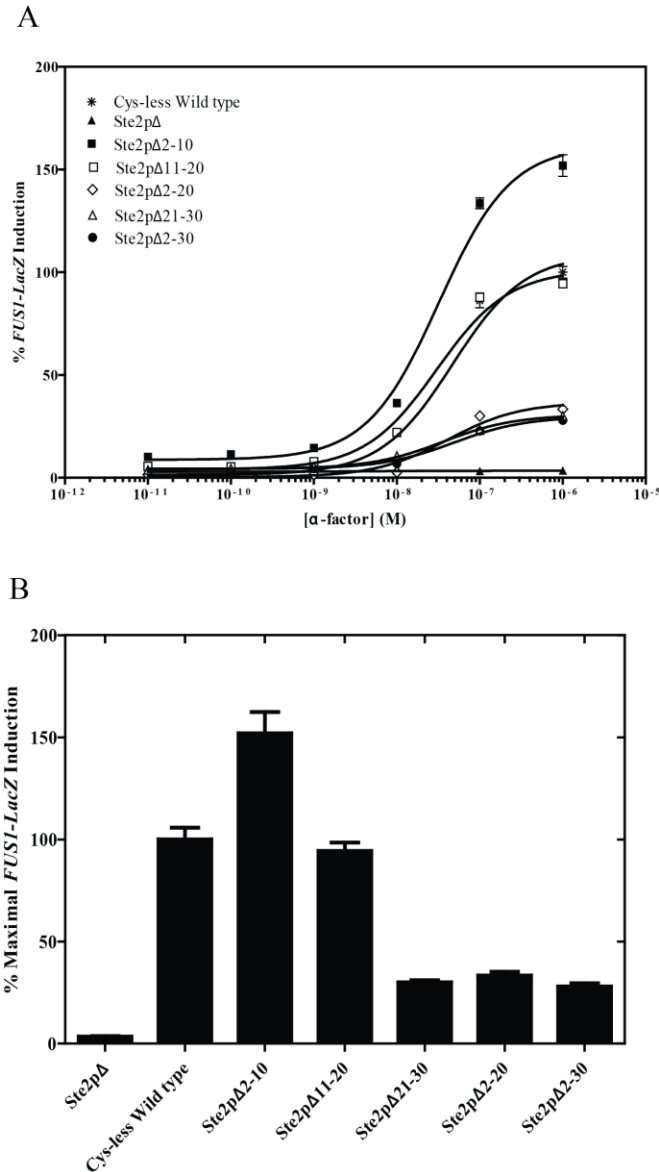


**Figure 3.7. (A). Phormone-induced *FUS1-LacZ* induction. Dose-response curves for  $\alpha$ -factor stimulated *FUS1-lacZ* induction of the N-terminal deletion mutants. Data are expressed as a percentage of the maximal response stimulated by the full length wild type receptor. (B). Maximal induction (%) is determined from the data on panel A with the highest concentration of  $\alpha$ -factor (1  $\mu$ M). Results represent average from three independent experiments performed in quadruplicate. One-way ANOVA followed by Dunnett's post hoc test was used to determine statistical significance ( $n = 4$ ;  $p < 0.05$ ).**

In *FUS1-LacZ* induction assays (**Table 3.2** and Figure 3.7A) all mutant receptors exhibited potencies ( $EC_{50}$  values) similar, not less than or greater than 30%, of that of wild type receptor. Maximal responses produced by the mutants reflect efficacy (intrinsic activity) of the receptors. In contrast, potency ( $EC_{50}$ ), the molar concentration of an agonist required to produce 50% of the maximal response to the agonist, reflects a complex function of both efficacy and affinity. Therefore, increased maximal signaling by Ste2p $\Delta$ 2-10 indicates that deletion of the residues 2-10 in the N-terminus enhances the intrinsic signaling activity of the receptor. Also constitutive signaling, as measured by gene reporter activity in the absence of added  $\alpha$ -factor, was the same as wild type for each receptor (data not shown). In contrast, the maximal signaling activity or efficacy, (*FUS1-LacZ* expression obtained at  $1 \times 10^{-6}$  M  $\alpha$ -factor) exhibited variation among the receptors with signaling between 28% (Ste2p $\Delta$ 2-30) and 152% (Ste2p $\Delta$ 2-10) of the wild type (**Table 3.2** and Figure 3.7). Out of the five mutants tested, Ste2p $\Delta$ 2-20, Ste2p $\Delta$ 21-30, and Ste2p $\Delta$ 2-30 exhibited a significant decrease in signaling ( $p < 0.05$ ), Ste2p $\Delta$ 11-20 exhibited similar activity as the wild type and Ste2p $\Delta$ 2-10 appeared to increase the signaling activity.

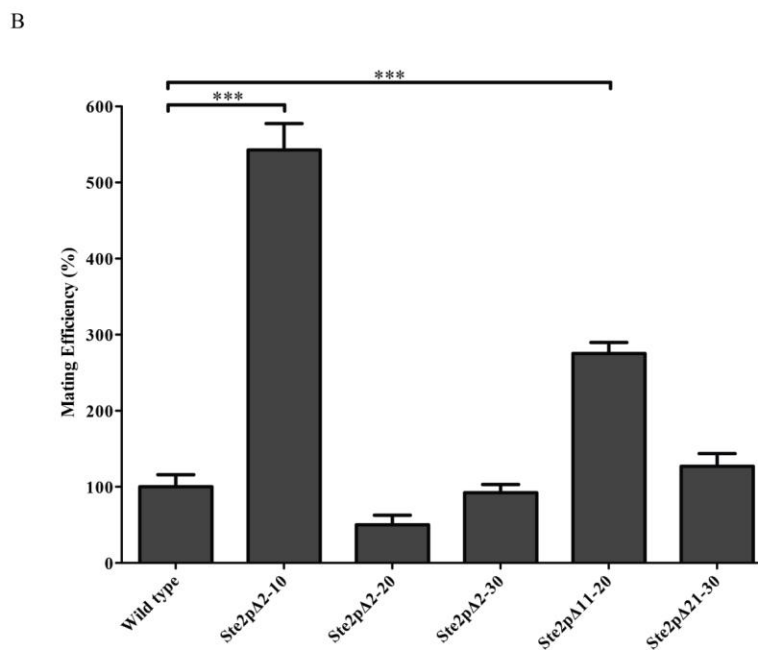
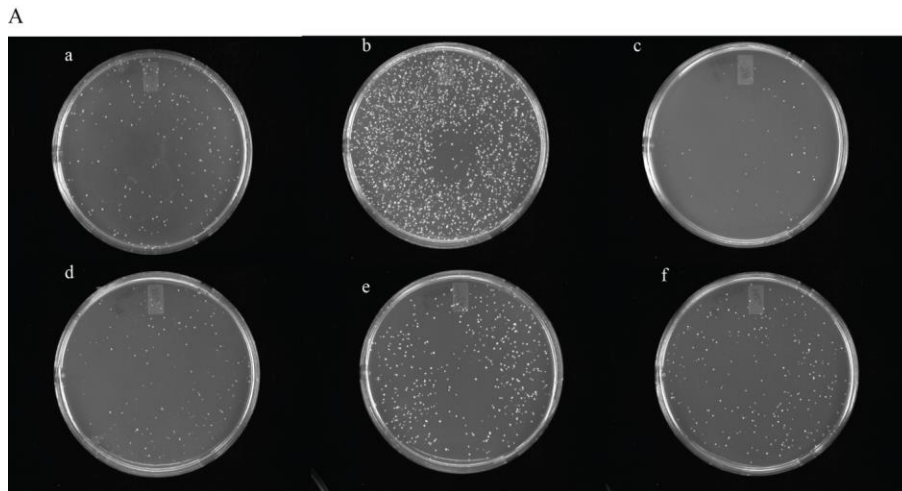


**Figure 3.8. (A).** Auxotrophic *MAT $\alpha$*  strain (TBR1 was mated with *MAT $\alpha$*  *STE2 $\Delta$*  yeast strain (LM012) expressing wild type (a) Ste2pΔ2-10 (b), Ste2pΔ2-20 (c) Ste2pΔ21-30 (d), Ste2pΔ11-20 (e) and Ste2pΔ2-30 (f). **(B).** Mating efficiency of the strains were analyzed and compared to that of the wild type. Statistical significance was analyzed at  $p < 0.001$  by using GraphPad Prism.

The two mutants Ste2p $\Delta$ 2-10 and Ste2p $\Delta$ 11-20 exhibited enhanced mating efficiency ( $p < 0.001$ ) (Figure 3.8). Statistical analyses revealed that the mating efficiency of the Ste2p $\Delta$ 2-20, Ste2p $\Delta$ 2-30, and Ste2p $\Delta$ 21-30 was not significantly different from that of the wild type at  $p < 0.001$ .

**Table 3.2. Signaling activities of Ste2p mutants.**

Receptors	Relative growth arrest activity <sup>a</sup>	Relative maximal <i>FUS1-LacZ</i> Induction <sup>b</sup>	EC <sub>50</sub> (nM) <sup>c</sup>	Maximal <i>FUS1-LacZ</i> induction/Surface expression <sup>d</sup>
Wild type	1.00 ± 0.05	1.00 ± 0.06	46 ± 5	1.00 ± 0.06
Ste2pΔ2-10	1.02 ± 0.04	1.52 ± 0.01	32 ± 4	1.7 ± 0.08
Ste2pΔ2-20	0.96 ± 0.04	0.39 ± 0.03	56 ± 2	1.3 ± 0.07
Ste2pΔ11-20	1.06 ± 0.05	0.94 ± 0.04	36 ± 3	3.6 ± 0.30
Ste2pΔ21-30	0.95 ± 0.05	0.30 ± 0.01	44 ± 1	1.8 ± 0.18
Ste2pΔ2-30	0.72 ± 0.04	0.28 ± 0.02	48 ± 1	3.1 ± 0.20

<sup>a</sup>Relative growth arrest activity (halo size ±SEM) was compared to that of the Cys-less wild type receptor at 1.0 μg of α-factor applied to a disk (the halo size of the Cys-less wild type was 23mm).

<sup>b</sup>Relative maximal *FUS1-LacZ* induction (±SEM) of each mutant was calculated with respect to Cys-less wild type receptor when induced with the highest concentration of α-factor (1 μM).

<sup>c</sup>Determined from *FUS1-lacZ* assays. EC<sub>50</sub> (potency) reflects the concentration of α-factor required to cause half-maximal induction.

<sup>d</sup>Maximal *FUS1-LacZ* induction of each mutant was normalized to its surface expression level and compared to that of the Cys-less wild type.

We have shown that deletion of portions of the N-terminal tail of Ste2p decreased the surface expression level of mutant receptors without any significant change in their binding affinities (**Table 3.1**). Although surface expression of Ste2p has been found to affect signaling activity as determined by *FUS1-LacZ* reporter assay (Figure 3.7), the calculated signaling activities do not take into account the level of surface expression. Therefore, to compare the signaling activities of the mutants based on the cell surface expression the maximal *FUS1-LacZ* activation was normalized to the amount of receptor on the cell surface as determined by saturation binding experiments. Interestingly, although the apparent signaling activity of the mutants was weaker than that of the wild type, this normalization revealed that the maximum *FUS1-LacZ* response of the mutants was in fact stronger than the wild type (Figure 3.9). We observed that truncation of the N-terminus significantly enhanced the relative *FUS1-LacZ* response by 2- to 3-fold. Thus, receptors lacking portions of the N-terminus are actually more effective with respect to signaling than the wild type.

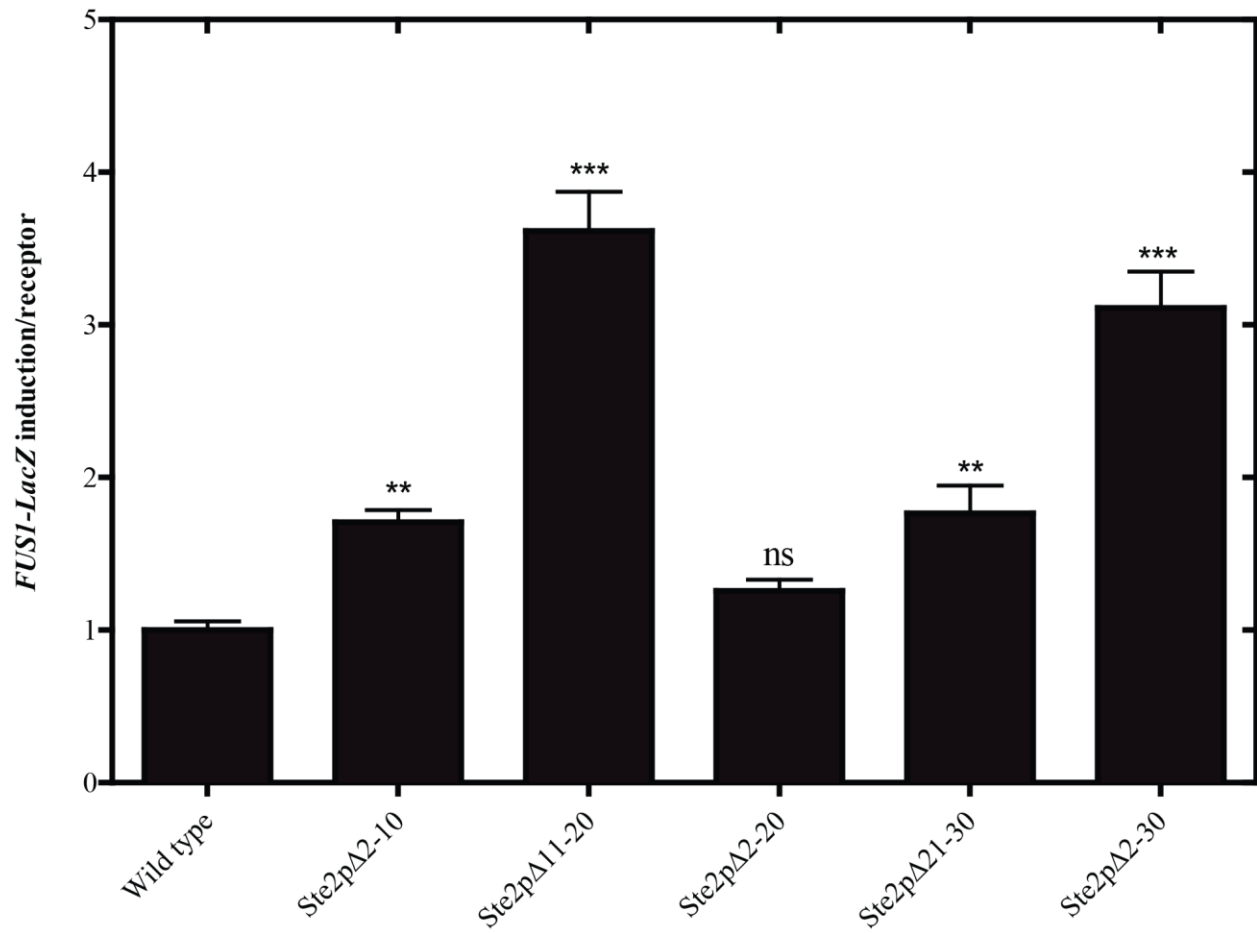


**Figure 3.9. Normalized *FUS1-LacZ* activity of each receptor construct as compared the wild type. The maximal signaling activity of each construct was normalized to the number of receptors expressed on the cell surface. One way ANOVA was carried out at  $p < 0.05$  to determine statistical significance using GraphPad Prism**

In order to further evaluate the relationship of signaling to surface expression of various Ste2ps, we ascertained the surface expression and signaling activity with the same wild type receptor expressed at various levels. The wild type Ste2p was expressed under the control of Copper-inducible promoter *CUP1* from the *URA3* based plasmid pCBEC2 (52). We performed growth arrest and *FUS1-LacZ* assays to determine if there was any correlation between the surface expression level and signaling activities. Relative surface expression levels at various concentrations of  $\text{CuSO}_4$  was determined using a fluorescent  $\alpha$ -factor analogue  $[\text{K}^7(\text{NBD}),\text{Nle}^{12}]\alpha$ -factor (35,53) by flow cytometer. We were able to regulate the surface expression level of Ste2p in a dose-dependent manner such that incubation with increasing concentrations of  $\text{CuSO}_4$  led to increasing the amount of  $[\text{K}^7(\text{NBD}),\text{Nle}^{12}]\alpha$ -factor on the surface as measured by mean fluorescence intensity (Figure 3.10). As judged from Figure 3.10B, there was a large increase in the number of receptors at 50  $\mu\text{M}$   $\text{CuSO}_4$ .

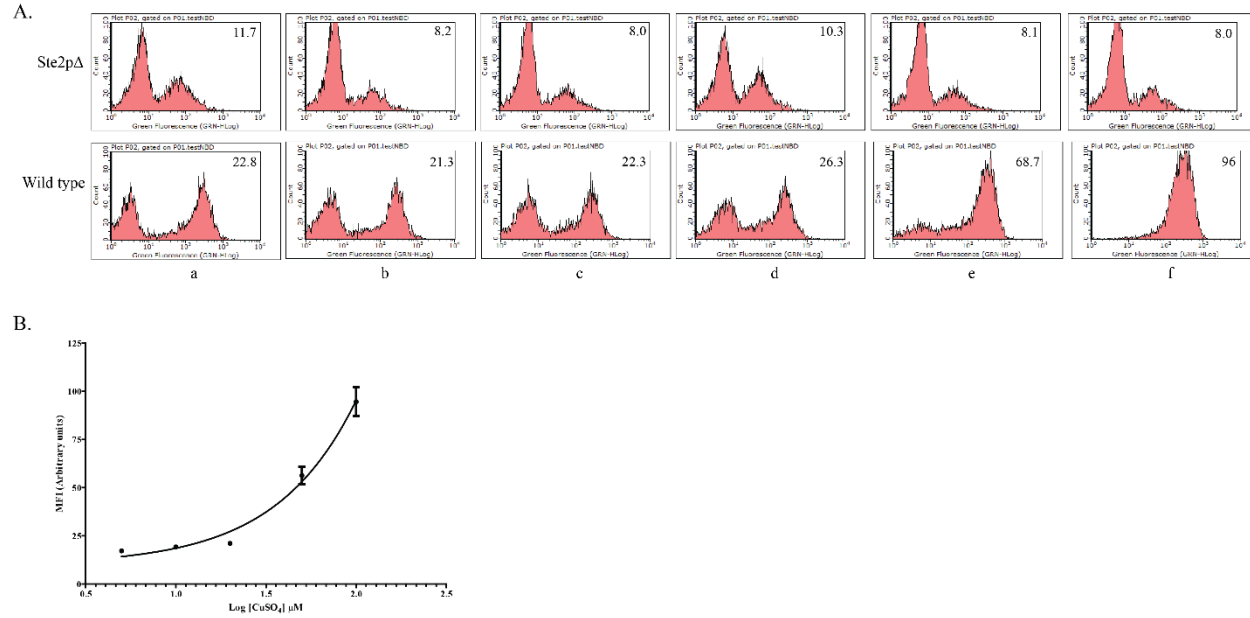


**Figure 3.10. Receptor expression level at the cell surface determined by flow Cytometry. (Wild type Ste2p expressed under the control of copper-inducible promoter at different concentrations of CuSO<sub>4</sub>. A) FACS histograms of cells expressing no receptors (top panels) and wild type (bottom panels) in the presence of saturating concentration of the ligand. The concentrations of CuSO<sub>4</sub> (μM) were 0 (a), 5 (b), 10 (c), 20 (d), 50 (e) and 100 (f) B). The histograms represent the number of cells (Y-axis) plotted against the fluorescence intensity (X-axis). The mean fluorescence intensity obtained from the histograms (insert number, upper right hand corner of histograms) was analyzed using non-linear regression analysis in GraphPad Prism.**

Growth arrest assay indicated that the halos were turbid with indistinct edges at lower receptor expression levels. However, at higher expression levels, the halos were less turbid with distinct edges (Figure 3.11A). The results indicated that halo size was similar at the various concentrations of  $\text{CuSO}_4$  used in the experiment. The result is consistent with previous studies in which it has been shown that halo size produced by cells with different receptor expression level was similar (54). In *FUS1-LacZ* induction assays increasing signal was observed as the concentration of  $\text{CuSO}_4$  increased (Figure 3.11B).

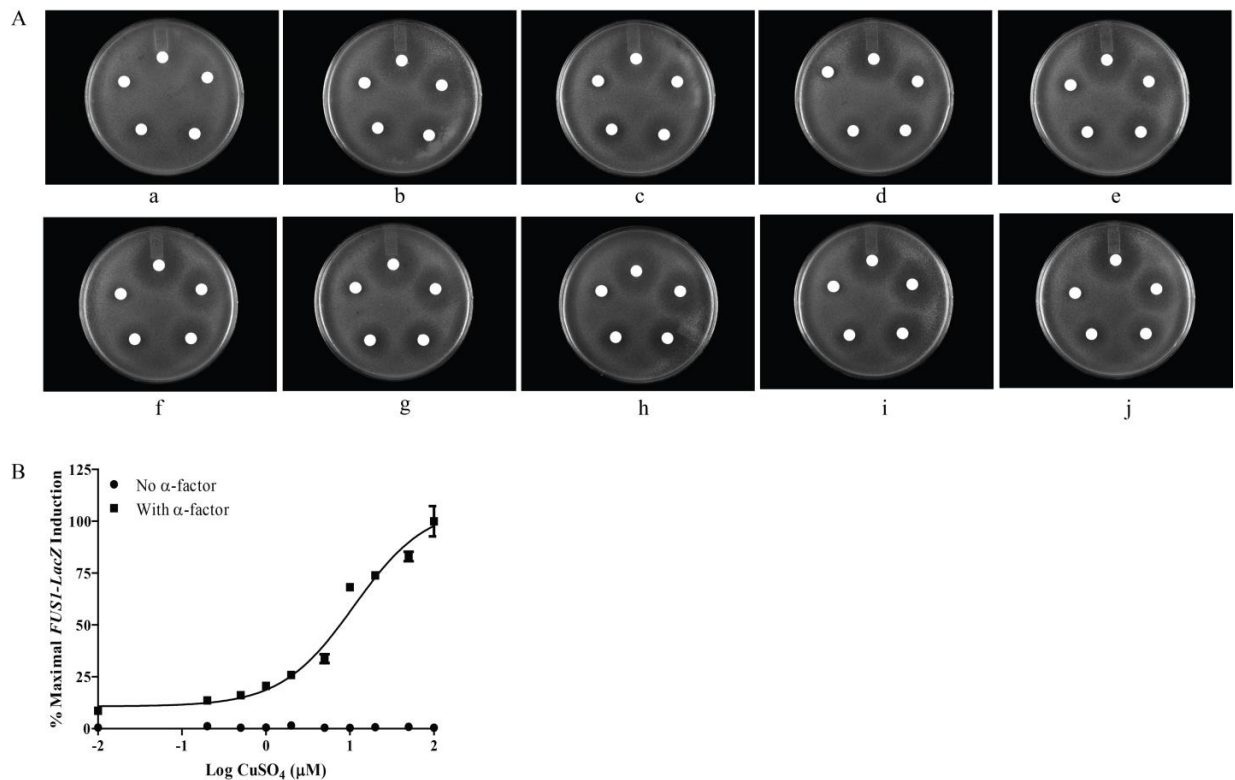


**Figure 3.11. Signaling activities of the wild type receptor expressed at different levels. (A) Growth arrest assay at various concentrations of CuSO<sub>4</sub> (μM): (a) 0 (No added CuSO<sub>4</sub>) (b) 0.2, (c) 0.5, (d) 1.0, (e) 2.0, (f) 5.0, (g) 10.0, (h) 20.0, (i) 50.0, (j) 100. (B) *FUS1-LacZ* induction at different concentrations of CuSO<sub>4</sub> (μM): 0 (no added CuSO<sub>4</sub>), 0.2, 0.5, 1.0, 2.0, 5.0, 10, 20, 50 and 100. Data from *FUS1-LacZ* assay were analyzed by non-linear regression analysis using GraphPad Prism.**

Detection of increase in *FUS1-LacZ* activity (Figure 3.11B) was more sensitive to lower CuSO<sub>4</sub> induction levels than was detection of surface expression of Ste2p (Figure 3.10A & B). These results supported our hypothesis that signaling activity judged by the gene induction assay is correlated to receptor expression levels, although this relationship is not clear at lower expression levels due to the inability of flow cytometry to detect receptor expression above the background level at CuSO<sub>4</sub> levels below 20 μM.

## Discussion

The N-termini of several GPCRs have been reported to play roles in receptor function such as constraining receptor activation (17) or acting as a tethered ligand (55). The N-terminus of Ste2p was previously associated with dimerization (24,25,56), mating (26,57) and as a site for glycosylation (23). Consistent with previous studies (49,50), we found that the N-terminus was important for cell surface expression but not required for ligand binding. Our experiments on the N-terminus indicated that deletion of N-terminal regions resulted in enhanced signaling as analyzed by *FUS1-LacZ* assays when normalized to Ste2p surface expression.

It is generally assumed that the signaling activity of Ste2p is independent of receptor expression level (45,58,59). This assumption was based on signaling activities determined by the growth arrest assay and direct measurement of surface receptor expression level determined by a binding assay (54). In addition, the Dumont group supported this conclusion based on their analysis of the *FUS1-LacZ* assay (43). However, interpretation of the Gehret *et al.* (43) experiments involving the signaling activity as determined by the *FUS1-LacZ* assay was complicated by the fact that only the total expression, not the surface expression of Ste2p, was evaluated for the two strains: Ste2p expressed from the normal chromosomal *STE2* locus versus Ste2p expressed under repressed condition from the *GALI* promoter (absence of galactose and the presence of glucose). The interpretation is also complicated by the concerns that receptor expression level on the cell surface and the number of G protein subunits available to interact with the activated receptor can affect the signaling activity. It has been reported that the number of G proteins is approximately equal to the number of receptors in cells containing normal chromosomal copies of the genes encoding receptors and G protein subunits (60-62). Therefore,

if the available G proteins are saturated with the receptors expressed on the surface, increasing the expression level of Ste2p beyond the available of G proteins will not increase signaling.

The *FUS1-LacZ* reporter gene assay has been used as a quantitative assay for measurement of pheromone-induced signaling through Ste2p and its mutants in numerous studies (27,47,51,63,64). Our analyses with wild type receptor expressed under the control of a copper-inducible promoter *CUPI* demonstrated that signaling activity as measured by *FUS1-LacZ* was dependent on the number of surface expressed receptors (Figure 3.10 & 3.11B). This observation is consistent with the idea that the signaling activity as determined by the *FUS1-LacZ* assay is dependent on the surface expression level of Ste2p. However, the signaling activity as determined by growth arrest assay does not correlate to the level of expression at the levels of copper used in the experiments (Figure 3.11). The difference in the two measurements of signaling activities indicates that the long-term growth arrest assay is relatively less responsive to the amount of receptor expressed at the cell surface. The apparent differences in the results of the two assays may be a consequence of difference in the level of receptor expression in cells grown in suspension versus cells grown on agar or the time frame of the assays.

Mutants that were found to exhibit the greatest reduction in cell surface expression demonstrated marked changes in the banding pattern for Ste2p on SDS-PAGE (Figures 3.3 and 3.4). It is probable that the changes in the banding pattern were due to altered glycosylation of the mutants because of either deletion of, or proximity to, the mutation of the two Ste2p glycosylation sites at N25 and N32. Accordingly, deglycosylation of the receptors resulted in the collapse of several bands into a major band which is consistent with previous studies in our lab (30) and others (23). However, removal of the two glycosylation sites does not affect receptor activity or subcellular localization (23). Thus reduced surface expression cannot be attributed

simply to changes in the glycosylation pattern of the receptors. It has been reported previously that the charged residues in the N-terminus are important for proper orientation of the receptor in the membrane (49). It is reasonable that a combination of the modification in the glycosylation pattern and changes in the electrostatic properties of the N-terminus influence the localization of Ste2p and its orientation in the plasma membrane.

Despite reduced surface expression and altered glycosylation, the mutant receptors were still functional, *i.e.*, they exhibited similar ligand binding affinity and responded to ligand effectively in both growth arrest and gene induction assays. When the signaling activities of the mutant Ste2ps were normalized to the number of receptors that bound  $\alpha$ -factor, the mutants actually exhibited a greater response than wild type. In fact the Ste2p $\Delta$ 11-20 and Ste2p $\Delta$ 2-30 mutants are more than 3-fold more effective than the full-length receptor in the signaling efficacies as measured by the reporter gene assay. Nevertheless, the activity of the Ste2p $\Delta$ 2-20 receptor was similar to wild type receptor showing that regulation by the N-terminus governing signaling response is complex and cannot be divided onto linear domains. Our control experiments with wild type receptor at various expression levels support the conclusion that maximal signaling activity as measured by gene reporter is dependent on receptor expression levels on the cell surface.

For measurement of signaling activities, we used pheromone-induced growth arrest and *FUS1-lacZ* assays. The growth arrest activities of the mutants were found to be similar to the wild type with the exception of Ste2p $\Delta$ 2-30. The reduced signaling of Ste2p $\Delta$ 2-30 mutant may be attributed to inefficient targeting to the membrane (49). However, this mutant construct still binds the ligand efficiently and signals. This mutant was reported previously to exhibit weaker growth arrest activity with indistinct halo edges as compared to ours (57). As shown in our

control experiment with the wild type receptor, the fuzzy halo may result from poor expression level on the cell surface (Figure 10A). The difference in the signaling activity by growth arrest may also be attributed to the differences in strain background and promoter used in our study as compared to that of *Shi, et al.* (57). We expressed the receptor from a constitutively active *GPD* promoter while they used an inducible *GALI* promoter. Further examination of signaling activities using a more sensitive, quantitative and shorter term reporter gene activation assay (*FUS1-LacZ*) revealed that the signaling activity of the mutants was enhanced as compared to the wild type when receptor expression levels at the cell surface are taken into account to normalize signaling activities.

The results from the gene induction assay (Figure 3.9) indicate that the N-terminus of Ste2p is involved in negative regulation of signaling activity by this GPCR. In fact, the N-terminus of another GPCR, GPR56, has been reported to constrain receptor activity (17). The N-terminus of GPR61, an orphan GPCR that is abundantly expressed in the brain, was also reported to be essential for constitutive activity (65). Thus the results from our analysis of the role of the N-terminus of Ste2p in its function, and those of others involving different mammalian GPCRs, indicate an increasing importance for the N-terminus in the biology of GPCRs. Although the N-terminus may not be essential for GPCR signaling, its role in the regulation of signaling has been ignored to some extent in previous studies. The N-terminus may be required for fine tuning the signaling process and thus may be an important drug target for future drug design studies in which the GPCR function can be regulated more specifically.

In order for the N-terminus to be involved in negative regulation of Ste2p signal transduction, it is likely that the N-terminus interacts with receptor domains that are important

for signal transduction. A secondary structure analysis suggested that regions of the N-terminus, in particular residues 20-30, have a strong tendency to form  $\beta$ -sheet structures, (25,57). It is possible that removal of portions of the N-terminal domain lowers either intramolecular interactions within Ste2p or intermolecular contacts with other domains of the Ste2p dimer (24,25). The sum of these  $\beta$ -sheet-like contacts may help to maintain the receptor in its inactive conformation and their removal would thereby facilitate transition to an activated state upon ligand binding. We speculate that the interacting domain with the N-terminus is the extracellular loop one (EL1) as mutation of residues in this loop has been found to change the glycosylation patterns of the receptor and its ability to be activated, and a structure prediction also indicates a tendency to form sheet secondary structures (30,57). However, we do not exclude the possibility of interactions with other Ste2p domains. Overall, this study demonstrates that important information about receptor regulation can be obtained from the study of the N-terminus.

## **Acknowledgments**

We thank Prof. Yury Chernoff, Georgia Tech University, for the pmCUPNMsGFPX plasmid as the source of the *CUPI* promoter. This research was supported by grant GM-22087 from the National Institute of General Medical Sciences, NIH.

## References

1. Venkatakrisnan, A. J., Deupi, X., Lebon, G., Tate, C. G., Schertler, G. F., and Babu, M. M. (2013) Molecular signatures of G-protein-coupled receptors. *Nature* **494**, 185-194
2. Fredriksson, R., Lagerstrom, M. C., Lundin, L. G., and Schioth, H. B. (2003) The G-protein-coupled receptors in the human genome form five main families. Phylogenetic analysis, paralogon groups, and fingerprints. *Molecular pharmacology* **63**, 1256-1272
3. O'Hayre, M., Vazquez-Prado, J., Kufareva, I., Stawiski, E. W., Handel, T. M., Seshagiri, S., and Gutkind, J. S. (2013) The emerging mutational landscape of G proteins and G-protein-coupled receptors in cancer. *Nature reviews. Cancer* **13**, 412-424
4. Salon, J. A., Lodowski, D. T., and Palczewski, K. (2011) The significance of G protein-coupled receptor crystallography for drug discovery. *Pharmacological reviews* **63**, 901-937
5. Kobilka, B. K. (2011) Structural insights into adrenergic receptor function and pharmacology. *Trends in pharmacological sciences* **32**, 213-218
6. Kristiansen, K. (2004) Molecular mechanisms of ligand binding, signaling, and regulation within the superfamily of G-protein-coupled receptors: molecular modeling and mutagenesis approaches to receptor structure and function. *Pharmacology & therapeutics* **103**, 21-80
7. Gether, U. (2000) Uncovering molecular mechanisms involved in activation of G protein-coupled receptors. *Endocrine reviews* **21**, 90-113
8. Umanah, G. K., Huang, L., Ding, F. X., Arshava, B., Farley, A. R., Link, A. J., Naider, F., and Becker, J. M. (2010) Identification of residue-to-residue contact between a peptide ligand and its G protein-coupled receptor using periodate-mediated dihydroxyphenylalanine cross-linking and mass spectrometry. *The Journal of biological chemistry* **285**, 39425-39436

9. Eilers, M., Hornak, V., Smith, S. O., and Konopka, J. B. (2005) Comparison of class A and D G protein-coupled receptors: common features in structure and activation. *Biochemistry* **44**, 8959-8975
10. Oldham, W. M., and Hamm, H. E. (2008) Heterotrimeric G protein activation by G-protein-coupled receptors. *Nature reviews. Molecular cell biology* **9**, 60-71
11. Kobilka, B. K. (2007) G protein coupled receptor structure and activation. *Biochimica et biophysica acta* **1768**, 794-807
12. Lagerstrom, M. C., and Schioth, H. B. (2008) Structural diversity of G protein-coupled receptors and significance for drug discovery. *Nature reviews. Drug discovery* **7**, 339-357
13. Beinborn, M. (2006) Class B GPCRs: a hidden agonist within? *Molecular pharmacology* **70**, 1-4
14. Ersoy, B. A., Pardo, L., Zhang, S., Thompson, D. A., Millhauser, G., Govaerts, C., and Vaisse, C. (2012) Mechanism of N-terminal modulation of activity at the melanocortin-4 receptor GPCR. *Nature chemical biology* **8**, 725-730
15. Scarborough, R. M., Naughton, M. A., Teng, W., Hung, D. T., Rose, J., Vu, T. K., Wheaton, V. I., Turck, C. W., and Coughlin, S. R. (1992) Tethered ligand agonist peptides. Structural requirements for thrombin receptor activation reveal mechanism of proteolytic unmasking of agonist function. *The Journal of biological chemistry* **267**, 13146-13149
16. Vassart, G., Pardo, L., and Costagliola, S. (2004) A molecular dissection of the glycoprotein hormone receptors. *Trends in biochemical sciences* **29**, 119-126
17. Paavola, K. J., Stephenson, J. R., Ritter, S. L., Alter, S. P., and Hall, R. A. (2011) The N terminus of the adhesion G protein-coupled receptor GPR56 controls receptor signaling activity. *The Journal of biological chemistry* **286**, 28914-28921
18. Andersson, H., D'Antona, A. M., Kendall, D. A., Von Heijne, G., and Chin, C. N. (2003) Membrane assembly of the cannabinoid receptor 1: impact of a long N-terminal tail. *Molecular pharmacology* **64**, 570-577

19. Hague, C., Chen, Z., Pupo, A. S., Schulte, N. A., Toews, M. L., and Minneman, K. P. (2004) The N terminus of the human alpha1D-adrenergic receptor prevents cell surface expression. *The Journal of pharmacology and experimental therapeutics* **309**, 388-397
20. Dunham, J. H., Meyer, R. C., Garcia, E. L., and Hall, R. A. (2009) GPR37 surface expression enhancement via N-terminal truncation or protein-protein interactions. *Biochemistry* **48**, 10286-10297
21. Dohlman, H. G., Thorner, J., Caron, M. G., and Lefkowitz, R. J. (1991) Model systems for the study of seven-transmembrane-segment receptors. *Annual review of biochemistry* **60**, 653-688
22. Slessareva, J. E., and Dohlman, H. G. (2006) G protein signaling in yeast: new components, new connections, new compartments. *Science* **314**, 1412-1413
23. Montesana, P. E., and Konopka, J. B. (2001) Mutational analysis of the role of N-glycosylation in alpha-factor receptor function. *Biochemistry* **40**, 9685-9694
24. Overton, M. C., and Blumer, K. J. (2002) The extracellular N-terminal domain and transmembrane domains 1 and 2 mediate oligomerization of a yeast G protein-coupled receptor. *The Journal of biological chemistry* **277**, 41463-41472
25. Uddin, M. S., Kim, H., Deyo, A., Naider, F., and Becker, J. M. (2012) Identification of residues involved in homodimer formation located within a beta-strand region of the N-terminus of a Yeast G protein-coupled receptor. *Journal of receptor and signal transduction research* **32**, 65-75
26. Shi, C., Kendall, S. C., Grote, E., Kaminskyj, S., and Loewen, M. C. (2009) N-terminal residues of the yeast pheromone receptor, Ste2p, mediate mating events independently of G1-arrest signaling. *Journal of cellular biochemistry* **107**, 630-638
27. Marsh, L. (1992) Substitutions in the hydrophobic core of the alpha-factor receptor of *Saccharomyces cerevisiae* permit response to *Saccharomyces kluyveri* alpha-factor and to antagonist. *Molecular and cellular biology* **12**, 3959-3966

28. Son, C. D., Sargsyan, H., Naider, F., and Becker, J. M. (2004) Identification of ligand binding regions of the *Saccharomyces cerevisiae* alpha-factor pheromone receptor by photoaffinity cross-linking. *Biochemistry* **43**, 13193-13203
29. Dohlman, H. G., Goldsmith, P., Spiegel, A. M., and Thorner, J. (1993) Pheromone action regulates G-protein alpha-subunit myristoylation in the yeast *Saccharomyces cerevisiae*. *Proceedings of the National Academy of Sciences of the United States of America* **90**, 9688-9692
30. Hauser, M., Kauffman, S., Lee, B. K., Naider, F., and Becker, J. M. (2007) The first extracellular loop of the *Saccharomyces cerevisiae* G protein-coupled receptor Ste2p undergoes a conformational change upon ligand binding. *The Journal of biological chemistry* **282**, 10387-10397
31. Turcatti, G., Nemeth, K., Edgerton, M. D., Meseth, U., Talabot, F., Peitsch, M., Knowles, J., Vogel, H., and Chollet, A. (1996) Probing the structure and function of the tachykinin neurokinin-2 receptor through biosynthetic incorporation of fluorescent amino acids at specific sites. *The Journal of biological chemistry* **271**, 19991-19998
32. Ganusova, E. E., Ozolins, L. N., Bhagat, S., Newnam, G. P., Wegrzyn, R. D., Sherman, M. Y., and Chernoff, Y. O. (2006) Modulation of prion formation, aggregation, and toxicity by the actin cytoskeleton in yeast. *Molecular and cellular biology* **26**, 617-629
33. Sherman, F. (1991) Getting started with yeast. *Methods in enzymology* **194**, 3-21
34. Reynolds, T. B., and Fink, G. R. (2001) Bakers' yeast, a model for fungal biofilm formation. *Science* **291**, 878-881
35. Bajaj, A., Celic, A., Ding, F. X., Naider, F., Becker, J. M., and Dumont, M. E. (2004) A fluorescent alpha-factor analogue exhibits multiple steps on binding to its G protein coupled receptor in yeast. *Biochemistry* **43**, 13564-13578
36. Huang, L. Y., Umanah, G., Hauser, M., Son, C., Arshava, B., Naider, F., and Becker, J. M. (2008) Unnatural amino acid replacement in a yeast G protein-coupled receptor in its native environment. *Biochemistry* **47**, 5638-5648

37. Slauch, J. M., Mahan, M. J., and Mekalanos, J. J. (1994) Measurement of transcriptional activity in pathogenic bacteria recovered directly from infected host tissue. *BioTechniques* **16**, 641-644
38. Rath, S. K., Naider, F., and Becker, J. M. (1988) Peptide analogues compete with the binding of alpha-factor to its receptor in *Saccharomyces cerevisiae*. *The Journal of biological chemistry* **263**, 17333-17341
39. David, N. E., Gee, M., Andersen, B., Naider, F., Thorner, J., and Stevens, R. C. (1997) Expression and purification of the *Saccharomyces cerevisiae* alpha-factor receptor (Ste2p), a 7-transmembrane-segment G protein-coupled receptor. *The Journal of biological chemistry* **272**, 15553-15561
40. Pinson, B., Chevallier, J., and Urban-Grimal, D. (1999) Only one of the charged amino acids located in membrane-spanning regions is important for the function of the *Saccharomyces cerevisiae* uracil permease. *The Biochemical journal* **339 ( Pt 1)**, 37-42
41. Umanah, G. K., Huang, L. Y., Maccarone, J. M., Naider, F., and Becker, J. M. (2011) Changes in conformation at the cytoplasmic ends of the fifth and sixth transmembrane helices of a yeast G protein-coupled receptor in response to ligand binding. *Biochemistry* **50**, 6841-6854
42. Wang, H. X., and Konopka, J. B. (2009) Identification of amino acids at two dimer interface regions of the alpha-factor receptor (Ste2). *Biochemistry* **48**, 7132-7139
43. Gehret, A. U., Connelly, S. M., and Dumont, M. E. (2012) Functional and physical interactions among *Saccharomyces cerevisiae* alpha-factor receptors. *Eukaryotic cell* **11**, 1276-1288
44. Jenness, D. D., Li, Y., Tipper, C., and Spatrick, P. (1997) Elimination of defective alpha-factor pheromone receptors. *Molecular and cellular biology* **17**, 6236-6245
45. Blumer, K. J., Reneke, J. E., and Thorner, J. (1988) The STE2 gene product is the ligand-binding component of the alpha-factor receptor of *Saccharomyces cerevisiae*. *The Journal of biological chemistry* **263**, 10836-10842

46. Lin, J. C., Duell, K., and Konopka, J. B. (2004) A microdomain formed by the extracellular ends of the transmembrane domains promotes activation of the G protein-coupled alpha-factor receptor. *Molecular and cellular biology* **24**, 2041-2051
47. Akal-Strader, A., Khare, S., Xu, D., Naider, F., and Becker, J. M. (2002) Residues in the first extracellular loop of a G protein-coupled receptor play a role in signal transduction. *The Journal of biological chemistry* **277**, 30581-30590
48. Overton, M. C., Chinault, S. L., and Blumer, K. J. (2003) Oligomerization, biogenesis, and signaling is promoted by a glycoprotein A-like dimerization motif in transmembrane domain 1 of a yeast G protein-coupled receptor. *The Journal of biological chemistry* **278**, 49369-49377
49. Harley, C. A., and Tipper, D. J. (1996) The role of charged residues in determining transmembrane protein insertion orientation in yeast. *The Journal of biological chemistry* **271**, 24625-24633
50. Sen, M., and Marsh, L. (1994) Noncontiguous domains of the alpha-factor receptor of yeasts confer ligand specificity. *The Journal of biological chemistry* **269**, 968-973
51. Trueheart, J., Boeke, J. D., and Fink, G. R. (1987) Two genes required for cell fusion during yeast conjugation: evidence for a pheromone-induced surface protein. *Molecular and cellular biology* **7**, 2316-2328
52. Gebhart, D., Bahrami, A. K., and Sil, A. (2006) Identification of a copper-inducible promoter for use in ectopic expression in the fungal pathogen *Histoplasma capsulatum*. *Eukaryotic cell* **5**, 935-944
53. Tantry, S., Ding, F. X., Dumont, M., Becker, J. M., and Naider, F. (2010) Binding of fluorinated phenylalanine alpha-factor analogues to Ste2p: evidence for a cation-pi binding interaction between a peptide ligand and its cognate G protein-coupled receptor. *Biochemistry* **49**, 5007-5015
54. Shah, A., and Marsh, L. (1996) Role of Sst2 in modulating G protein-coupled receptor signaling. *Biochemical and biophysical research communications* **226**, 242-246

55. Adams, M. N., Ramachandran, R., Yau, M. K., Suen, J. Y., Fairlie, D. P., Hollenberg, M. D., and Hooper, J. D. (2011) Structure, function and pathophysiology of protease activated receptors. *Pharmacology & therapeutics* **130**, 248-282
56. Shi, C., Paige, M. F., Maley, J., and Loewen, M. C. (2009) In vitro characterization of ligand-induced oligomerization of the *S. cerevisiae* G-protein coupled receptor, Ste2p. *Biochimica et biophysica acta* **1790**, 1-7
57. Shi, C., Kaminskyj, S., Caldwell, S., and Loewen, M. C. (2007) A role for a complex between activated G protein-coupled receptors in yeast cellular mating. *Proceedings of the National Academy of Sciences of the United States of America* **104**, 5395-5400
58. Reneke, J. E., Blumer, K. J., Courchesne, W. E., and Thorner, J. (1988) The carboxy-terminal segment of the yeast alpha-factor receptor is a regulatory domain. *Cell* **55**, 221-234
59. Konopka, J. B., Jenness, D. D., and Hartwell, L. H. (1988) The C-terminus of the *S. cerevisiae* alpha-pheromone receptor mediates an adaptive response to pheromone. *Cell* **54**, 609-620
60. Yi, T. M., Kitano, H., and Simon, M. I. (2003) A quantitative characterization of the yeast heterotrimeric G protein cycle. *Proceedings of the National Academy of Sciences of the United States of America* **100**, 10764-10769
61. Hao, N., Yildirim, N., Wang, Y., Elston, T. C., and Dohlman, H. G. (2003) Regulators of G protein signaling and transient activation of signaling: experimental and computational analysis reveals negative and positive feedback controls on G protein activity. *The Journal of biological chemistry* **278**, 46506-46515
62. Bardwell, L. (2005) A walk-through of the yeast mating pheromone response pathway. *Peptides* **26**, 339-350
63. Dube, P., and Konopka, J. B. (1998) Identification of a polar region in transmembrane domain 6 that regulates the function of the G protein-coupled alpha-factor receptor. *Molecular and cellular biology* **18**, 7205-7215

64. Mathew, E., Bajaj, A., Connelly, S. M., Sargsyan, H., Ding, F. X., Hajduczok, A. G., Naider, F., and Dumont, M. E. (2011) Differential interactions of fluorescent agonists and antagonists with the yeast G protein coupled receptor Ste2p. *Journal of molecular biology* **409**, 513-528
65. Toyooka, M., Tujii, T., and Takeda, S. (2009) The N-terminal domain of GPR61, an orphan G-protein-coupled receptor, is essential for its constitutive activity. *Journal of neuroscience research* **87**, 1329-1333

## **Chapter 4**

**Formation of Ste2p dimers by a conserved tyrosine residue in the N-terminus that has multiple contacts with the extracellular loop 1**

## **Abstract**

Ste2p, a *Saccharomyces cerevisiae* G protein-coupled receptor (GPCR) that responds to the 13 amino acid-peptide,  $\alpha$ -factor pheromone, initiates the yeast mating pathway after ligand binding. This receptor has been used as a model to understand the molecular mechanism of signal transduction by GPCRs, which play essential roles in signal transduction in eukaryotes. Single and double cysteine mutants of Ste2p were analyzed by disulfide cross-linking to determine intramolecular and intermolecular interactions. A conserved tyrosine residue (Y26) in the extracellular N-terminus was found to be a part of a Ste2p dimer intermolecular interface. Y26-mediated dimerization was hindered by mutations at V109 and T114, two residues in the extracellular loop 1 (ECL1), suggesting an interaction between Y26 and V109 or T114. The amount of Ste2p dimerization was affected by ligand binding suggesting a conformational change in the N-terminus of the receptor upon activation. In this study we identified a specific residue in the N-terminus that is involved in dimerization, found interactions between the N-terminus and ECL1, and suggested that the N-terminus changes conformational upon receptor activation.

## Introduction

Transmission of extracellular signals across the plasma membrane by receptor-mediated signaling is one of the most fundamental biological processes. G protein-coupled receptors (GPCRs) are by far the largest and most versatile signaling molecules on the cell surface that are involved in communication between the extracellular and intracellular environment of a cell. These receptors serve as highly versatile membrane sensors responding to a broad range of signals, including photons, hormones, neurotransmitters, ions and lipids (1-3) and translate them into cellular response. These receptors play crucial roles in many physiological and pathophysiological processes (4). Not surprisingly, GPCRs are therapeutic targets for a major portion of currently used drugs (1,5-8). The pharmacological relevance of these receptors is firmly established by the fact that approximately 30% of the known drugs on the market are designed to target GPCRs (9).

The structural hallmark of GPCRs is their seven transmembrane domains connected by alternating extracellular and intracellular loops. Ligand binding promotes a conformational change in the receptor that triggers the cellular response via intracellular transducers, the heterotrimeric ( $\alpha$ ,  $\beta$ ,  $\gamma$  subunits) guanine (G-) nucleotide binding proteins and/or  $\beta$ -arrestin (10). The conformational changes involve the movement of transmembrane domains (11-16). However, concomitant changes are also expected to occur in other domains of the receptor including the loop regions and the N- as well the C-termini.

Structurally, a GPCR can be divided into three parts: (i) the extracellular region consisting of the N-terminus and the three extracellular loops (ECL1-ECL3), (ii) the transmembrane domains (TM1-TM7), and (iii) the intracellular region consisting of three intracellular loops (ICL1-ICL3), an intracellular amphipathic helix (H8) that is part of the C-

terminus close to TM7, and the remaining portion of the C-terminus. Although all GPCRs contain these three distinct regions, the majority of studies have focused on the transmembrane helices. However, a growing number of studies indicate that the N-terminus also plays an important role in receptor function (17-20). For example, studies with class B secretin GPCRs indicate that the N-terminus is the ligand binding domain for these receptors (21). It has been proposed that binding of the cognate ligand to the N-terminus induces a conformational change in the receptor's N-terminus that enables a built-in agonist epitope to dock near the top of transmembrane domain 6 and this in turn triggers a conformational change in the heptahelical bundle, thereby initiating the downstream signaling (22). In class C glutamate receptors, the conserved N-terminal Venus flytrap module in the N-terminus has been reported to regulate ligand binding and receptor activation (17,19,20,23). The N-termini of protease-activated receptors (PARs) and glycoprotein hormone receptors (GpHRs) have also been associated with receptor activation (24,25). The N-terminus of adhesion G protein-coupled receptor GPR56 has been reported to constrain receptor activity (26). Truncation of the N-terminus of several GPCRs including CB1 cannabinoid (27),  $\alpha_{1D}$  adrenergic (28) and GPR37 (29) has been shown to enhance cell surface expression.

The *Saccharomyces cerevisiae* pheromone receptor Ste2p is a GPCR activated upon binding  $\alpha$  factor, a 13-residue peptide, triggering the activation of a cytoplasmic heterotrimeric G protein in *MATa* haploid cells (30). Ste2p has been used as a model for understanding structure-function relationships of GPCRs using the power of yeast genetics and analysis of the yeast pheromone response pathway. Although Ste2p lacks strong sequence similarity to mammalian GPCRs, some mammalian GPCRs have been expressed in yeast and are capable of activating the

yeast mating pathway (31,32). Ste2p also exhibits signaling when expressed in mammalian cells (33).

The N-terminus of Ste2p is ~50 amino acids long and contains two glycosylation sites, neither of which are essential for receptor function (34). The N-terminus was also reported to be involved in forming a domain for Ste2p dimerization (35,36). Previous studies of the first extracellular loop using the substituted cysteine accessibility method (SCAM) reported that several residues (L102C, N105C, S108C, Y111C and T114C) in this loop were inaccessible to the sulfhydryl reagent (MTSEA-biotin) used to assess accessibility (37). It was also reported that mutation of these residues to cysteine affected the glycosylation pattern of the receptor. Because two glycosylation sites of the receptor are located in the N-terminus at N25 and N32 (34) and the mutations in the ECL1 affected the glycosylation pattern, we hypothesize that the N-terminus interacts with ECL1. More recently, several residues in the N-terminus including Y26C, were also found to be inaccessible to MTSEA-biotin and the Y26C mutant also exhibited markedly increased dimerization (35). This residue is in the consensus sequence of N-glycosylation N-X-S/T (where X is any amino acid except Pro). The tyrosine in this position is conserved among the  $\alpha$ -factor receptors in several fungal species (Figure 4.1). This observation stimulated this investigation into whether ECL1 interacts with N-terminus.

## Materials and Methods

**Media, Reagents, Strains, and Plasmids:** The *Saccharomyces cerevisiae* strain LM102 [*MATa ste2 FUS1-lacZ::URA3 bar1 ura3 leu2 his4 trp1 met1*] (38) was used for growth arrest, *FUS1-lacZ* gene induction and saturation binding assays, and the protease-deficient strain BJS21 [*MATa, prc1-407 prb1-1122 pep4-3 leu2 trp1 ura3-52 ste2::Kan<sup>R</sup>*] (39) was used for protein isolation, immunoblot analyses, and disulfide cross-linking studies in order to lower receptor degradation during analysis. To facilitate disulfide cross-linking, plasmid pBEC2-FXa was constructed from plasmid pBEC2 containing a Cys-less Ste2p using primers to introduce tandem Factor Xa protease cleavage sites between residues T78 and P79 in ICL1 (37). The plasmid pBEC2-FXa containing C-terminal FLAG<sup>TM</sup> and His-tagged *STE2* with a tandem Factor Xa cleavage site was transformed by the method of Geitz (40). Transformants were selected by growth on yeast media (41) lacking tryptophan (designated as MLT) to maintain selection for the plasmid. The cells were cultured in MLT (2% glucose, 1% casamino acids (Research Products International Corp., IL, USA), 0.17% yeast nitrogen base without ammonium sulfate (Research Products International Corp., IL, USA), 0.5% ammonium sulfate (Research Products International Corp., IL, USA), amino acid dropout mix containing (arginine 0.026 g/L, asparagine 0.058 g/L, Aspartic acid 0.14 g/L, glutamic acid 0.14 g/L, histidine 0.028 g/L, isoleucine 0.058 g/L, leucine 0.083 g/L, lysine 0.042 g/L, methionine 0.028 g/L, phenylalanine 0.69 g/L, serine 0.52 g/L, threonine 0.28 g/L, tyrosine 0.042 g/L, valine 0.21 g/L, adenine sulfate 0.058 g/L, uracil 0.028 g/L) and grown to mid log phase at 30°C with shaking (200 rpm) for all assays.

### ***Growth Arrest Assays***

*S. cerevisiae* strain LM102 expressing Cys-less Ste2p (ICL1-Xa<sub>2</sub>) and Cys mutants were grown at 30°C overnight in MLT, harvested, washed three times with water, and resuspended to a final concentration of  $5 \times 10^6$  cells/mL (42). Cells (1 mL) were combined with 3.5 mL of agar noble (1.1%) and poured as a top agar lawn onto a MLT medium agar plate. Filter disks (BD, Franklin Lakes, NJ) impregnated with  $\alpha$ -factor (4, 2, 1, 0.5, and 0.25  $\mu$ g/disk) were placed on the top agar. The plates were incubated at 30°C for 24h and then observed for clear halos around the disks. The experiment was repeated at least three times, and reported values represent the mean of these tests.

### ***FUS1-lacZ Gene Induction Assay***

Cells expressing Cys-less Ste2p (ICL1-Xa<sub>2</sub>) and Cys mutants were grown at 30°C in MLT, harvested, washed three times with fresh medium and resuspended to a final concentration of  $5 \times 10^7$  cells/mL. Cells (500  $\mu$ l) were combined with  $\alpha$ -factor pheromone (final concentration of 1  $\mu$ M) and incubated at 30°C for 90 min. The cells were transferred to a 96-well flat bottom plate (Corning Incorporated, Corning, NY) in triplicate, permeabilized with 0.5% Triton X-100 in 25 mM PIPES buffer (pH 7.2) and then  $\beta$ -galactosidase assays were carried out using fluorescein di- $\beta$ -galactopyranoside (Molecular Probes, Inc., Eugene, OR) as a substrate as described previously (43). The reaction mixtures were incubated at 37°C for 60 min and 1.0 M Na<sub>2</sub>CO<sub>3</sub> was added to stop the reaction. The fluorescence of the samples (excitation of 485 nm and emission of 530 nm) was determined using a 96-well plate reader Synergy2 (BioTek Instruments, Inc., Winooski, VT). The data were analyzed using Prism software (GraphPad Prism version 6.02 for Windows, GraphPad Software, San Diego CA). The experiments were repeated at least three times and reported values represent the mean of these tests.

### ***Binding Assays***

Cells (LM102) expressing different receptor constructs were grown at 30°C for ~20 hours at 30°C with shaking. Fifty  $\mu\text{L}$  of cells were reinoculated into fresh medium and grown for ~16 hours to an OD of ~1.8. Cells were washed with 15mM sodium acetate buffer, pH 4.6 containing sodium azide (10 mM final concentration), resuspended to a final concentration of  $5 \times 10^7$  cells/ml. Cells were incubated with various concentrations of  $\alpha$ -factor for 30 minutes at room temperature in the dark, washed three times with 15 mM sodium acetate buffer containing sodium azide (10 mM final concentration), and analyzed on a EMD Millipore (MA, USA) flow cytometer (Guava 6HT-2L) using excitation at 488 nm and emission at 525. The mean fluorescence intensity obtained at various concentrations of fluorescent  $\alpha$ -factor analogue [K<sup>7</sup>(NBD),Nle<sup>12</sup>] were determined. The samples were protected from light during pre-incubations and flow cytometry analysis. The mean fluorescence obtained from the Guava was analyzed by GraphPad Prism using non-linear regression analysis. Because of significant day-to-day variation in the absolute values of the measured mean fluorescence intensity, all comparisons between different strains displayed in the figures show assays performed in parallel within the same experiment.

### ***Immunoblots***

Immunoblot analysis of Ste2p was carried out as described previously (44). Cells (BJS21) expressing various Ste2p constructs grown in MLT were used to prepare total cell membranes as previously described (37,45). For studies of disulfide cross-linking, membranes were solubilized in SDS sample buffer (30% glycerol, 3% SDS, 0.01% bromphenol blue, 0.1875 M Tris, pH 6.8) without 2-mercaptoethanol. Proteins were fractionated by SDS-PAGE (10% acrylamide, 0.1% SDS was used in the running buffer) along with pre-stained Precision Plus protein standards

(BioRad) and transferred to an Immobilon<sup>TM</sup>P membrane (Millipore Corp., Bedford, MA). The blot was probed with anti-FLAG<sup>TM</sup> M2 antibody (Sigma/Aldrich Chemical, St. Louis, MO), and bands were visualized with the West Pico chemiluminescent detection system (Pierce) using ChemiDoc<sup>TM</sup> XRS+ system (BioRad, Hercules, CA). The intensity of Ste2p signals was measured by densitometry using Image Lab<sup>TM</sup> software (version 4.1, BioRad, Hercules, CA). Multiple repeats of immunoblot experiments yielded similar results.

Constitutively-expressed membrane protein Pma1p was used as a loading control as described previously (46) using Pma1p antibody (Thermo Scientific, Rockford, IL).

#### ***Disulfide Cross-Linking with Cu-Phenanthroline***

Disulfide cross-linking was carried out as described previously (44). One hundred  $\mu\text{g}$  of membrane protein preparation was treated with a fresh preparation (pH 7.4) of Cu(II)-1,10-phenanthroline (Cu-P; final concentration, 2.5  $\mu\text{M}$  CuSO<sub>4</sub> and 7.5  $\mu\text{M}$  phenanthroline). The reaction was carried out at room temperature for 20 min, terminated with 50 mM EDTA, and kept on ice for 20 min followed by adding SDS sample buffer without 2-mercaptoethanol. The membrane preparation was incubated in the absence or presence  $\alpha$ -factor (1  $\mu\text{M}$  final concentration) for 30 min prior to Cu-P treatment in experiments performed to examine the influence of ligand on dimerization.

#### ***Factor Xa digestion***

The membrane protein preparation (40  $\mu\text{g}$ ) was incubated with 0.4 unit of Factor Xa (Novagen) in Factor Xa cleavage buffer (0.1M NaCl, 50 mM Tris-HCl, 5 mM CaCl<sub>2</sub>, pH 8.0) containing 0.1% Triton X-100 for 16h at 4°C. Each sample was divided into two aliquots. The reactions were terminated by adding one-third the volume of Laemmli sample buffer (30% glycerol, 3% SDS, 0.01% bromphenol blue, 0.1875 M Tris, pH 6.8). To one aliquot  $\beta$ -mercaptoethanol (final

concentration, 1%, v/v) was added for reducing conditions. Samples were analyzed by SDS-PAGE and Western blotting as described above.

## Results

### *Expression and Biological Activities of Cys Mutant Receptors:*

To determine intramolecular interaction between the N-terminus (NT) and extracellular loop 1 (ECL1) of Ste2p, one residue (Y26) in the NT and five residues (N105, S108, V109, Y111 and T114) in the ECL1 were chosen for mutation to Cys to investigate possible interactions by assaying for the formation of disulfide linkages. These residues were chosen for several reasons: (i) Y26 was found to be conserved in the N-terminal domains of  $\alpha$ -factor pheromone receptors of the fungi *Saccharomyces cerevisiae*, *Ashybya gossypii*, *Candida albicans*, *Candida dubliniensis*, *Candida tropicalis*, *Debaryomyces hansenii*, *Eremothecium cymbalariae*, *Kluyveromyces lactis*, *Lachancea kluyveri*, *Naumovozyma castellii*, *Naumovozyma dairenesis*, and *Scheffersomyces stipitis*. The N-terminal regions of the  $\alpha$ -factor pheromone receptors of these fungi were compared by amino acid sequence alignment. TMHMM 2.0 (47) was used to predict N-terminal regions and Clustal Omega (48) was used for alignment (Figure 4.1). All twelve receptors analyzed in this study were predicted to have an N-terminal domain of a 45-53 residues. The multiple sequence alignment of the N-terminal domain of these receptors demonstrated that only two residues, Y26 and F38, in the entire N-terminus were absolutely conserved, (ii) Y26 was suggested to be solvent inaccessible as determined by the substituted cysteine accessibility method. and the Y26C mutant demonstrated a greatly increased dimerization in a previous study (35), (iii) Y26 is located within one of the two known glycosylation motifs (associated with N25 & N32) of Ste2p (34), (iv) it is located within a predicted beta strand in the N-terminus (35,49), and (v) mutation of residues N105, S108, V109, Y111 and T114 to Cys led to changes in the glycosylation pattern of the receptors, although the glycosylation sites are located in the N-terminus at N25 and N32 (37).

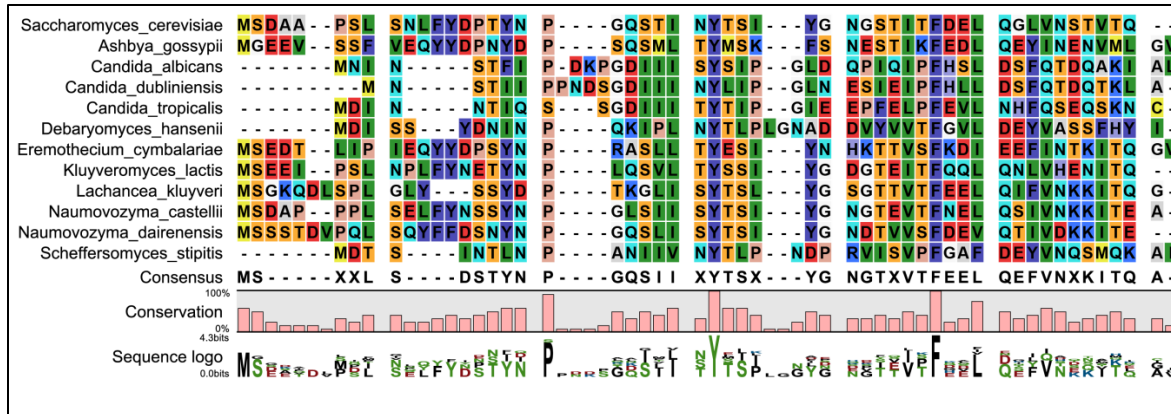


**Figure 4.1. Sequence alignments of yeast pheromone  $\alpha$ -factor receptors from different fungi. The N-terminal regions of *S. cerevisiae*, *Ashbya gossypii*, *Candida albicans*, *Candida dubliniensis*, *Candida tropicalis*, *Debaryomyces hansenii*, *Eremothecium cymbalariae*, *Kluyveromyces lactis*, *Lachancea kluyveri*, *Naumovozyma castellii*, *Naumovozyma dairenensis*, and *Scheffersomyces stipitis*  $\alpha$ -factor pheromone receptors were compared by amino acid sequence alignment. TMHMM 2.0 (47) was used to predict N-terminal regions for alignment by Clustal Omega (48). Sequence conservation is shown at the bottom of the aligned sequences. Graphical representation (sequence logo) shows sequence conservation.**

To eliminate non-specific cross-linking, the template for the introduction of these mutations was a Cys-less receptor (37). The Cys-less template also contained two C-terminal epitope tags (FLAG and 6XHIS) and tandem Factor Xa cleavage sites (IEGRIEGR) in the first intracellular loop in order to facilitate detection of interdomain cross-linking (Figure 4.2). The Cys-less Ste2p-FLAG-His receptor (referred to herein as “wild-type”) and the receptor with the Factor Xa cleavage sites in ICL1 (referred to herein as “ICL1-Xa<sub>2</sub>”) demonstrated similar expression levels as well as almost identical biological activities in growth arrest and *FUS1-LacZ* assays indicating that incorporating the protease cleavage sites did not alter receptor function (Figure 4.3).

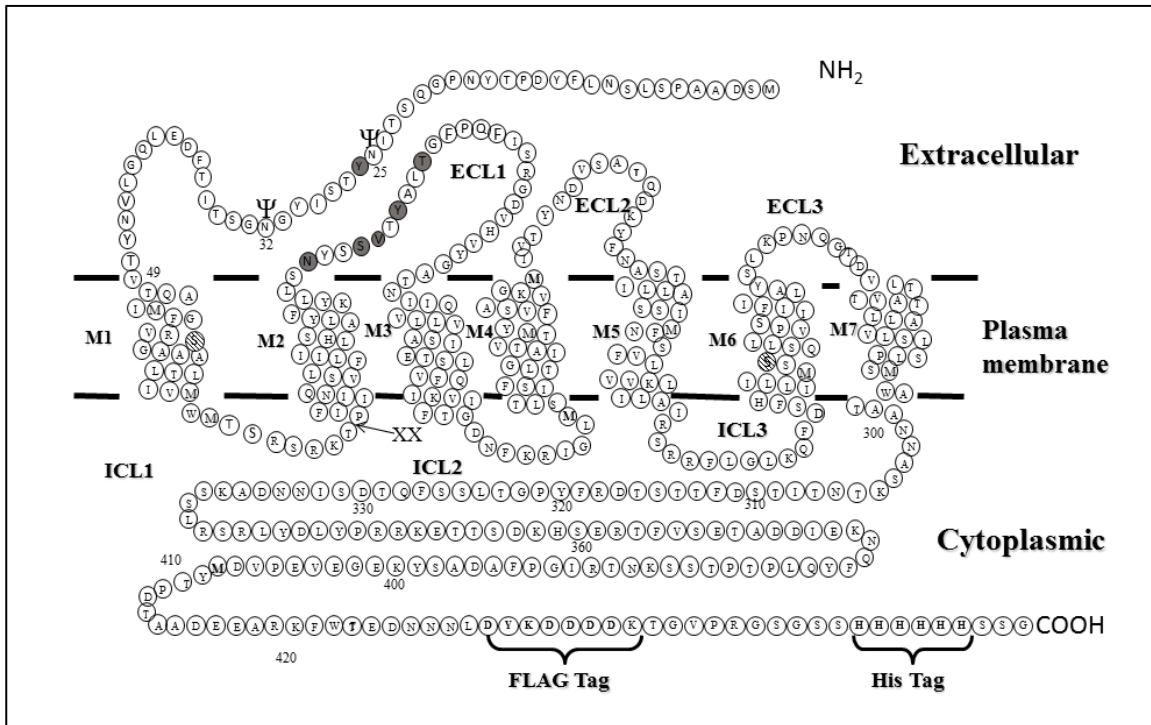


**Figure 4.2. Diagram of Ste2p showing positions of Cys mutations and modifications introduced to facilitate disulfide cross-linking and inter- and intra-molecular interactions. The tandem Factor Xa protease cleavage sites engineered into ICL1 are marked with “XX”. The FLAG and HIS epitope tags engineered into the C-terminus are also shown. The two endogenous Cys residues (C59 and C252 – hatched circles) were mutated to Ser to generate Cys-less Ste2p. The sites of Cys mutation engineered into the NT and ECL1 regions for disulfide cross-linking (Y26C, N105C, S108C, V109C, Y111C and T114C) are shown in grey circles. The two known glycosylation sites are shown with “ψ” symbol.**

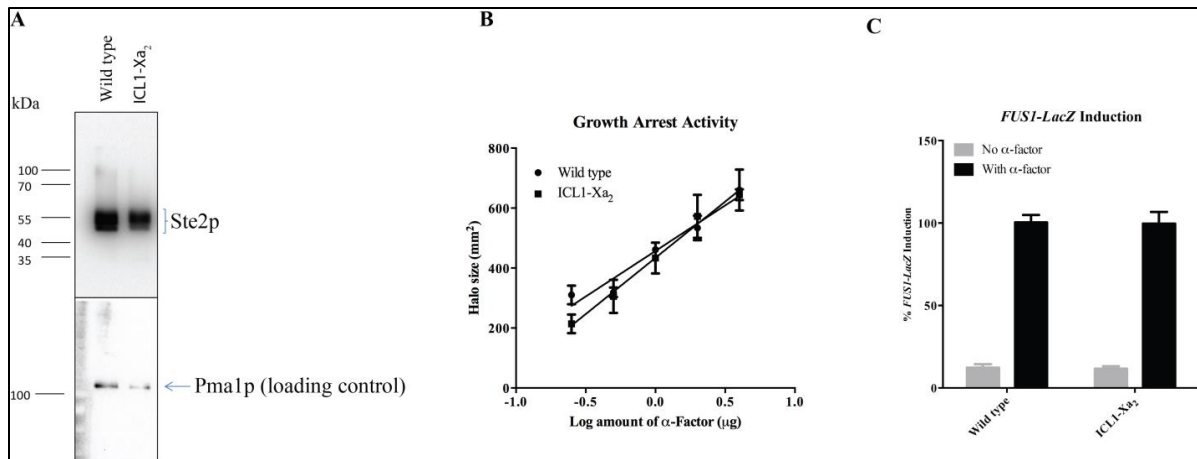


**Figure 4.3. Comparison of the expression levels and signaling activities of the WT and ICL1-Xa<sub>2</sub> receptor used in this study. ICL1-Xa<sub>2</sub> is the Cys-less receptor containing the C-terminal FLAG and His epitope tags and a tandem Factor Xa digestion site in IL1. Wild-type is the Cys-less receptor without the Factor Xa digestion site containing the FLAG and His epitopes. (A) total membranes prepared from the cells expressing wild-type and ICL1-Xa<sub>2</sub> constructs were immunoblotted using anti-FLAG antibody. The bottom panel shows the same immunoblot re-probed using antibody against Pma1p, a constitutively expressed plasma membrane protein used as a loading control. (B) The zone of growth inhibition of strains carrying the indicated receptors was measured at various concentrations of  $\alpha$ -factor. (C) Signaling activities of the constructs determined by pheromone-induced *FUS1-LacZ* activity. The grey bars represent the constitutive signaling and the black bars represent the  $\alpha$ -factor induced signaling activity. The signaling was normalized to that of the wild-type construct.**

The signaling activities of the cysteine mutants were examined by pheromone-induced growth arrest and *FUS1-LacZ* induction assays. The growth arrest assay is a sensitive test that is used to determine the ability of cells expressing Ste2p to maintain pheromone-induced cell

division arrest over a period of 24h. The *FUS1-LacZ* induction assay, on the other hand, measures an early response of the yeast cell to pheromone. The strains used in this study were engineered with a reporter gene construct consisting of a fusion between *FUS1* promoter and the *lacZ* gene encoding the enzyme  $\beta$ -galactosidase (50). The *FUS1-LacZ* assay allows for fast, sensitive detection of mating pathway activation by assessing the induction of  $\beta$ -galactosidase activity in response to mating pheromone. The growth arrest activity of the mutants varied from 33-90% of the ICL1-Xa<sub>2</sub> control whereas the *FUS1-LacZ* activity varied from 30-90% of the ICL1-Xa<sub>2</sub> control (Table 4.1). It was noticed that growth arrest activity and *FUS1-LacZ* activities of some mutants were different. For example, S108C exhibited 65% growth arrest compared to the ICL1-Xa<sub>2</sub> control and 30% *FUS1-LacZ* activity. The Y26C/V109C exhibited 34% growth arrest activity and 72% *FUS1-LacZ* activity. The difference between the *FUS1-LacZ* activity and cell division arrest (growth arrest activity) has been observed in many studies and has been explained on the basis of the amount of time after pheromone exposure when the response was measured (51-53).

**Table 4.1. Biological activities of Cys mutant receptors**

Receptor	Growth arrest activity <sup>1</sup>	$\beta$ -galactosidase activity	
		Basal Activity <sup>2</sup>	Induced Activity <sup>3</sup>
ICL1-Xa2	1.00	1.00±0.16	1.00±0.05
Y26C	0.60	1.12±0.10	0.53±0.03
N105C	0.79	0.97±0.18	0.43±0.01
Y26C/N105C	0.40	1.04±0.16	0.47±0.04
S108C	0.65	1.01±0.14	0.30±0.02
Y26C/S108C	0.59	0.97±0.21	0.45±0.02
V109C	0.84	0.95±0.12	0.89±0.01
Y26C/V109C	0.34	0.97±0.05	0.72±0.02
Y111C	0.90	0.97±0.04	0.30±0.01
Y26C/Y111C	0.70	0.94±0.04	0.64±0.01
T114C	0.87	1.00±0.04	0.57±0.01
Y26C/T114C	0.75	0.98±0.01	0.39±0.02

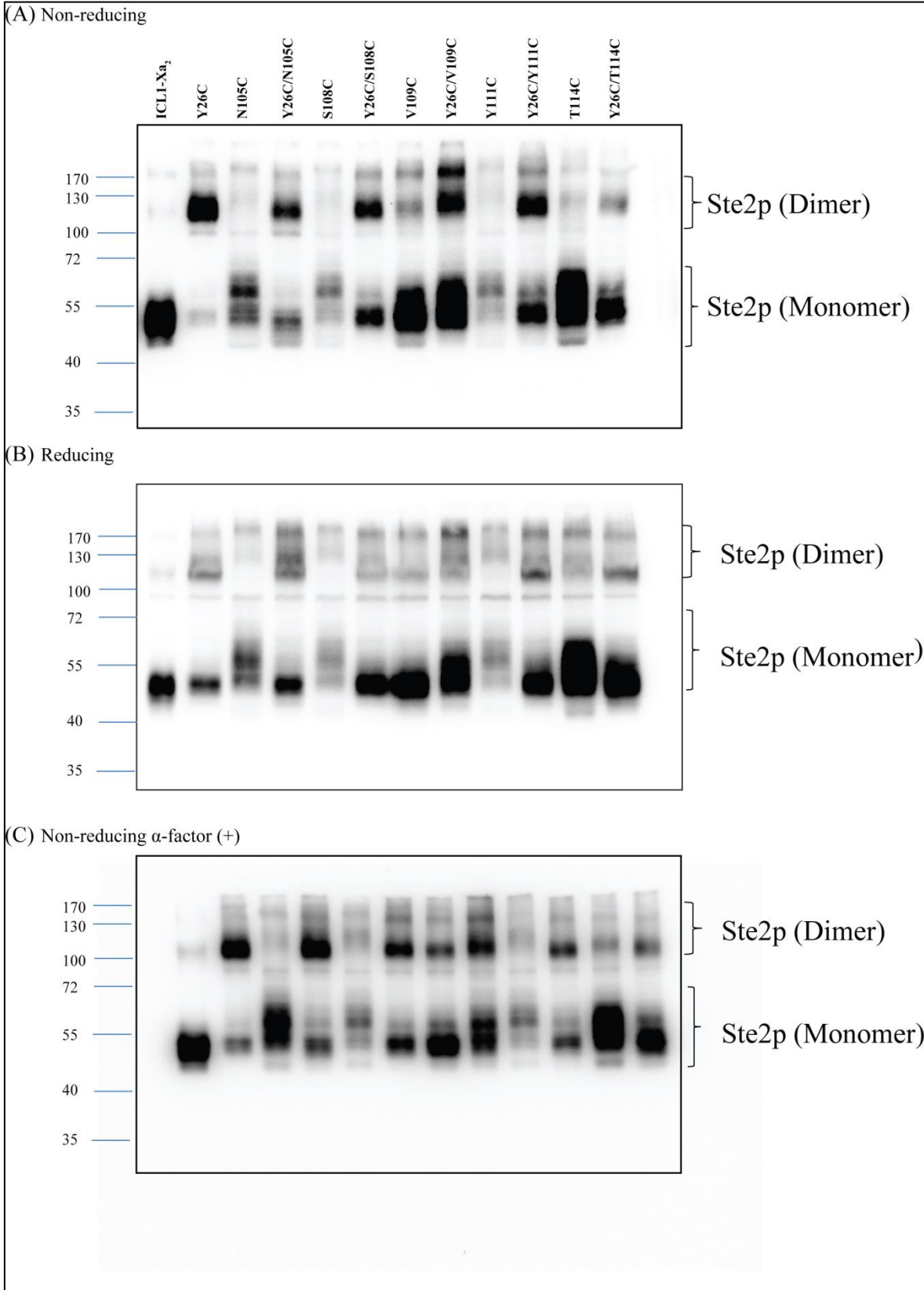
<sup>1</sup>Relative halo size was compared to the halo size of the ICL1-Xa<sub>2</sub> receptor at 1  $\mu$ g of  $\alpha$ -factor applied to a disc. The standard deviation of the halo activity for all receptors was within  $\pm 0.1$  (three replicates).

<sup>2</sup>Relative activity ( $\pm$ standard deviation) compared with basal activity of the ICL1-Xa<sub>2</sub>.

<sup>3</sup>Relative activity ( $\pm$ standard deviation) compared with induced activity of the ICL1-Xa<sub>2</sub> at 1  $\mu$ M of  $\alpha$ -factor.

The expression level of each single and double-Cys mutant receptor was determined by Western blot analysis. All mutant receptors showed several bands between 44 and 55 kDa (Figure 4.4A). The multiple bands are typical of Ste2p expression and are due to differences in the glycosylation state, which does not influence receptor function (34). Although the two intrinsic Cys residues have been substituted, a weak band at ~110 kDa, corresponding to a dimerized form of Ste2p, was observed for the ICL1-Xa<sub>2</sub> receptor. This band is likely a native, noncovalent dimer which was not disrupted by membrane protein preparation or SDS-PAGE. Such dimers have been observed on SDS-PAGE gels in our lab (35,43,44,54) and those of others working with Ste2p (49,55,56). Although the Cys constructs were expressed as judged by the Western blot, there was a large variability in the amount of receptor expressed, the glycosylation pattern, and the distribution of monomer to dimer among these mutants (Figure 4.4A).

**Figure 4.4. (A) Ste2p expression levels of various Cys mutants. Whole cell lysates from cells expressing various mutants were prepared as described in Materials and Methods. The cell lysates were run on SDS-PAGE gel under non-reducing conditions; the gel was blotted and probed using antibody against the C-terminal FLAG epitope tag to detect the presence of Ste2p at either the monomer or dimer positions, (B) Effect of reducing agent ( $\beta$ -mercaptoethanol) on dimerization. Cell lysates prepared from cells were run on SDS-PAGE under reducing conditions; the gel was blotted and probed with anti-FLAG antibody to detect the presence of Ste2p at either the monomer or dimer positions, (C) Effect of ligand binding on dimerization. Cell lysates were incubated with  $\alpha$ -factor (1 $\mu$ M final concentration); the membrane extracts were run on SDS-PAGE gel under non-reducing conditions; the gel was blotted and probed with anti-FLAG antibody to detect the presence Ste2p at either the monomer or dimer positions. Molecular mass markers (kDa) are indicated on the left-hand side.**



### ***The N-terminal Cys Mutant Y26C Forms Dimers:***

Ste2p is observed on immunoblots predominantly as a monomer of about 50 kDa as most non-covalent interactions between receptors are disrupted by the conditions of the SDS-PAGE. However, some SDS-resistant dimers persist as had been observed in many studies (37,43,44,55,57,58). Consistent with the previous studies, Ste2p was observed predominantly as a monomer at about 50 Kda with a small amount SDS-resistant dimer at about ~110 kDa in our Cys-less construct ICL1-Xa<sub>2</sub> (Lane ICL1-Xa<sub>2</sub>, Figure 4.4A). On the other hand, Y26C exhibited a strong dimer with a small amount of monomer (Lane Y26C, Figure 4.4A). The single Cys mutants N105C, S108C, V109C, Y111C and T114C showed predominantly as a monomer with a small amount of dimer. Additionally, with the exception of V109C, Ste2p banding pattern in the other single Cys mutants was different from the ICL1-Xa<sub>2</sub> control as exhibited by diffuse bands between ~55 and ~70 Kda. The diffuse banding pattern was attributed to changes in the glycosylation pattern of the receptors as these bands collapsed into a major monomeric band upon treatment with PNGase (37). The Ste2p expression levels of these mutants were also weaker than that of the ICL1-Xa<sub>2</sub> when the loading control (not shown) is taken into account. The low expression level of the ECL1 single mutants (N105C, S108C, Y111C, and T114C) was also observed previously (37). The expression levels of the double Cys mutants were also weaker than that of the ICL1-Xa<sub>2</sub> when the amount of protein loading is considered (Figure 4.4A). The banding pattern of the double Cys mutants was also different from the ICL1-Xa<sub>2</sub> as exhibited by a strong band (at about 50 Kda) along with a small amount of diffused bands between ~50 and ~70 Kda. Since the diffused banding pattern was not observed in Y26C and observed in N105C, S108C, Y111C and T114C, the differential banding pattern in the double Cys mutants can be attributed to mutations in ECL1.

The majority of the double Cys mutants exhibited stronger dimer with weaker monomer as compared to those of the ICL1-Xa<sub>2</sub> under non-reducing condition (Figure 4.4A). As stated above, the ICL1-Xa<sub>2</sub> and virtually all of the single Cys mutants of Ste2p exhibited no or faint bands at about 110 kDa consistent with a small amount of dimerized Ste2p. Since strong dimer was demonstrated in the majority of the double Cys mutants containing Y26C and weak dimer in the corresponding single Cys mutants, the dimers formed by these mutants can be attributed to Y26C. The dimer bands at ~110 kDa of the all the double Cys mutants decreased by the addition of  $\beta$ -mercaptoethanol indicating the involvement of disulfide bonds in stabilization of the dimer (Compare Figure 4.4A & B; See **Table 4.2**).

Analysis of the ratio of dimer to monomer in the gels under non-reducing conditions showed that the dimer/monomer ratio of Y26C was ~28 fold greater than that of the ICL1-Xa<sub>2</sub> control, whereas that of the double Cys mutants (Y26C/N105C, Y26C/S108C, Y26C/V109C, Y26C/Y111C and Y26C/T114C) ranged from about 4- to 8-fold greater (**Table 4.2**). The dimer ratio of the single Cys mutants ranged from 2-4 fold greater than that of the ICL1-Xa<sub>2</sub> control. Under reducing conditions, the dimer to monomer ratio of the Y26C and all the double Cys mutants decreased significantly ( $p < 0.05$ ), whereas the ratio did not change in any of the other single Cys mutants suggesting that the dimerization in the double Cys mutants were maintained by Y26C. No significant difference was observed in the ratio of dimer to monomer ratio among Y26C/N105C, Y26C/S108C and Y26C/Y111C. Also no significant difference in the ratio was observed between the Y26C/V109C and Y26C/T114C. These results indicate that the dimerization by Y26C is affected by mutation at positions V109C and T114C, whereas mutation at other positions did not affect dimerization.

**Table 4.2. Dimer to monomer ratio of Cys mutants in non-reducing and reducing conditions**

Receptor	Non-reducing <sup>1</sup>	Reducing <sup>2</sup>
ICL1-Xa <sub>2</sub>	1.0	1.0
Y26C*	27.9	12.3
N105C	2.2	2.3
Y26C/N105C*	8.0	5.9
S108C	3.1	2.3
Y26C/S108C*	8.3	4.4
V109C	3.7	2.2
Y26C/V109C*	5.7	3.4
Y111C	4.4	3.2
Y26C/Y111C*	8.2	4.5
T114C	1.9	1.3
Y26C/T114C*	4.1	2.6

<sup>1</sup>Relative dimer to monomer ratio of the Cys mutants as compared to that of the ICL1-Xa<sub>2</sub> in the absence of β-ME.

<sup>2</sup>Relative dimer to monomer ratio of the Cys mutants as compared to that of the ICL1-Xa<sub>2</sub> in the presence of β-ME.

Significant difference (p<0.05) in dimer to monomer ratio of the receptors in non-reducing and reducing conditions is indicated by “\*”. The dimer to monomer ratio of the mutants of the all the mutants was normalized to that of the ICL1-Xa<sub>2</sub>. The standard deviation of the relative dimer to monomer ratio for all receptors was within ±0.6.

***Conformational Changes in the N-terminus Upon Ligand Binding:*** It is generally believed that activation of GPCRs upon ligand binding results in a conformational change involving rearrangement of the various receptor domains (59-62). Previous studies have also shown that binding of  $\alpha$ -factor affected Ste2p dimer formation (36,44,58). Additionally, the N-terminus of Ste2p was reported to be involved in dimerization in several studies (35,36). A commonly used method to examine ligand-induced conformational change in GPCRs is disulfide cross-linking involving cysteine-substituted mutant receptors. This strategy can be used to determine the differences in disulfide formation between two receptor monomers containing Cys residues in the presence and absence of ligand (58,63,64). We investigated whether incubation with  $\alpha$ -factor would influence dimerization of the mutants examined in this study. We observed that dimer formation by the ICL1-Xa<sub>2</sub> control and majority of the mutants was not affected by agonist. However, three mutants (Y26C, Y26C/N105C and Y26C/S108C) exhibited a significant difference in the ratio of dimer to monomer in the absence or presence of agonist (Compare Figure 4.4A & C; see Figure 4.5). The dimer to monomer ratio of Y26C significantly decreased upon incubation with  $\alpha$ -factor. On the other hand, the dimer to monomer ratio of Y26C/N105C and Y26C/S108C increased significantly. These results suggest that  $\alpha$ -factor binding induces conformational changes in the N-terminus and EL1 of Ste2p which alters the availability of the Y26C, Y26C/N105C and Y26C/S108C residues for cross-linking, whereas for the other mutants of the ECL1 dimerization is not affected by ligand binding. These results indicate that the dimer interface formed by the N-terminus of the receptor changes upon receptor activation.

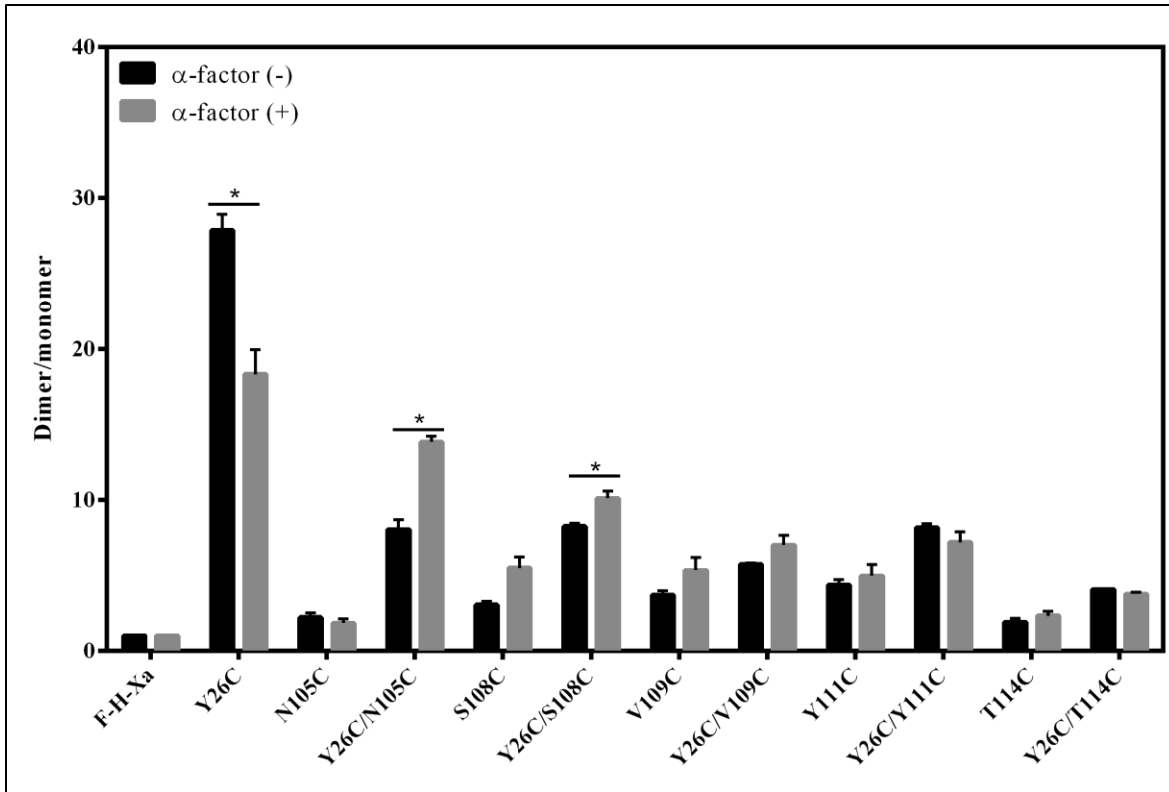


**Figure 4.5. Effect of ligand binding on dimerization. Band intensity of dimer and monomer forms of Ste2p was quantified from Western blots (Figure 4.4A & C) using Image Lab (version 4.1). The dimer/monomer ratio of the mutants was normalized to that of the ICL1-Xa<sub>2</sub>. Black and grey bars represent the ratio of dimer to monomer in the absence or presence of  $\alpha$ -factor, respectively. Statistical significance ( $p < 0.05$ ) in the dimer-monomer ratio is indicated by an asterisk.**

***Determination of intramolecular interaction between N-terminus and extracellular loop 1:***

The experiments described above indicated that dimerization mediated by Y26C was hindered by the V109C and T114C mutations in ECL1 suggesting a possible interaction between Y26C and these two positions in Ste2p. To test this idea, we took advantage of the protease (Factor Xa) digestion site engineered into ICL1 of Ste2p. If cross-linking between Y26C and V109C or T114C occurred, subsequent Factor Xa digestion would yield a full-length receptor, which can be detected by antibody against the C-terminal FLAG epitope tag (Figure 4.6, right panel). In contrast, if cross-linking did not occur, the receptor would be cut into two fragments, and a 42 kDa band would be detected on immunoblots using the C-terminal FLAG antibody (Figure 4.6, left panel). As expected, digestion of ICL1-Xa<sub>2</sub> receptor with Factor Xa led to detection of a 42 kDa fragment, and this digestion also lowered the total amount of Ste2p detected in both the monomer and dimer (non-disulfide) form (compare lanes 1 and 2 in Figure 4.7A). In contrast, the 42 kDa fragment protease digestion fragment was not detected in Y26C/V109C and Y26C/T114C mutants (lanes 4 and 6 in Figure 4.7A). Similar results were obtained when the receptors were incubated without (lanes 1-6) or with  $\alpha$ -factor (lanes 7-12) before digestion with Factor Xa. The monomer bands (~55 kDa) are due to incomplete Factor Xa digestion. We performed partial digestion because a longer incubation led to degradation of proteins.

To ascertain if the interaction was indeed due to disulfide cross-linking, all of the receptors showed the 42 kDa band, when treated with a reducing agent ( $\beta$ -mercaptoethanol) after protease digestion in both the presence and absence of  $\alpha$ -factor (Figure 4.7B). These results demonstrate that Y26 in the extracellular N-terminus and V109 and T114 in ECL1 of Ste2p molecule are in close proximity and provide evidence that the N-terminus and ECL1 may interact via these contacts.

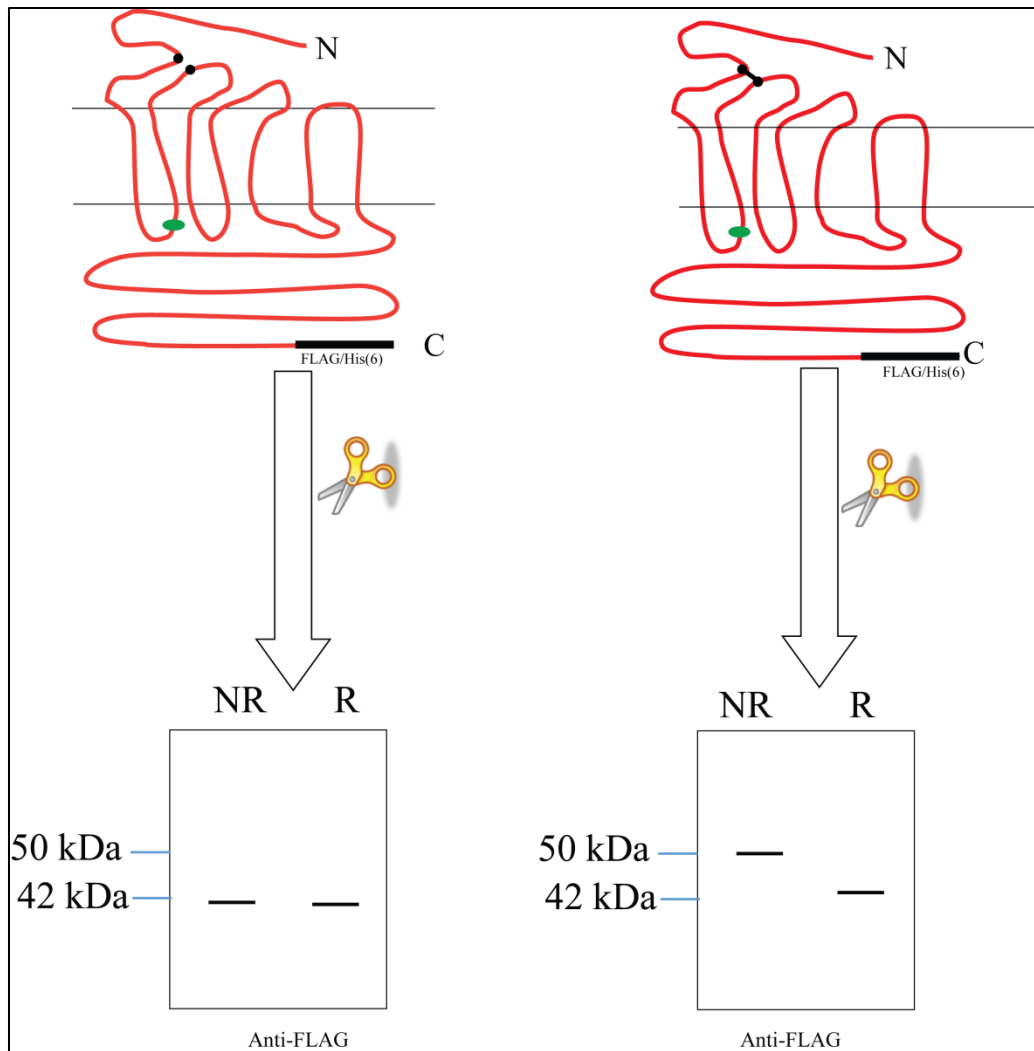


**Figure 4.6. Diagram showing the schematic of determination of intramolecular interaction using protease Factor Xa digestions followed by immunoblot detection using antibody against the C-terminal FLAG epitope tag. Non-reducing and reducing conditions of the sample buffer is indicated by NR and R respectively. The diagram of immunoblot on the left shows no interaction and the diagram of the immunoblot on the right shows a positive interaction. The N and C-termini of Ste2p are indicated by N and C, respectively. The green in ICL1 indicates the location of the protease Factor Xa cleavage site. The FLAG and His (6) epitope tags are shown in black.**

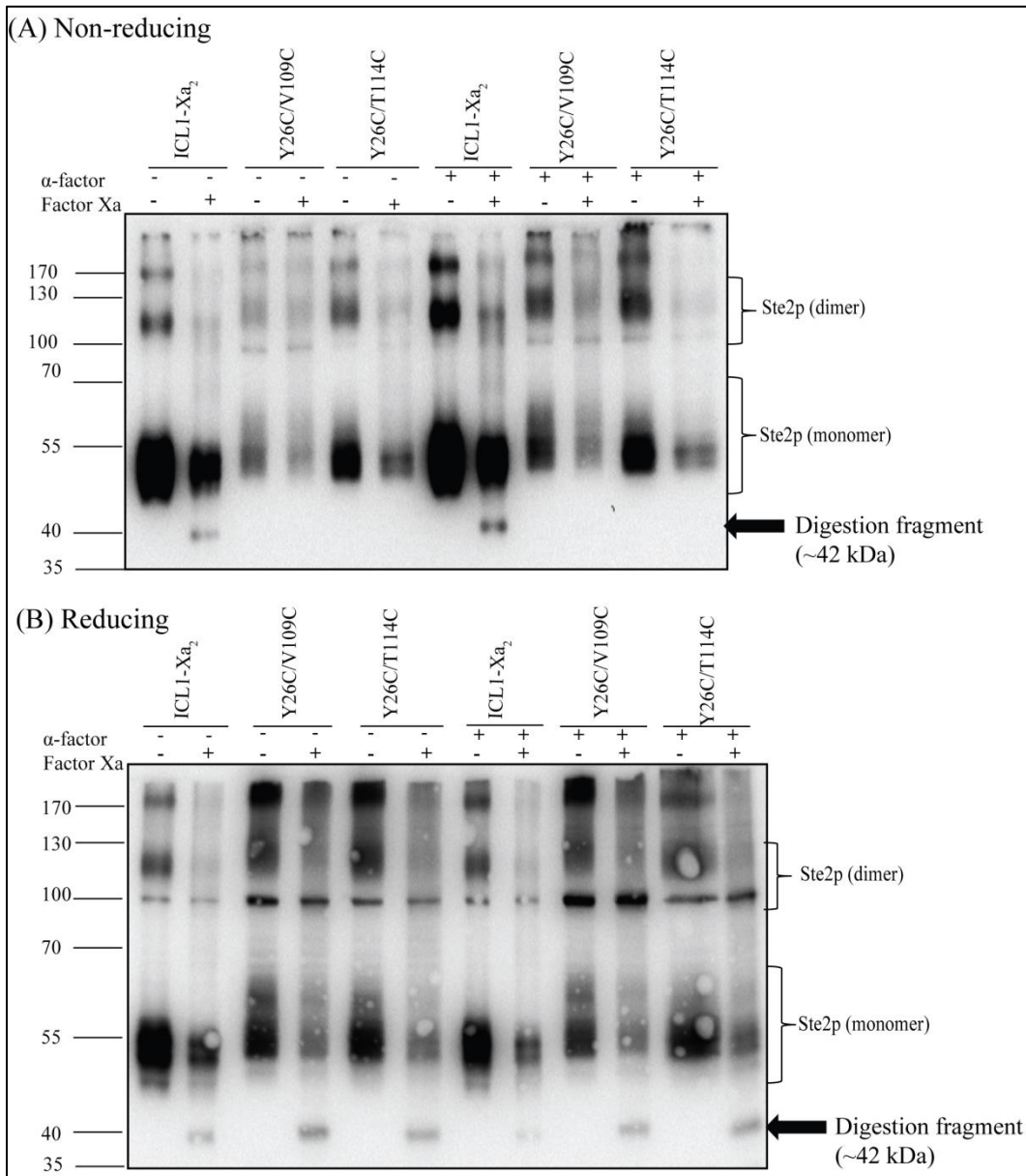


**Figure 4.7. Factor Xa digestion.** Membranes prepared from cells expressing the indicated receptors were prepared and digested as described in Materials and Methods. The samples were separated by SDS-PAGE in non-reducing (A) and reducing (B) conditions. The 42 kDa Ste2p fragment detected is marked with an arrow. The molecular markers are shown on the left.

## Discussion

We herein present data indicating a role for a highly conserved tyrosine residue in the N-terminus of Ste2p in dimerization and interaction with ECL1. Specifically, we identified Tyr26 as a key residue that is important for Ste2p dimerization facilitated by two residues Val109 and Thr114 in ECL1. Furthermore, using disulfide cross-linking methodology, we provide evidence that Tyr26 interacts with Val109 or Thr114. We also present data suggesting that the N-terminus-mediated dimer interface of the receptor changes upon receptor activation. The disulfide cross-linking studies were carried out with Ste2p in its membrane-bound state. The maximum distance between  $\alpha$ -carbons linked by disulfide bonds was shown to be about 7Å (65). Thus, these experiments should identify amino acid side chains that are within this distance. Cysteine residues engineered into GPCRs has been applied to facilitate disulfide bond formation in several GPCRs including Ste2p (44,54,58,61,66-69).

It had been suggested that the N-terminus of Ste2p is involved in dimerization (35,36). Our results support these findings and furthermore identified a specific residue in the N-terminus that facilitates Ste2p dimerization. The mutant receptor Y26C showed significantly increased dimerization over that of the ICL1-Xa2 (Figures 4A, 4B & **Table 4.2**). The finding that Y26C participates in dimer formation is in good agreement with the recently published results that Y26C is inaccessible to the sulfhydryl reagent MTSEA-Biotin (35) since the Y26C-Y26C interaction might render Y26C inaccessible. The fact that this residue formed a linkage suggests that the Ste2p-Ste2p interactions involving this region of the N-terminus have significant spatial restrictions which might make this region relatively rigid. This is consistent with the prediction that this region of the receptor has a  $\beta$  strand (35,70,71). Thus our mutational analysis defines a specific residue (Y26C) that appears to be involved in Ste2p dimerization.

It is interesting that N-terminus-mediated dimerization was hindered by mutations in the ECL1 of the receptor. This is consistent with the idea that the N-terminus interacts with extracellular loop 1. It had been shown previously that mutations in ECL1 affected the glycosylation pattern of the receptor (37), although the glycosylation sites are located in the N-terminus (34). The mutant receptors Y26C, Y26C/N105C, Y26C/S108C, Y26C/V109C, Y26C/Y111C and Y26C/T114C exhibited markedly increased dimerization over that of the ICL1-Xa<sub>2</sub> (Figures 4A, 4B & **Table 4.2**). The dimerization of these mutants was reversed by treatment with  $\beta$ -ME. On the other hand, the single Cys mutants (N105C, S108C, V109C, Y111C and T114C) exhibited weak dimerization as compared to the mutants containing Y26C mutation (Figures 4A, 4B & **Table 4.2**) and no significant decrease in dimerization was observed when treated with  $\beta$ -ME, indicating that the small amount of dimers formed by these mutants was due to SDS-resistant association between receptors that is not mediated by disulfide bonds. Out of the five double Cys mutants tested, two mutants (Y26C/V109C and Y26C/T114C) exhibited decreased dimerization as compared to the other three (Y26C/N105C, Y26C/S108C and Y26C/Y111C) indicating that Y26C-mediated dimerization was prevented by mutations at positions V109C or T114C. These results are consistent with the idea that interaction of Y26C with either V109C or T114C will hinder Y26C-Y26C interaction thus reducing dimerization. On the other hand, the other positions (N105C, S108C, Y111C) do not interact with Y26C and thus Y26C-Y26C interaction is not affected thereby dimerization maintained by Y26C does not change. These results suggest that Y26C interacts with these two positions. Since Y26C is located adjacent to a glycosylation site (N25), it is expected that mutations blocking the interaction might influence the glycosylation pattern. Indeed, it was observed previously that

mutation in these positions affect the glycosylation pattern (37). Thus these findings suggest that Y26 interacts with V109 and T114.

It is important to note that reduced dimerization of Y26C/V109C and Y26C/T114C might result from non-specific effects of mutation rather than interaction between the N-terminus and ECL1. To ascertain if specific interactions between Y26C and the two residues in ECL1 existed, we used disulfide cross-linking followed by Factor Xa digestion. We found that these two residues (V109C and T114C) in EL1 indeed cross-link with Y26C (Figure 4.8). This strategy has been used previously in our lab to determine the involvement of TM regions in dimerization (44). These results support previous studies in which mutation T114C along with N105C, S108C, and Y111C was found to change glycosylation pattern of the receptor. Our study identified the specific residues in EL1 and N-terminus that interact with each other. This finding led us to believe that the N-terminus and EL1 are in close proximity and these two domains have strong interactions that might play an important role in negative regulation of signaling as discussed in chapter 3 of this dissertation.

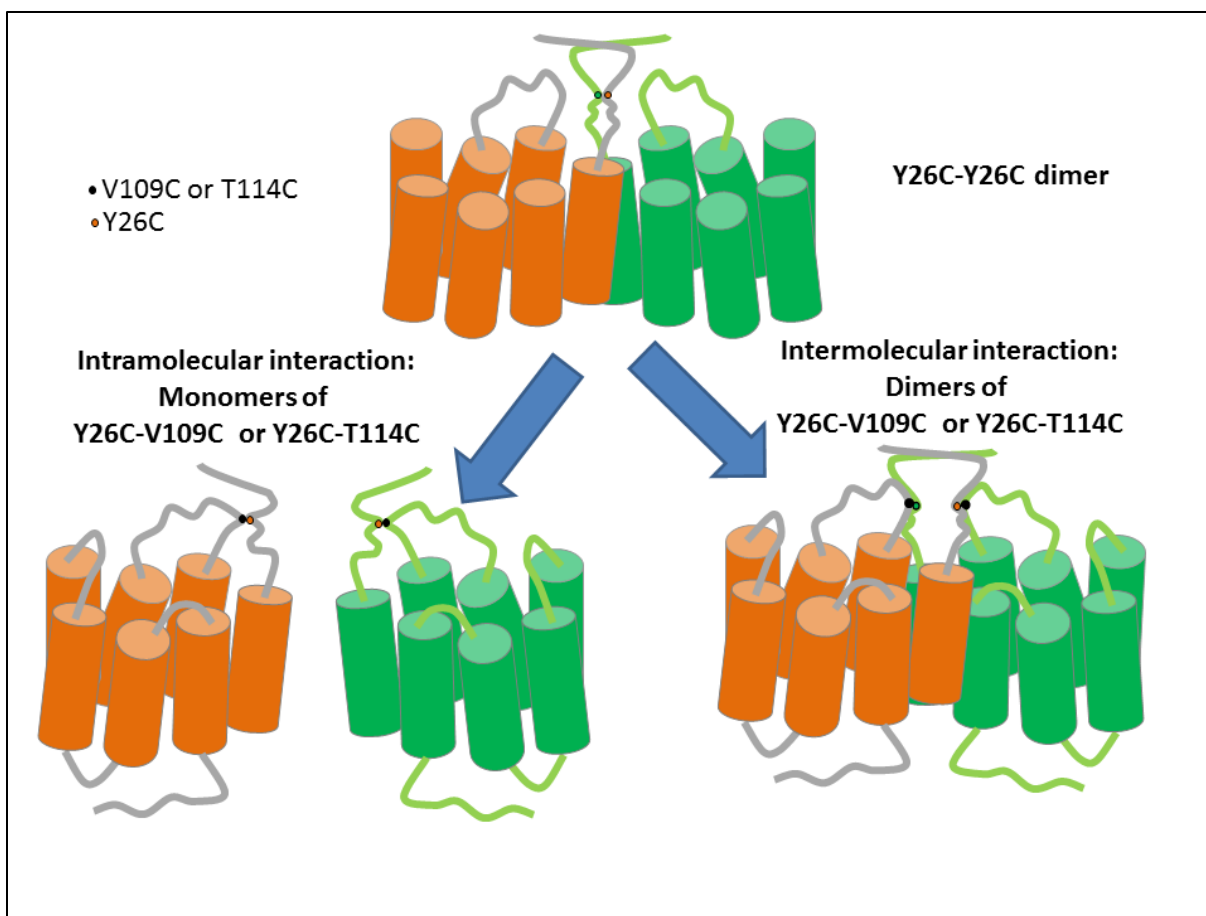


**Figure 4.8. Ste2p dimer mediated by Y26 and its interaction with ECL1. Two Ste2p molecules (orange and green) are shown with the positions of Y26 (green and orange dots), V109 (black) and T114 (black). Intramolecular and intermolecular interactions are shown on the left and right panels, respectively.**

The finding that NT is involved in Ste2p dimerization led us to propose that at least four dimerization interfaces can exist in Ste2p. In addition to the TM1, TM4, TM7 interfaces previously found (36,44,58), our data suggest that NT-NT interactions are also involved in direct contacts in the Ste2p dimer. The results described in this study show that cysteine residue introduced in the N-terminus (NT) forms a disulfide bond with its counterpart in another Ste2p

monomer (Figure 4.8). Since Y26C-mediated dimerization is prevented by Cys mutations at V109 and T114, these two residues in ECL1 are in close proximity to Y26C in the receptor. These results also suggest that the distance between Y26C and V109C or T114C is closer than that of Y26C of another Ste2p molecule in a Ste2p dimer mediated by Y26C-Y26C interaction because introduction of Cys at these positions competes out Y26C-Y26C interaction. It is also possible that Y26C-mediated dimerization was prevented by intermolecular interaction between Y26C of one Ste2p molecule with V109C or T114C of a second Ste2p molecule.

We also report here that the N-terminus of Ste2p is a dimer interface that changes upon receptor activation. Specifically, dimerization of Y26C, Y26C/N105C, and Y26C/S108C was found to change in the presence of  $\alpha$ -factor. The dimerization mediated by Y26C was found to decrease in the presence of  $\alpha$ -factor indicating that the dimer interface at the N-terminus of the receptor moves away from each other during receptor activation. The movement of the N-terminus may affect other domains of the receptor including ECL1 and TM domains which are believed to be involved in receptor activation. On the other hand, the dimerization mediated by Y26C/N105C and Y26C/S108C mutants was found to increase suggesting that the dimer interface mediated by Y26C moves closer to each other. Previous studies in our lab demonstrated that solvent accessibility of several residues (Y101, Y106, and A112) in ECL1 changes upon incubation with  $\alpha$ -factor thereby indicating the involvement of this region in receptor activation (37). A  $3_{10}$  helix was also predicted between residues 106-114 in the ECL1. Our results suggest that Y26 interacts with two residues (V109 and T114) in this region that are part of the  $3_{10}$  helix. It is possible that in the presence of  $\alpha$ -factor, the N-terminus moves away due to conformational changes in the ECL1 thereby affecting Y26-mediated dimerization. On the other hand, N105 and S108 are adjacent to these interacting residues in ECL1 (V109 and T114). Thus changes in these

two residues (N105 and S108) may influence the conformation of the ECL1 thereby affecting dimerization of Y26C/N105C and Y26C/S108C receptors, resulting in increased dimer formation due to bring the Y26 closer to each other.

GPCRs have been believed to exist and function as monomers for many years. Nevertheless, a growing number of studies demonstrated that GPCRs form dimers or higher-ordered oligomers, which have been proposed to be essential for modulation of receptor function (1,63,72-77). In most receptors, the transmembrane domains were reported to be involved in receptor dimerization/oligomerization. However, several studies demonstrated the extracellular N-terminal domain of Ste2p is also associated with dimerization (35,36). The residue identified in this study, Y26C, is highly conserved in fungal GPCRs. Conserved residues are often important for structure and function of proteins and conservation is stronger at protein-protein interfaces compared to elsewhere on the protein surface (78-81). Thus analysis of sequence conservation in a protein family is a useful strategy to identify key residues that are important for protein function (82-91). Protein-protein interaction sites are subjected to substantial selective pressure to maintain critical interactions throughout the course of evolution (92,93).

These findings provide valuable information relating to the arrangement of the receptor in which the N-terminus appear to face each other. In the absence of a crystal structure for Ste2p, the disulfide cross-linking results contributes to understanding structural features of the functional receptor such as inter-amino terminal interactions that may be involved in oligomerization.

## References

1. George, S. R., O'Dowd, B. F., and Lee, S. P. (2002) G-protein-coupled receptor oligomerization and its potential for drug discovery. *Nature reviews. Drug discovery* **1**, 808-820
2. Venkatakrisnan, A. J., Deupi, X., Lebon, G., Tate, C. G., Schertler, G. F., and Babu, M. M. (2013) Molecular signatures of G-protein-coupled receptors. *Nature* **494**, 185-194
3. O'Hayre, M., Vazquez-Prado, J., Kufareva, I., Stawiski, E. W., Handel, T. M., Seshagiri, S., and Gutkind, J. S. (2013) The emerging mutational landscape of G proteins and G-protein-coupled receptors in cancer. *Nature reviews. Cancer* **13**, 412-424
4. Pierce, K. L., Premont, R. T., and Lefkowitz, R. J. (2002) Seven-transmembrane receptors. *Nature reviews. Molecular cell biology* **3**, 639-650
5. Howard, A. D., McAllister, G., Feighner, S. D., Liu, Q., Nargund, R. P., Van der Ploeg, L. H., and Patchett, A. A. (2001) Orphan G-protein-coupled receptors and natural ligand discovery. *Trends in pharmacological sciences* **22**, 132-140
6. Carrieri, A., Perez-Nueno, V. I., Lentini, G., and Ritchie, D. W. (2013) Recent Trends and Future Prospects in Computational GPCR Drug Discovery: From Virtual Screening to Polypharmacology. *Current topics in medicinal chemistry* **13**, 1069-1097
7. McNeely, P. M., Naranjo, A. N., and Robinson, A. S. (2012) Structure-function studies with G protein-coupled receptors as a paradigm for improving drug discovery and development of therapeutics. *Biotechnology journal* **7**, 1451-1461

8. Fotiadis, D., Jastrzebska, B., Philippsen, A., Muller, D. J., Palczewski, K., and Engel, A. (2006) Structure of the rhodopsin dimer: a working model for G-protein-coupled receptors. *Current opinion in structural biology* **16**, 252-259
9. Overington, J. P., Al-Lazikani, B., and Hopkins, A. L. (2006) How many drug targets are there? *Nature reviews. Drug discovery* **5**, 993-996
10. Lefkowitz, R. J., and Shenoy, S. K. (2005) Transduction of receptor signals by beta-arrestins. *Science* **308**, 512-517
11. Kobilka, B. K., Kobilka, T. S., Daniel, K., Regan, J. W., Caron, M. G., and Lefkowitz, R. J. (1988) Chimeric alpha 2-,beta 2-adrenergic receptors: delineation of domains involved in effector coupling and ligand binding specificity. *Science* **240**, 1310-1316
12. Schoneberg, T., Liu, J., and Wess, J. (1995) Plasma membrane localization and functional rescue of truncated forms of a G protein-coupled receptor. *The Journal of biological chemistry* **270**, 18000-18006
13. Filipek, S., Stenkamp, R. E., Teller, D. C., and Palczewski, K. (2003) G protein-coupled receptor rhodopsin: a prospectus. *Annual review of physiology* **65**, 851-879
14. Hargrave, P. A., Hamm, H. E., and Hofmann, K. P. (1993) Interaction of rhodopsin with the G-protein, transducin. *BioEssays : news and reviews in molecular, cellular and developmental biology* **15**, 43-50
15. Khorana, H. G. (1992) Rhodopsin, photoreceptor of the rod cell. An emerging pattern for structure and function. *The Journal of biological chemistry* **267**, 1-4
16. Rao, V. R., Cohen, G. B., and Oprian, D. D. (1994) Rhodopsin mutation G90D and a molecular mechanism for congenital night blindness. *Nature* **367**, 639-642

17. Kristiansen, K. (2004) Molecular mechanisms of ligand binding, signaling, and regulation within the superfamily of G-protein-coupled receptors: molecular modeling and mutagenesis approaches to receptor structure and function. *Pharmacology & therapeutics* **103**, 21-80
18. Kobilka, B. K. (2007) G protein coupled receptor structure and activation. *Biochimica et biophysica acta* **1768**, 794-807
19. Lagerstrom, M. C., and Schioth, H. B. (2008) Structural diversity of G protein-coupled receptors and significance for drug discovery. *Nature reviews. Drug discovery* **7**, 339-357
20. Ersoy, B. A., Pardo, L., Zhang, S., Thompson, D. A., Millhauser, G., Govaerts, C., and Vaisse, C. (2012) Mechanism of N-terminal modulation of activity at the melanocortin-4 receptor GPCR. *Nature chemical biology* **8**, 725-730
21. Beinborn, M. (2006) Class B GPCRs: a hidden agonist within? *Molecular pharmacology* **70**, 1-4
22. Dong, M., Pinon, D. I., Asmann, Y. W., and Miller, L. J. (2006) Possible endogenous agonist mechanism for the activation of secretin family G protein-coupled receptors. *Molecular pharmacology* **70**, 206-213
23. Kobilka, B. K., and Deupi, X. (2007) Conformational complexity of G-protein-coupled receptors. *Trends in pharmacological sciences* **28**, 397-406
24. Scarborough, R. M., Naughton, M. A., Teng, W., Hung, D. T., Rose, J., Vu, T. K., Wheaton, V. I., Turck, C. W., and Coughlin, S. R. (1992) Tethered ligand agonist peptides. Structural requirements for thrombin receptor activation reveal mechanism of proteolytic unmasking of agonist function. *The Journal of biological chemistry* **267**, 13146-13149

25. Vassart, G., Pardo, L., and Costagliola, S. (2004) A molecular dissection of the glycoprotein hormone receptors. *Trends in biochemical sciences* **29**, 119-126
26. Paavola, K. J., Stephenson, J. R., Ritter, S. L., Alter, S. P., and Hall, R. A. (2011) The N terminus of the adhesion G protein-coupled receptor GPR56 controls receptor signaling activity. *The Journal of biological chemistry* **286**, 28914-28921
27. Andersson, H., D'Antona, A. M., Kendall, D. A., Von Heijne, G., and Chin, C. N. (2003) Membrane assembly of the cannabinoid receptor 1: impact of a long N-terminal tail. *Molecular pharmacology* **64**, 570-577
28. Hague, C., Chen, Z., Pupo, A. S., Schulte, N. A., Toews, M. L., and Minneman, K. P. (2004) The N terminus of the human alpha1D-adrenergic receptor prevents cell surface expression. *The Journal of pharmacology and experimental therapeutics* **309**, 388-397
29. Dunham, J. H., Meyer, R. C., Garcia, E. L., and Hall, R. A. (2009) GPR37 surface expression enhancement via N-terminal truncation or protein-protein interactions. *Biochemistry* **48**, 10286-10297
30. Bardwell, L. (2005) A walk-through of the yeast mating pheromone response pathway. *Peptides* **26**, 339-350
31. Dowell, S. J., and Brown, A. J. (2009) Yeast assays for G protein-coupled receptors. *Methods in molecular biology* **552**, 213-229
32. King, K., Dohlman, H. G., Thorner, J., Caron, M. G., and Lefkowitz, R. J. (1990) Control of yeast mating signal transduction by a mammalian beta 2-adrenergic receptor and Gs alpha subunit. *Science* **250**, 121-123

33. Yin, D., Gavi, S., Shumay, E., Duell, K., Konopka, J. B., Malbon, C. C., and Wang, H. Y. (2005) Successful expression of a functional yeast G-protein-coupled receptor (Ste2) in mammalian cells. *Biochemical and biophysical research communications* **329**, 281-287
34. Montesana, P. E., and Konopka, J. B. (2001) Mutational analysis of the role of N-glycosylation in alpha-factor receptor function. *Biochemistry* **40**, 9685-9694
35. Uddin, M. S., Kim, H., Deyo, A., Naider, F., and Becker, J. M. (2012) Identification of residues involved in homodimer formation located within a beta-strand region of the N-terminus of a Yeast G protein-coupled receptor. *Journal of receptor and signal transduction research* **32**, 65-75
36. Overton, M. C., and Blumer, K. J. (2002) The extracellular N-terminal domain and transmembrane domains 1 and 2 mediate oligomerization of a yeast G protein-coupled receptor. *The Journal of biological chemistry* **277**, 41463-41472
37. Hauser, M., Kauffman, S., Lee, B. K., Naider, F., and Becker, J. M. (2007) The first extracellular loop of the *Saccharomyces cerevisiae* G protein-coupled receptor Ste2p undergoes a conformational change upon ligand binding. *The Journal of biological chemistry* **282**, 10387-10397
38. Marsh, L. (1992) Substitutions in the hydrophobic core of the alpha-factor receptor of *Saccharomyces cerevisiae* permit response to *Saccharomyces kluyveri* alpha-factor and to antagonist. *Molecular and cellular biology* **12**, 3959-3966
39. Son, C. D., Sargsyan, H., Naider, F., and Becker, J. M. (2004) Identification of ligand binding regions of the *Saccharomyces cerevisiae* alpha-factor pheromone receptor by photoaffinity cross-linking. *Biochemistry* **43**, 13193-13203

40. Turcatti, G., Nemeth, K., Edgerton, M. D., Meseth, U., Talabot, F., Peitsch, M., Knowles, J., Vogel, H., and Chollet, A. (1996) Probing the structure and function of the tachykinin neurokinin-2 receptor through biosynthetic incorporation of fluorescent amino acids at specific sites. *The Journal of biological chemistry* **271**, 19991-19998
41. Sherman, F. (1991) Getting started with yeast. *Methods in enzymology* **194**, 3-21
42. Huang, L. Y., Umanah, G., Hauser, M., Son, C., Arshava, B., Naider, F., and Becker, J. M. (2008) Unnatural amino acid replacement in a yeast G protein-coupled receptor in its native environment. *Biochemistry* **47**, 5638-5648
43. Umanah, G. K., Huang, L., Ding, F. X., Arshava, B., Farley, A. R., Link, A. J., Naider, F., and Becker, J. M. (2010) Identification of residue-to-residue contact between a peptide ligand and its G protein-coupled receptor using periodate-mediated dihydroxyphenylalanine cross-linking and mass spectrometry. *The Journal of biological chemistry* **285**, 39425-39436
44. Kim, H., Lee, B. K., Naider, F., and Becker, J. M. (2009) Identification of specific transmembrane residues and ligand-induced interface changes involved in homo-dimer formation of a yeast G protein-coupled receptor. *Biochemistry* **48**, 10976-10987
45. David, N. E., Gee, M., Andersen, B., Naider, F., Thorner, J., and Stevens, R. C. (1997) Expression and purification of the *Saccharomyces cerevisiae* alpha-factor receptor (Ste2p), a 7-transmembrane-segment G protein-coupled receptor. *The Journal of biological chemistry* **272**, 15553-15561
46. Pinson, B., Chevallier, J., and Urban-Grimal, D. (1999) Only one of the charged amino acids located in membrane-spanning regions is important for the function of the *Saccharomyces cerevisiae* uracil permease. *The Biochemical journal* **339** ( Pt 1), 37-42

47. Krogh, A., Larsson, B., von Heijne, G., and Sonnhammer, E. L. (2001) Predicting transmembrane protein topology with a hidden Markov model: application to complete genomes. *Journal of molecular biology* **305**, 567-580
48. Sievers, F., Wilm, A., Dineen, D., Gibson, T. J., Karplus, K., Li, W., Lopez, R., McWilliam, H., Remmert, M., Soding, J., Thompson, J. D., and Higgins, D. G. (2011) Fast, scalable generation of high-quality protein multiple sequence alignments using Clustal Omega. *Molecular systems biology* **7**, 539
49. Shi, C., Paige, M. F., Maley, J., and Loewen, M. C. (2009) In vitro characterization of ligand-induced oligomerization of the *S. cerevisiae* G-protein coupled receptor, Ste2p. *Biochimica et biophysica acta* **1790**, 1-7
50. Trueheart, J., Boeke, J. D., and Fink, G. R. (1987) Two genes required for cell fusion during yeast conjugation: evidence for a pheromone-induced surface protein. *Molecular and cellular biology* **7**, 2316-2328
51. McCaffrey, G., Clay, F. J., Kelsay, K., and Sprague, G. F., Jr. (1987) Identification and regulation of a gene required for cell fusion during mating of the yeast *Saccharomyces cerevisiae*. *Molecular and cellular biology* **7**, 2680-2690
52. Dube, P., DeCostanzo, A., and Konopka, J. B. (2000) Interaction between transmembrane domains five and six of the alpha -factor receptor. *The Journal of biological chemistry* **275**, 26492-26499
53. Parrish, W., Eilers, M., Ying, W., and Konopka, J. B. (2002) The cytoplasmic end of transmembrane domain 3 regulates the activity of the *Saccharomyces cerevisiae* G-protein-coupled alpha-factor receptor. *Genetics* **160**, 429-443

54. Umanah, G. K., Huang, L. Y., Maccarone, J. M., Naider, F., and Becker, J. M. (2011) Changes in conformation at the cytoplasmic ends of the fifth and sixth transmembrane helices of a yeast G protein-coupled receptor in response to ligand binding. *Biochemistry* **50**, 6841-6854
55. Gehret, A. U., Bajaj, A., Naider, F., and Dumont, M. E. (2006) Oligomerization of the yeast alpha-factor receptor: implications for dominant negative effects of mutant receptors. *The Journal of biological chemistry* **281**, 20698-20714
56. Blumer, K. J., Reneke, J. E., and Thorner, J. (1988) The STE2 gene product is the ligand-binding component of the alpha-factor receptor of *Saccharomyces cerevisiae*. *The Journal of biological chemistry* **263**, 10836-10842
57. Yesilaltay, A., and Jenness, D. D. (2000) Homo-oligomeric complexes of the yeast alpha-factor pheromone receptor are functional units of endocytosis. *Molecular biology of the cell* **11**, 2873-2884
58. Wang, H. X., and Konopka, J. B. (2009) Identification of amino acids at two dimer interface regions of the alpha-factor receptor (Ste2). *Biochemistry* **48**, 7132-7139
59. Bukusoglu, G., and Jenness, D. D. (1996) Agonist-specific conformational changes in the yeast alpha-factor pheromone receptor. *Molecular and cellular biology* **16**, 4818-4823
60. Farrens, D. L., Altenbach, C., Yang, K., Hubbell, W. L., and Khorana, H. G. (1996) Requirement of rigid-body motion of transmembrane helices for light activation of rhodopsin. *Science* **274**, 768-770
61. Zeng, F. Y., Hopp, A., Soldner, A., and Wess, J. (1999) Use of a disulfide cross-linking strategy to study muscarinic receptor structure and mechanisms of activation. *The Journal of biological chemistry* **274**, 16629-16640

62. Luo, X., Zhang, D., and Weinstein, H. (1994) Ligand-induced domain motion in the activation mechanism of a G-protein-coupled receptor. *Protein engineering* **7**, 1441-1448
63. Bouvier, M. (2001) Oligomerization of G-protein-coupled transmitter receptors. *Nature reviews. Neuroscience* **2**, 274-286
64. Park, P. S., Filipek, S., Wells, J. W., and Palczewski, K. (2004) Oligomerization of G protein-coupled receptors: past, present, and future. *Biochemistry* **43**, 15643-15656
65. Srinivasan, N., Sowdhamini, R., Ramakrishnan, C., and Balaram, P. (1990) Conformations of disulfide bridges in proteins. *International journal of peptide and protein research* **36**, 147-155
66. Li, J. H., Han, S. J., Hamdan, F. F., Kim, S. K., Jacobson, K. A., Bloodworth, L. M., Zhang, X., and Wess, J. (2007) Distinct structural changes in a G protein-coupled receptor caused by different classes of agonist ligands. *The Journal of biological chemistry* **282**, 26284-26293
67. Yu, H., Kono, M., McKee, T. D., and Oprian, D. D. (1995) A general method for mapping tertiary contacts between amino acid residues in membrane-embedded proteins. *Biochemistry* **34**, 14963-14969
68. Li, J. H., Hamdan, F. F., Kim, S. K., Jacobson, K. A., Zhang, X., Han, S. J., and Wess, J. (2008) Ligand-specific changes in M3 muscarinic acetylcholine receptor structure detected by a disulfide scanning strategy. *Biochemistry* **47**, 2776-2788
69. Ward, S. D., Hamdan, F. F., Bloodworth, L. M., Siddiqui, N. A., Li, J. H., and Wess, J. (2006) Use of an in situ disulfide cross-linking strategy to study the dynamic properties of the cytoplasmic end of transmembrane domain VI of the M3 muscarinic acetylcholine receptor. *Biochemistry* **45**, 676-685

70. Shi, C., Kaminskyj, S., Caldwell, S., and Loewen, M. C. (2007) A role for a complex between activated G protein-coupled receptors in yeast cellular mating. *Proceedings of the National Academy of Sciences of the United States of America* **104**, 5395-5400
71. Shi, C., Kendall, S. C., Grote, E., Kaminskyj, S., and Loewen, M. C. (2009) N-terminal residues of the yeast pheromone receptor, Ste2p, mediate mating events independently of G1-arrest signaling. *Journal of cellular biochemistry* **107**, 630-638
72. Milligan, G. (2007) G protein-coupled receptor dimerisation: molecular basis and relevance to function. *Biochimica et biophysica acta* **1768**, 825-835
73. Devi, L. A. (2001) Heterodimerization of G-protein-coupled receptors: pharmacology, signaling and trafficking. *Trends in pharmacological sciences* **22**, 532-537
74. Milligan, G. (2004) G protein-coupled receptor dimerization: function and ligand pharmacology. *Molecular pharmacology* **66**, 1-7
75. Milligan, G. (2008) A day in the life of a G protein-coupled receptor: the contribution to function of G protein-coupled receptor dimerization. *British journal of pharmacology* **153 Suppl 1**, S216-229
76. Maurice, P., Kamal, M., and Jockers, R. (2011) Asymmetry of GPCR oligomers supports their functional relevance. *Trends in pharmacological sciences* **32**, 514-520
77. Ferre, S., Ciruela, F., Woods, A. S., Lluís, C., and Franco, R. (2007) Functional relevance of neurotransmitter receptor heteromers in the central nervous system. *Trends in neurosciences* **30**, 440-446
78. Bordner, A. J., and Abagyan, R. (2005) Statistical analysis and prediction of protein-protein interfaces. *Proteins* **60**, 353-366

79. Caffrey, D. R., Somaroo, S., Hughes, J. D., Mintseris, J., and Huang, E. S. (2004) Are protein-protein interfaces more conserved in sequence than the rest of the protein surface? *Protein science : a publication of the Protein Society* **13**, 190-202
80. Elcock, A. H., and McCammon, J. A. (2001) Identification of protein oligomerization states by analysis of interface conservation. *Proceedings of the National Academy of Sciences of the United States of America* **98**, 2990-2994
81. Valdar, W. S., and Thornton, J. M. (2001) Conservation helps to identify biologically relevant crystal contacts. *Journal of molecular biology* **313**, 399-416
82. Manning, J. R., Jefferson, E. R., and Barton, G. J. (2008) The contrasting properties of conservation and correlated phylogeny in protein functional residue prediction. *BMC bioinformatics* **9**, 51
83. Capra, J. A., and Singh, M. (2007) Predicting functionally important residues from sequence conservation. *Bioinformatics* **23**, 1875-1882
84. Panchenko, A. R., Kondrashov, F., and Bryant, S. (2004) Prediction of functional sites by analysis of sequence and structure conservation. *Protein science : a publication of the Protein Society* **13**, 884-892
85. Berezin, C., Glaser, F., Rosenberg, J., Paz, I., Pupko, T., Fariselli, P., Casadio, R., and Ben-Tal, N. (2004) ConSeq: the identification of functionally and structurally important residues in protein sequences. *Bioinformatics* **20**, 1322-1324
86. del Sol, A., Pazos, F., and Valencia, A. (2003) Automatic methods for predicting functionally important residues. *Journal of molecular biology* **326**, 1289-1302
87. Pupko, T., Bell, R. E., Mayrose, I., Glaser, F., and Ben-Tal, N. (2002) Rate4Site: an algorithmic tool for the identification of functional regions in proteins by surface

- mapping of evolutionary determinants within their homologues. *Bioinformatics* **18 Suppl 1**, S71-77
88. Landgraf, R., Xenarios, I., and Eisenberg, D. (2001) Three-dimensional cluster analysis identifies interfaces and functional residue clusters in proteins. *Journal of molecular biology* **307**, 1487-1502
89. Armon, A., Graur, D., and Ben-Tal, N. (2001) ConSurf: an algorithmic tool for the identification of functional regions in proteins by surface mapping of phylogenetic information. *Journal of molecular biology* **307**, 447-463
90. Mirny, L. A., and Shakhnovich, E. I. (1999) Universally conserved positions in protein folds: reading evolutionary signals about stability, folding kinetics and function. *Journal of molecular biology* **291**, 177-196
91. Casari, G., Sander, C., and Valencia, A. (1995) A method to predict functional residues in proteins. *Nature structural biology* **2**, 171-178
92. Guharoy, M., and Chakrabarti, P. (2005) Conservation and relative importance of residues across protein-protein interfaces. *Proceedings of the National Academy of Sciences of the United States of America* **102**, 15447-15452
93. Biswas, S., Guharoy, M., and Chakrabarti, P. (2009) Dissection, residue conservation, and structural classification of protein-DNA interfaces. *Proteins* **74**, 643-654

## **Chapter 5**

### **Conclusions, summary and future studies**

## Summary

This dissertation describes the identification of a discrete structure that is involved in homodimer formation of Ste2p, the yeast  $\alpha$ -factor receptor, a model system for mammalian GPCR peptide hormone receptors. The Substituted Cysteine Accessibility Method (SCAM) was used to determine the accessibility of residues in the N-terminus and disulfide cross-linking was used to determine dimer formation by these residues. These studies revealed that certain residues in the extracellular N-terminus were solvent inaccessible and that these residues also promote increased dimers formation. The pattern of accessibility combined with the disulfide cross-linking results suggested the presence of a  $\beta$ -strand structure in the N-terminus which was predicted previously by bioinformatics analysis of this region. Deletion mutagenesis revealed that the N-terminus is involved in negative regulation of signaling. Further analysis of the N-terminus revealed that a conserved tyrosine residue in the  $\beta$ strand plays a critical role in receptor dimerization and likely interacts with two residues (V109 and T114) in ECL1 of the receptor. Furthermore, the Ste2p dimer interface was found to change upon receptor activation thereby supporting the emerging idea that dimerization plays an important role in receptor function.

The Substituted Cysteine Accessibility Method (SCAM) was used to determine the accessibility of residues in the N-terminus and disulfide cross-linking was used to determine if the N-terminus is part of a dimer interface for Ste2p. The results of these assays indicate that certain residues in a short segment of the N-terminus of Ste2p do not react with a water-soluble biotinylation reagent and appeared to be involved in receptor dimerization. Interestingly, the pattern of solvent accessibility was found to be consistent with a  $\beta$ -sheet-like structure involving the stretch of residues G20-Y30. It was also found that the dimer interface changed in response to pheromone indicating a change in conformation of the N-terminus upon receptor activation.

These findings suggest that the N-terminus of Ste2p possesses a discrete structural domain that appears to participate in the signaling mechanism. Interestingly, a  $\beta$ -strand was predicted in this region by sequence analysis (1,2).

Deletion mutagenesis demonstrated that the N-terminus constrains Ste2p signaling activity. The N-terminus of GPR56, an adhesion GPCR, has also been reported to constrain receptor activation (3). Previous studies with Ste2p demonstrated a role of the N-terminus in dimerization (4-6), mating (1,2) and as a site of glycosylation domains(7). Our studies revealed a previously unrecognized role of the N-terminus: the constraint of signaling activities by stabilizing the inactive state of the receptor. The proposed interaction between the N-terminus and other domain(s) of the receptor may function to stabilize the inactive state of the receptor. Thus, removal of portions of the N-terminal domain may affect Ste2p dimerization or interaction with other domain(s) of the receptor that is important for activation (4,5). In fact, the  $\beta$ -sheet like contacts found in the N-terminus may help to maintain the receptor in its inactive conformation and removal of these residues would thereby facilitate transition to an activated state upon ligand binding. Previous studies indicated a possible interaction between the N-terminus with the extracellular loop one (ECL1), based on changes in glycosylation pattern of the receptor which were observed upon mutation of residues in ECL1, although glycosylation sites are located in the N-terminus (8).

An evolutionarily conserved tyrosine residue, Y26, in the N-terminus was found to play key role in receptor dimerization. Two residues in the ECL1 (V109 and T114) facilitate Y26-mediated dimerization. The disulfide cross-linking studies indicated that Tyr26 interacted with Val109 or Thr114. The dimer interface of the receptor was found to change in response to pheromone indicating a role for dimerization mediated by the N-terminus in receptor activation.

Because the maximum distance between  $\alpha$ -carbons linked by disulfide bonds is about 7Å (9), the amino acid side chains identified using this method should be very close (within 7Å). This strategy has been used to identify interacting residues in several GPCRs including Ste2p (10-17).

## **Future studies**

Despite the remarkable progress made in the structural biology of GPCRs, a clear understanding of the extracellular N-terminus and its significance in signal transduction remains ambiguous. In addition, although dimerization is a widely observed phenomenon in GPCRs, the functional significance of this phenomenon for the vast majority of GPCRs is still debated. The results obtained during the course of the studies for this dissertation will aid in understanding the role of the N-terminus and dimerization in GPCR signal transduction. However, in order to fully understand the role of this extracellular domain and dimerization in receptor function, further studies are necessary. A few suggestions are outlined below to elucidate the role of the Ste2p N-terminus and dimerization.

The results obtained in Chapter 2 indicate that SCAM was useful in determining the accessibility of residues in the extracellular N-terminus. Although these experiments revealed the accessibility of residues in the inactive state of the receptor, it is not known whether the accessibility of these residues is changed upon receptor activation. This information is important since conformational changes also occur in the N-terminus upon receptor activation as indicated by changes in dimerization in the absence and presence of  $\alpha$ -factor. Therefore, SCAM studies of the residues in the presence of  $\alpha$ -factor will provide information regarding conformational changes in the N-terminus that leads to receptor activation.

The results described in Chapter 3 of this dissertation indicate that removal of the N-terminus affects signaling and surface expression. However, no specific residue(s) in the N-terminus was identified as being most responsible for this effect. Alanine scanning mutagenesis in this region might reveal the specific residue(s) responsible for signaling and/or surface expression. Furthermore, the N-terminus was suggested to be involved in negative regulation but the mechanism of the regulation is still unknown. The N-terminus possesses two glycosylation sites located at N25 and N32. A previous report indicated that mutation of these two glycosylation sites to glutamine did not influence receptor function. However, our studies with Cys mutation in the glycosylation sites indicate that signaling activity was altered. Thus it appears that glycosylation in the Ste2p affects signaling but a thorough investigation of the role of this post-translational modification on receptor function is warranted. For example, three forms of receptor mutants having none, one or two glycosylation sites can be tested for functional properties to determine if glycosylation plays a role in receptor function.

Disulfide cross-linking studies demonstrated that a conserved tyrosine residue (Y26) in the N-terminus interacts with V109 or T114 in ECL1. However, these experiments were carried out using membranes prepared from cells expressing these receptors. Thus it is not known if the interaction also occurs in whole cells. Therefore, cross-linking studies using whole cells can be done to determine the interaction *in vivo*. The Y26C mutant functions as a major dimer interface for Ste2p, and exists as a dimer even in the absence of pheromone. The Y26C mutant exhibited weaker growth arrest activity compared to that of the wild type. On the other hand, Y26A mutant does not form promote dimerization, but exhibits increased signaling activity suggesting that dimerization prevents signaling. Although the growth arrest activity of the Y26C and Y26A mutants was similar, *FUS1-LacZ* activities of the Y26A mutant was higher indicating that signal

transduction by dimer and monomer is different. Conformational changes in the receptor resulting from the activation of a Ste2p dimer may be different from that of the monomer thereby initiating a signal. SCAM and disulfide cross-linking can be used to understand the conformational changes which occur in the dimerized receptor in response to pheromone. Identification of the residues and domains that are involved in GPCR dimerization might establish the foundation for the design of drugs that specifically affect the signaling crosstalk between the components of the receptor dimer/oligomer.

## References

1. Shi, C., Kaminskyj, S., Caldwell, S., and Loewen, M. C. (2007) A role for a complex between activated G protein-coupled receptors in yeast cellular mating. *Proceedings of the National Academy of Sciences of the United States of America* **104**, 5395-5400
2. Shi, C., Kendall, S. C., Grote, E., Kaminskyj, S., and Loewen, M. C. (2009) N-terminal residues of the yeast pheromone receptor, Ste2p, mediate mating events independently of G1-arrest signaling. *Journal of cellular biochemistry* **107**, 630-638
3. Paavola, K. J., Stephenson, J. R., Ritter, S. L., Alter, S. P., and Hall, R. A. (2011) The N terminus of the adhesion G protein-coupled receptor GPR56 controls receptor signaling activity. *The Journal of biological chemistry* **286**, 28914-28921
4. Overton, M. C., and Blumer, K. J. (2002) The extracellular N-terminal domain and transmembrane domains 1 and 2 mediate oligomerization of a yeast G protein-coupled receptor. *The Journal of biological chemistry* **277**, 41463-41472
5. Uddin, M. S., Kim, H., Deyo, A., Naider, F., and Becker, J. M. (2012) Identification of residues involved in homodimer formation located within a beta-strand region of the N-terminus of a Yeast G protein-coupled receptor. *Journal of receptor and signal transduction research* **32**, 65-75
6. Shi, C., Paige, M. F., Maley, J., and Loewen, M. C. (2009) In vitro characterization of ligand-induced oligomerization of the *S. cerevisiae* G-protein coupled receptor, Ste2p. *Biochimica et biophysica acta* **1790**, 1-7
7. Montesana, P. E., and Konopka, J. B. (2001) Mutational analysis of the role of N-glycosylation in alpha-factor receptor function. *Biochemistry* **40**, 9685-9694

8. Hauser, M., Kauffman, S., Lee, B. K., Naider, F., and Becker, J. M. (2007) The first extracellular loop of the *Saccharomyces cerevisiae* G protein-coupled receptor Ste2p undergoes a conformational change upon ligand binding. *The Journal of biological chemistry* **282**, 10387-10397
9. Srinivasan, N., Sowdhamini, R., Ramakrishnan, C., and Balaram, P. (1990) Conformations of disulfide bridges in proteins. *International journal of peptide and protein research* **36**, 147-155
10. Li, J. H., Han, S. J., Hamdan, F. F., Kim, S. K., Jacobson, K. A., Bloodworth, L. M., Zhang, X., and Wess, J. (2007) Distinct structural changes in a G protein-coupled receptor caused by different classes of agonist ligands. *The Journal of biological chemistry* **282**, 26284-26293
11. Yu, H., Kono, M., McKee, T. D., and Oprian, D. D. (1995) A general method for mapping tertiary contacts between amino acid residues in membrane-embedded proteins. *Biochemistry* **34**, 14963-14969
12. Zeng, F. Y., Hopp, A., Soldner, A., and Wess, J. (1999) Use of a disulfide cross-linking strategy to study muscarinic receptor structure and mechanisms of activation. *The Journal of biological chemistry* **274**, 16629-16640
13. Li, J. H., Hamdan, F. F., Kim, S. K., Jacobson, K. A., Zhang, X., Han, S. J., and Wess, J. (2008) Ligand-specific changes in M3 muscarinic acetylcholine receptor structure detected by a disulfide scanning strategy. *Biochemistry* **47**, 2776-2788
14. Ward, S. D., Hamdan, F. F., Bloodworth, L. M., Siddiqui, N. A., Li, J. H., and Wess, J. (2006) Use of an in situ disulfide cross-linking strategy to study the dynamic properties

- of the cytoplasmic end of transmembrane domain VI of the M3 muscarinic acetylcholine receptor. *Biochemistry* **45**, 676-685
15. Wang, H. X., and Konopka, J. B. (2009) Identification of amino acids at two dimer interface regions of the alpha-factor receptor (Ste2). *Biochemistry* **48**, 7132-7139
  16. Kim, H., Lee, B. K., Naider, F., and Becker, J. M. (2009) Identification of specific transmembrane residues and ligand-induced interface changes involved in homo-dimer formation of a yeast G protein-coupled receptor. *Biochemistry* **48**, 10976-10987
  17. Umanah, G. K., Huang, L. Y., Maccarone, J. M., Naider, F., and Becker, J. M. (2011) Changes in conformation at the cytoplasmic ends of the fifth and sixth transmembrane helices of a yeast G protein-coupled receptor in response to ligand binding. *Biochemistry* **50**, 6841-6854

## **VITA**

Mohammad Seraj Uddin was born in Cox's bazar, Bangladesh. He graduated from the University of Chittagong, Bangladesh and received Bachelor of Science degree in Microbiology. He received Master of Science degree in Microbiology from the same university. After his Master degree, he worked as a lecturer in the Department of Microbiology, University of Chittagong. He was accepted to the Ph.D. program in Microbiology Department at the University of Tennessee, Knoxville. He did his graduate work in Dr. Jeffrey M. Becker's laboratory. Throughout the course of his time in this program, he served as a graduate teaching and research assistant. He received his Doctor of Philosophy degree in Microbiology in August, 2013.